INVESTIGATING THE CONTROLS ON SURFACE OCEAN DIMETHYL SULPHIDE CONCENTRATIONS AT REGIONAL TO GLOBAL SCALES

Christopher James Miles

A thesis submitted to the School of Environmental Sciences at the University of East Anglia, for the degree of Doctor of Philosophy

September 2012

For my parents and for my brother....

Abstract

This thesis details a series of investigations into the controls on surface ocean concentrations of the climatically relevant, biogenic sulphur compound, dimethyl sulphide (DMS) at regional to global scales. The primary focus is upon the role of solar irradiance and metrics of biological activity in modulating DMS concentrations using bivariate and multivariate statistical techniques in conjunction with three different data sets from multiple spatial and temporal scales.

Firstly, a statistical investigation into the proposed strong positive relationship between surface DMS concentration and the average mixed layer irradiance (solar radiation dose: SRD) was undertaken using DMS data from a series of cruise tracks from the Atlantic Meridional Transect (AMT) programme, primarily from the oligotrophic Atlantic gyres. Positive correlations were found between DMS and (a) SRD formulations using concurrently sampled *in situ* data (ρ=0.55 n=65 p<0.01), (b) SRD formulations based on using climatological data (ρ=0.74 n=65 p<0.01) and (c) a ultraviolet radiation dose (ρ= 0.67 n=54 p<0.01).

The next analysis investigated whether the inclusion of a biological variable (chlorophyll or primary production) alongside irradiance could explain additional variance in DMS concentrations. This analysis employed a database of cruise data from a range of biogeochemical domains, latitudes and trophic conditions (AMT, the Barents Sea, the Atmospheric Chemistry Studies in the Oceanic Environment (ACSOE) research campaign and the DImethyl Sulphide biogeochemistry within a COccolithophore bloom (DISCO) study. Using multiple linear regression (MLR) analyses, it was found that the combination of, *in situ* rate of primary production and underwater irradiance accounted for significant variance in DMS concentrations in data from discrete depths within the euphotic zone (R^2 = 0.55), from near-surface waters (R^2 = 0.66) and within depth profile integrated data (R^2 = 0.40).

The final analysis is an investigation into global surface DMS dynamics using the global surface seawater DMS database (http://saga.pmel.noaa.gov/dms/) and satellite based retrievals of irradiance and primary production rates. A novel composite approach which combines multiple MLR models applied to Longhurst

biogeochemical provinces, and using monthly averaged data, explained maximum variance. Models developed within a randomly selected training subset were able to explain significant variance within the remaining validation subset using this composite approach (predicted vs. observed $\rho = 0.93$, $p = 0$, $n = 107$). Previous studies had been unable to identify a strong link between DMS and indicators of the biological community (e.g. chlorophyll) at large scales. Our results suggest that a link exists between ecosystem productivity and DMS concentrations, and moderated by processes directly influenced by solar irradiance. These findings on large scale ecosystem controls on DMS, based on remote-sensing datasets, provide an advancement in the understanding and prediction of global-scale surface DMS concentrations.

Contents

List of Tables

List of Figures

Figure 4.13: Predicted DMS (nmol l^{-1}) plotted against observed DMS data (nmol l^{-1}) within the validation data subset of the global DMS database (http://saga.pmel.noaa.gov/dms/). Predicted DMS is calculated using the "composite method" (see section 4.3.3.1 for details on composite method). Panel **(a)** shows the data with the axis limited to 10 nmol l^{-1} and panel, large red markers represent province monthly averaged data and smaller black markers represent the high resolution (non averaged) data. Panel **(b)** shows the same data on a $\log_{10}$ scale with no axis limitation. Also shown is the Spearman's rank correlation coefficient (ρ), the significance value (p) and the number of data points (n). Dashed line is a 1:1 trend line. 123

List of Abbreviations

ρ	Spearman's rank correlation coefficient
AMT	Atlantic Meridional Transect programme
ACSOE	Atmospheric Chemistry Studies in the Oceanic Environment
BAR	Barents Sea
BATS	Bermuda Atlantic Time Series
BGCD	Biogeochemical domain
BGCP	Biogeochemical province
C_{Atmos}	Concentration of DMS in the atmosphere
CbPM	Carbon based production model
CCN	Cloud condensation nuclei
CDNC	Cloud droplet number concentration
Chl	Chlorophyll
CoA	Coenzyme A
COD	Cloud optical depth
COS	carbonyl sulphide
C_{Water}	Concentration of DMS in seawater
DISCO	DImethyl Sulphide biogeochemistry within a COccolithophore bloom study
DMS	Dimethyl Sulphide
DMSP	Dimethylsulphoniopropionate
DMSPp	Dimethylsulphoniopropionate (particulate)
DMSPd	Dimethylsulphoniopropionate (dissolved)
DMSPt	Dimethylsulphoniopropionate (total)
DMSO	Dimethyl sulphoxide
DOM	Dissolved organic material
f	Fraction of surface irradiance
f_z	Fraction of surface irradiance at depth z
H	Henry's constant
HNLC	High nutrient low chlorophyll
HW	Hotelling-Williams test
I_0	Surface irradiance
$I_0 est$	Estimated surface irradiance
I_z	Underwater irradiance at depth z
$I_z insitu$	Underwater irradiance at depth z calculated using in situ data
$I_z sat$	Underwater irradiance at depth z calculated using climatological data
IEV	Independent Explanatory Variable

k	Transfer velocity for air sea gas exchange
K_d	Light attenuation coefficient
$K_{d\ TOT}$	Light attenuation coefficient for total solar irradiance
$K_{d\ UV}$	Light attenuation coefficient for UV irradiance
LWC	Liquid water content
MeSH	Methanethiol
MLD	Mixed layer depth
MLR	Multiple linear regression
MMPA	3-methiolpropionate
MODIS	Moderate Resolution Imaging Spectroradiometer
MTA	Methylthioacrylyl
MPA	3-mercaptopropionate
MSA	Methanesulphonic acid
NSS	Non-sea salt
n	Sample number
NPP	Net primary production rate
PSC	Phytoplankton size class
PFT	Phytoplankton functional type
p	p-value used to evaluate statistical significance
PAR	Photosynthetically active radiation
R	Multiple correlation coefficient
R^2	Multiple coefficient of determination
r	Pearson's product moment correlation coefficient
r^2	Bivariate coefficient of determination
RMBL	Remote marine boundary layer
ROS	Reactive oxygen species
SeaWiFS	Sea-viewing Wide Field-of-view Sensor
SRD	Solar radiation dose
SRD_{insitu}	Solar radiation dose calculated using *in situ* data
SRD_{cllim}	Solar radiation dose calculated using climatological data
TOA	Top of the atmosphere
UV	Ultraviolet radiation
VGPM	Vertically Generalised Production Model
$VGPM_{avg}$	Euphotic zone average net primary production rate using the VGPM model
z_eu	Depth of the euphotic zone
z	Depth

Acknowledgments

First and foremost I would like to thank my supervisors Parv Suntharalingam, Tom Bell and Tim Lenton for their tireless enthusiasm and support throughout my PhD. Thanks for the inspiration and for never doubting I could do it even when I doubted myself. It is impossible to articulate the gratitude I feel. Thanks to all the friends I made along the way that made my time at UEA special, you know who you are. Thanks to all the members of the Marine Trace Gas Biogeochemstiry group and the Earth System Science group for all the discussions and advice over the years. A special thanks must also go to Gill Malin for her words of advice and guidance throughout my PhD but especially at the end when I needed it the most. I would like to thank Sergio Vallina for his help and advice on the SRD calculation and for supplying some of the climatological data. Thanks to Dominic Kniveton and Jay Harman for their help with the acquisition and compilation of the UV data. I thank Paty Matrai, Kalle Olli, Paul Wassmann and María Vernet for providing the Barents Sea data. Thanks to Alex Poulton for providing the AMT primary production data and the British Oceanographic Data Centre (BODC) for providing the ACSOE and DISCO data. Thanks also goes to Robert O'Malley for supplying the climatological primary production data. I would also like to Valerie Livina for her statistical advice.

I dedicate this thesis to my parents Michael and Beverley and my brother Tim. Thanks for being you. Thanks also to Alex and Emily for all the years and for shelter in a storm. Without the support of family and friends this would not have been possible.

Chapter 1: Introduction

1.1 Introduction

In this introductory chapter I will provide the wider context for its content (section 1.2) before discussing in detail the processes and current knowledge surrounding its focus: the marine DMSP-DMS ecosystem and the factors which control the concentration of DMS in the surface ocean (section 1.3). The outline and motivation for this thesis is provided in section 1.4.

Two chapters in this thesis are published papers (chapters 2 (Miles et al. 2009) and 3 (Miles et al. 2012)) and so have their own introductions that are more comprehensive than might otherwise be found in a thesis chapter. Consequently there is the possibility for some overlap between this introduction and the introductions of these chapters. In addition, the methods are contained within each chapter rather than as a separate chapter.

1.2 Background

1.2.1 Gaia, biogeochemical cycles, climate and the CLAW hypothesis

Since the origin of life on Earth ~3.8 billion years ago (Mojzsis et al. 1996), life has persisted despite major perturbations to the earth system. These perturbations include modifications of the atmosphere's composition (e.g. the great oxidation (Goldblatt et al. 2006; Van Der Giezen and Lenton 2012)), almost complete glaciations ("Snowball Earth" (Kirschvink 1992; Kirschvink et al. 2000; Kopp et al. 2005)) and the Sun's brightness increasing by about 25% (faint young sun paradox (Sagan and Mullen 1972)).

The Gaia hypothesis (Lovelock and Margulis 1974b, a) proposed that life on Earth could contribute to the maintenance of habitable conditions via modifications and feedbacks within the biogeochemical cycles of the major elements (e.g. carbon, oxygen, hydrogen, nitrogen, phosphorus and sulphur) between the 4 major components of the "Earth system" (lithosphere, hydrosphere, atmosphere, and biosphere) .Via these feedbacks homeostasis within the system can emerge (Lovelock and Margulis 1974b) maintaining a state of low entropy (high order) as

evident in an atmosphere in chemical disequilibrium, in contrast to the atmospheres of Mars and Venus where no life has yet been found.

In 1987 the CLAW hypothesis (named after the initials of the authors) proposed a biogeochemical feedback between marine biogenic sulphur emissions in the form of dimethyl sulphide (DMS), cloud albedo and climate (Charlson et al. 1987) (see Figure 1.1). Earlier, Shaw (1983) had proposed that the emission and oxidation of DMS to SO_2 by OH, and further oxidation to H_2SO_4 by OH could lead to the nucleation of new particles in the remote marine boundary layer (RMBL) via gas phase H_2SO_4 to form non-sea salt sulphate aerosols ($NSS\text{-}SO_4^{-2}$). Furthermore it was suggested that $NSS\text{-}SO_4^{-2}$ were the primary source of cloud condensation nuclei (CCN) in the unperturbed RMBL. The equations of Twomey (1977) show that clouds forming in conditions with elevated CCN numbers will have a higher albedo. This is because of the Twomey first indirect effect: “more but smaller” cloud droplets have a higher albedo (Twomey 1991). Crucially, the CLAW authors recognised that a change in albedo propagated by biogenic DMS could feedback to either amplify or attenuate its production and so the biological regulation of climate could be possible (Charlson et al. 1987). It was unknown whether the sign of the feedback would be negative (countering any initial change) or positive (amplifying the initial change) (Charlson et al. 1987).

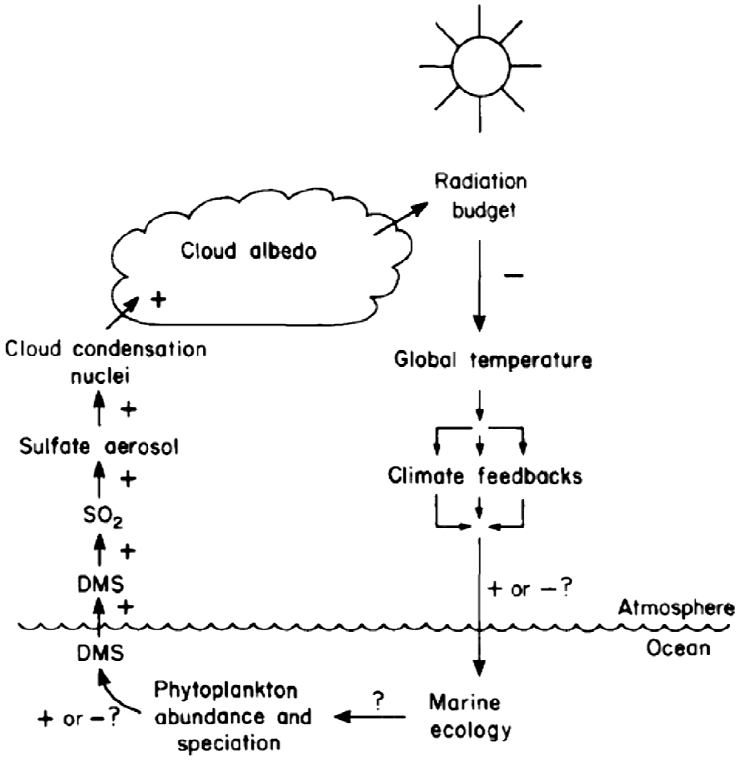

Figure 1.1*: Schematic of the CLAW hypothesis named after the initials of the authors Charlson, Lovelock, Andreae and Warren (Charlson et al. 1987). Reproduced from Andreae and Crutzen (1997).*

The apparent simplicity of CLAW belies huge complexities that span multiple spatial and temporal scales and scientific disciplines. In the 25 years since the publication of the CLAW hypothesis much research effort has been invested looking at the various stages of the loop with most of the linkages challenged to some extent (Ayers and Cainey 2007) with some calls to retire the CLAW hypothesis (Quinn and Bates 2011). Although much has been learnt, the stages of the CLAW loop are still subject to large uncertainties and relatively low levels of scientific understanding (Ayers and Cainey 2007; Harvey 2007)

The CLAW hypothesis proposed that DMS is oxidised largely by OH (NO_3 and IO are discussed but their contribution is considered minor) and that new sulphate aerosols are formed by homogenous nucleation in the marine boundary layer. These sulphate aerosols were thought to be the primary (perhaps only) source of CCN. CLAW proposed that the marine DMS flux could directly influence CCN numbers

(Charlson et al. 1987). Biogenic sulphur has been found to be ubiquitous in the remote marine aerosol and undoubtedly affects aerosol chemistry (Andreae and Rosenfeld 2008; Bates et al. 1992; Leck and Bigg 2005). Seasonal covariance has been observed between DMS, its oxidation products, and CCN from field observations and remote sensing studies (Ayers and Gillett 2000; Ayers and Gras 1991; Ayers et al. 1997; Putaud et al. 1992; Vallina et al. 2007), and between CCN and cloud optical depth (Boers et al. 1994).

However, it is now understood that the link between DMS and the CCN population is much more complicated than originally thought or implied by the CLAW hypothesis (Ayers and Gillett 2000; Quinn and Bates 2011; Von Glasow 2007). DMS is not only oxidised by OH but also by radicals of BrO and Cl. DMS is oxidised via two main pathways, H-abstraction and OH-addition with the relative contribution influenced by temperature. The addition pathway does not lead to H_2SO_4 and new particle formation but its products do contribute to the growth and chemical composition of existing particles (von Glasow and Crutzen 2004).The abstraction pathway leads by several intermediates to SO_2, which can be taken up by existing particles or further oxidised to H_2SO_4 or MSA. *Only* H_2SO_4 can lead to new particle formation (NSS-SO_4^{2-}) (Von Glasow 2007). The formation of new particles can only occur if H_2SO_4 is not scavenged by pre-existing aerosols before it can undergo homogenous nucleation to a secondary aerosol. Problematically, the nucleation of new particles is thought to be energetically less favourable than deposition onto existing particles (Andreae and Rosenfeld 2008). Modelling studies suggest that homogenous nucleation of new sulphate aerosols which can then act as CCN solely from DMS oxidation products is theoretically rare in the RMBL (Cainey and Harvey 2002; Carslaw et al. 2010; Korhonen et al. 2008; Pirjola et al. 2000; Woodhouse et al. 2010). There is only sparse field evidence for this occurrence but it is difficult to detect and measure nucleation events in the field (Andreae and Rosenfeld 2008; Carslaw et al. 2010). It is possible that the models or processes included within them are insufficient to represent the complexity of the real world situation (Andreae and Rosenfeld 2008; Faloona 2009).

The original CLAW study underestimated the potential for sea salt aerosols to act as CCN (Smith 2007). It was thought that sea salt aerosols were too large to act as CCN

and that the flux was small (Charlson et al. 1987). It has been shown that significant numbers of sea salt aerosols of the right size for CCN formation are entrained from the surface and can form CCN (O'Dowd and Smith 1993; O'Dowd et al. 1999; Murphy et al. 1998; Twohy and Anderson 2008). The primary control upon sea salt flux is wind speed and does not directly involve the biology of the surface ocean (Smith 2007; Twohy and Anderson 2008). Other potential sources of marine aerosols include biological products such as isoprene (Meskhidze and Nenes 2006) or viruses, bacteria, and organic material from dead cells (Bigg 2007; Leck and Bigg 2005, 2007).

Perhaps the least contested part of the CLAW loop is the relationship between the population of CCN and cloud albedo (Ayers and Cainey 2007). Clouds forming in air with elevated CCN numbers will form clouds with "more but smaller" cloud droplets, they will have a higher cloud droplet number concentration (CDNC) with a smaller cloud droplet effective radius (at a fixed liquid water content (LWC)) (Twomey 1991). Clouds with higher CDNC have an increased cloud optical depth (COD), reducing radiative transfer, and so a higher albedo (Twomey 1991). There are uncertainties regarding the effect of CCN/CNDC and cloud albedo. Increased CNDC may affect cloud lifetime (Albrecht 1989) with smaller cloud droplets decreasing precipitation efficiency , altering the LWC and augmenting cloud heights (Pincus and Baker 1994). Cloud processing (evaporation and condensation cycles) and CCN "rainout" events (losses) (Pandis et al. 1994) also increase the complexity of the relationship between aerosol-CCN populations and albedo (Andreae and Rosenfeld 2008).

In addition to the climatic role postulated by CLAW, oxidised DMS emissions are a potential source of carbonyl sulphide (COS) (Barnes et al. 1994). COS is oxidised in the stratosphere to form sulphate particles that influence the radiation budget via direct scattering of incoming radiation (Crutzen 1976). COS also influences the stratospheric ozone cycle (Crutzen 1976). Accurate estimates of DMS emissions are required to balance and constrain the global COS budget (Kettle et al. 2002; Suntharalingam et al. 2008).

1.2.2 Importance of understanding the controls on seawater DMS concentrations

Along with a role in climate (Charlson et al. 1987; Crutzen 1976), the global biogeochemical cycling of sulphur is important for life as sulphur is essential to the function of living cells (Nelson and Cox 2000). Figure 1.2a shows the pre-industrial global sulphur cycle. Sulphur is cycled between the terrestrial reservoir where it is abundant in rocks and soils, the oceanic reservoir where sulphate (SO_4^{-2}) is the second most abundant anion in seawater and the atmospheric reservoir. Major inter reservoir fluxes include volcanic SO_2 emissions, gaseous emissions from the terrestrial biosphere and the formation of sulphate aerosols over the oceans. The sea-air emission of DMS and its subsequent oxidation and deposition is the major flux of volatile sulphur from the oceans to the land (Brimblecombe et al. 1989; Graf et al. 1997).

The post industrial sulphur cycle (Figure 1.2b) has been heavily perturbed by terrestrial anthropogenic emissions, especially in the northern hemisphere. However, the trend for increasing sulphur emissions into the late 1980's has since been observed to be in decline throughout the 1990's and beyond (Stern 2006). In contrast, there has been an increase in the anthropogenic contribution of sulphur to the remote marine atmosphere from shipping along the major trade routes. Corbett et al. (1999) report that in 1993 ship sulphur emissions were around 4.24 Tg S y^{-1} which corresponds to ~20% of biogenic DMS emissions, increasing to around 4.72 Tg S y^{-1} by 2003 (Corbett and Koehler 2003). Despite the changes in anthropogenic sulphur sources, natural emissions of DMS remain the major source of volatile sulphur in the remote marine atmosphere (Bates et al. 1992; Watts 2000). The global sulphur cycle cannot be balanced without biogenic DMS emissions (Simó 2001).

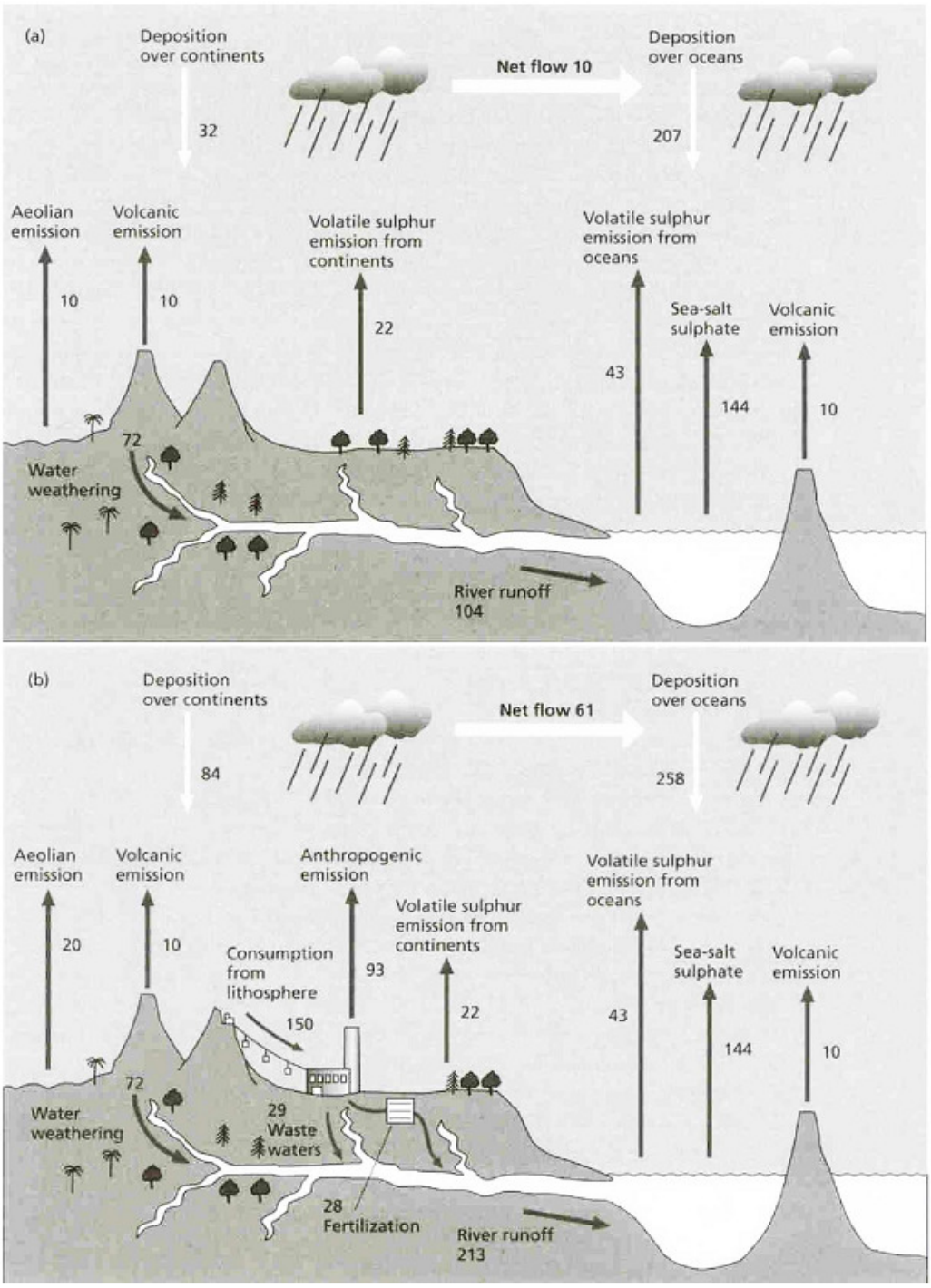

Figure 1.2: (a) *The natural, pre-industrial sulphur cycle and* ***(b)****, the post-industrial anthropogenically perturbed sulphur cycle. The fluxes between different reservoirs (atmosphere, ocean and land) are shown with black arrows with the numbers indicating their contribution to the total sulphur budget. Reproduced from Brimblecombe et al. (1989).*

The sea to air transfer of DMS at a constant wind speed and temperature depends primarily on the seawater DMS concentration (Elliott 2009; Liss and Slater 1974; Wanninkhof 1992). Annual global flux estimates are dependent upon a continuous, global field of sea surface DMS concentrations. The most commonly used fields are interpolated climatologies which represent a set of interpolated point measurements (Kettle and Andreae 2000; Lana et al. 2011a) or fields obtained using global models or simple parameterisations (Anderson et al. 2001; Aumont et al. 2002; Simó and Dachs 2002). The annual flux of DMS has been estimated to be 15 – 35 Tg S yr^{-1} (Elliott 2009) with the most recent estimate based upon an updated, interpolated climatology of ~28 Tg S yr^{-1} (Lana et al. 2011a). The significant uncertainties in estimating DMS flux are uncertainties in the parameterisation of sea-air gas exchange and uncertainties in the processes governing surface DMS concentrations. Reducing the uncertainty in calculating the surface DMS field used for flux estimates by furthering understanding of the controls on surface DMS concentrations is critical to constraining flux estimates.

To evaluate the role that DMS may play in current and future climate and how environmental changes may impact the sulphur cycle it is vital to understand the controls on DMS concentration. In order for the CLAW hypothesis to operate as proposed, any change in albedo caused by DMS-derived CCN must feedback to modulate the concentration of DMS in the surface ocean. It is critical to the CLAW hypothesis that changes in albedo dependent factors such as sea surface temperature or irradiance dependent processes influence the modulation of DMS.

1.3 Marine DMSP-DMS cycle

DMS results primarily from cleavage of its biological precursor molecule dimethylsulphoniopropionate (DMSP). DMS is an ecosystem product, with seawater concentrations the result of a complex interaction of sources and sinks only one of which is flux to the atmosphere (Simó 2001; Stefels et al. 2007). Seawater DMS concentrations display strong seasonal and latitudinal variation (Kettle et al. 1999; Lana et al. 2011a) (see Figure 4.1). Generally, highest DMS concentrations are observed at high latitudes with peaks that coincide with summer biomass whist low latitudes exhibit lower DMS concentrations with peaks in spring (smaller) and

summer (larger) (Kettle et al. 1999; Lana et al. 2011a). Analysis of the Bermuda Atlantic Time Series (BATS) data (Dacey et al. 1998) showed in oligotrophic environments that the summer DMS maximum is out of phase with the peak in biomass but coincident with maximum summer insolation (Toole et al. 2003). Typical open ocean concentrations of DMSP are around 10 nmol l^{-1} with DMS concentrations generally lower at 1-5 nmol l^{-1} with an average DMS concentration of 4.24 nmol l^{-1} for the recently updated global surface DMS database (http://saga.pmel.noaa.gov/dms/). However concentrations of DMS and DMSP can be much higher during localised algal blooms (e.g. maximum value of 420 nmol l^{-1} from the global DMS database).Both DMS and DMSP are rapidly degraded on timescales of hours to 1-2 days demonstrating fairly rapid production and loss rates (Kiene and Linn 2000).

1.3.1 DMSP synthesis

DMSP is a product of biological metabolism, synthesised inside the cells of some classes of marine phytoplankton (Keller et al. 1989). This process begins with the assimilation of sulphate across the cell membrane and ends in the biosynthesis of DMSP from methionine following several intermediate stages (Stefels 2000). DMSP is present in the marine ecosystem in two theoretically and operationally defined pools, particulate DMSP (DMSPp) and dissolved DMSP (DMSPd). DMSPp represents the intracellular DMSP within phytoplankton and organisms that have accumulated DMSP. DMSPd is the free DMSP in solution. Total DMSP (DMSPt) can be referred to either the sum of the two pools or it can refer to a single straight analysis without filtration.

1.3.2 Species dependence

The proportion of DMSP-carbon to total cell-carbon, the DMSP cell quota, is highly variable between different classes of marine phytoplankton (Archer 2007; Keller et al. 1989; Stefels et al. 2007). Intracellular concentrations can range from <0.1 nmol l^{-1} to 400 nmol l^{-1} (Archer 2007) with a range of 0-11% in DMSP cell quota between taxa (Stefels et al. 2007). High DMSP producers include members of the classes of Haptophyceae (including the coccolithophore *Emiliania huxleyi* and the prymnesiophyte *Phaeocystis spp.*) and Dinophyceae (dinoflagellates). Low DMSP

producers include the diatoms and prochlorophytes/cyanophytes (Stefels et al. 2007). Whilst the haptoyphyte sp. do not synthesise unusually high amounts of DMSP per cell volume their ability to form extensive blooms can yield high levels of DMSP (Stefels et al. 2007). Species composition affects ecosystem DMSP production the most (Stefels et al. 2007) with species composition varying in space and time, partly the result of environmental conditions such as temperature, salinity, irradiance and nutrient status (Longhurst 1995).

Table 1.1: *Major species groups and the mean ratios of DMSP:C, the proportion of cell carbon, and the mean ratios of DMSP:chl-a. Standard deviation is in brackets. Reproduced from Stefels et al. (2007) with references to individual studies therein.*

Species group	DMSP:C (mol:mol)	Proportion DMSP-carbon	DMSP:chl-*a* (mmol:g)
Diatoms (n = 22)	0.00086 (0.00126)	0.0043 (0.0063)	4 (6)
Chrysophytes (n = 6)	0.019 (0.015)	0.094 (0.075)	94 (75)
Dinoflagellates (n = 32)	0.022 (0.032)	0.111 (0.158)	111 (168)
Prasinophytes (n = 18)	0.005 (0.007)	0.025 (0.034)	25 (34)
Haptophytes (n = 32)	0.011 (0.007)	0.053 (0.037)	52 (37)
Prochlorophytes/Cyanophytes (n = 17)	0.0000015 (0.000004)	0.000008 (0.00002)	0.008 (0.02)

1.3.3 DMSP function(s)

Intracellular DMSP concentrations and the DMSP cell quota can also vary largely (0-100%) potentially influenced by environmental conditions such as temperature, irradiance, salinity and nutrients (Stefels et al. 2007). Phytoplankton exist in a highly dynamic environment subject to a range of environmental challenges, for example, changes to the abiotic environment caused by variations in irradiance intensity and wavelength, temperature, pH and salinity. These challenges occur on multiple temporal scales ranging from sub-hourly to diurnal to seasonal and influenced by temporal changes in vertical mixing and meteorology. Phytoplankton are also subject to environmental stresses from biotic factors such as grazing, bacterial and viral attack and the presence of environmental toxins and pollutants (Macintyre et al. 2000). Any strategy that maximises cellular efficiency over the relatively short lifetime of a phytoplankton cell is likely to offer a significant selective advantage (Simó 2001). Several cellular functions for DMSP have been proposed but the

physiological role(s) of DMSP and its breakdown products have not been resolved. The high cellular concentration observed within some species suggests it is not a by-product (Stefels 2000). DMSP may also have multiple roles within and between species (Simó 2001).

DMSP may act as a compatible solute (osmoprotectant) allowing the regulation of osmotic pressure within the cell countering changes in salinity (Dacey and Wakeham 1986; Stefels 2000; Vairavamurthy et al. 1985). Small molecules or osmolytes are accumulated within the cytoplasm where they act as compatible solutes, countering changes in cell volume that result from changes in the solute concentration around the cell which would otherwise cause water to cross the cell membrane (osmotic shock). Osmotic shock can occur when the salinity is increased or decreased relative to intracellular concentration. Under high salt concentrations water is drawn out of the cell whilst at low salt concentrations water may enter the cell causing the cell to swell or in the extreme causing it to burst. Increases in cellular DMSP concentration in response to increasing salinity have been observed in some species (Dickson and Kirst 1986; Stefels et al. 2007). High concentrations of DMSP are observed in some polar species and it has been suggested that DMSP may act as a cryoprotectant (Karsten et al. 1996).

Chemical defence strategies that reduce grazing rates should offer a selective advantage to marine phytoplankton (Strom 2002). The enzymatic cleavage of DMSP has been proposed as an activated chemical defence system (Wolfe and Steinke 1996; Wolfe et al. 1997). Activated defences are mildly toxic compounds stored by plants that are transformed to deterrent compounds upon tissue damage. In this case DMSP would be cleaved to DMS and acrylate upon grazing yielding high concentrations of acrylate in the food vacuoles of the grazer (Wolfe et al. 1997). Some laboratory studies have shown that DMSP producers experience lower levels of predation by zooplankton (Archer et al. 2001; Strom 2002; Wolfe et al. 1997) suggesting that DMSP (Strom 2002) or a product of its breakdown, acrylate (Wolfe et al. 1997), may act a grazing deterrent (see Figure 1.4 for details of DMSP breakdown pathways). Strom et al. (2003) investigated the effect of DMSP, DMS and acrylate upon the coccolithophorid *Emiliania huxleyi* by four dinoflagellate species. The addition of DMSP reduced grazing by all four dinoflagellate species

although the sensitivity of the grazers to DMSP and the percentage reduction in grazing varied between species from minor reductions to almost complete cessation. In addition the presence of DMSP reduced the grazing rates by the dinoflagellate species *Amphidinium longum* to similar levels upon five different algal species, including some non-DMSP producing species. This suggests that the effectiveness of DMSP as grazing deterrent depends upon the sensitivity of the grazer to DMSP. However, Strom et al. (2003) found that the addition of DMS and acrylate had no effect upon grazing rates. This would seem to refute the original DMSP active defence hypothesis which proposed that acrylate would impact grazers after prey ingestion. Instead Strom et al. (2003) propose that DMSP may act as a signalling compound for the presence of toxic algal cells.

DMS is released by grazing on phytoplankton species by zooplankton and so DMS may act as an attractant. Steinke et al. (2006) showed that the copepod *Temora longicornis* had the ability to detect DMS and it was suggested that copepods use DMS to detect grazing by smaller microzooplanktonic species upon which they feed. Steinke et al. (2006) also hypothesised that DMS could be released by phytoplankton as a mechanism to reduce microzooplankton grazing. Larger organisms are able to detect DMS and use it a signalling compound. Both seabirds (Bonadonna et al. 2006; Nevitt et al. 1995; Nevitt and Haberman 2003) and harbour seals (Kowalewsky et al. 2006) have been shown to use DMS to locate areas of high productivity which are coincident with good foraging grounds.

Stefels et al. (2000) proposed that DMSP may serve as an overflow mechanism for excess reduced sulphur (cystine and methionine) and carbon under conditions of unbalanced growth. At high irradiances carbon fixation rates exceed nitrate assimilation rates causing the accumulation of carbohydrates (Turpin 1991). When nitrogen is limited the S:N ratio within the cell can become unbalanced increasing the cellular concentrations of cystine and methionine. DMSP may be produced and potentially discarded in response to nitrogen limitation or high irradiances serving to regenerate intracellular nitrogen from methionine and as a sink for excess carbon (Stefels et al. 2000). Studies have shown an increase in DMSP production under nitrogen limitation (Bucciarelli and Sunda 2003; Turner et al. 1988) and under high

irradiances when nitrogen limitation is induced by iron limitation (Stefels and Van Leeuwe 1998).

Another potential function for DMSP is proposed by Sunda et al. (2002). The authors suggest that DMSP and a cascade of its breakdown products including DMS perform an antioxidant role within the cell scavenging harmful reactive oxygen species (ROS) generated in high light environments by photosynthesis or because of nutrient limitation. DMSP and DMS could therefore be involved in the maintenance of photosynthetic efficiency under high irradiances postponing photoinhibition. This could offer a significant selective advantage within the highly variable light environment of the mixed layer. The upregulation of DMSP production has been observed under nutrient limited conditions (Bucciarelli and Sunda 2003) and in response to high irradiances (Stefels and Van Leeuwe 1998). Sunda et al. (2002) report that DMS production via DMSP lyase activity increased in response to nutrient and UV induced oxidative stress. Sunda et al. (2002) observe that the largest increase in DMSP/cell volume and DMS/cell volume ratios (relative to cultures grown in light environments with no UV radiation) occurred when the irradiance spectrum was filtered for UVB (290-320nm) but included UVA (320-400nm).The antioxidant hypothesis and overflow hypothesis are not necessarily mutually exclusive (Stefels et al. 2007).

1.3.4 The DMS ecosystem: sources and sinks

In contrast to DMSP which is a product of algal synthesis, DMS is an ecosystem product, the result of a complex interaction of sources and sinks within the marine microbial food web (Simó 2001). Figure 1.3 gives a synopsis of the interaction between the biotic and abiotic components of the surface microbial ecosytem that constitute the major production and loss pathways for DMS, the balance of which ultimatly controls ambient DMS concentrations. The processes that dictate the magnitude of the DMS source are discussed in detail in section 1.3.4.1 and the major sinks for DMS are discussed in detail in section 1.3.4.2.

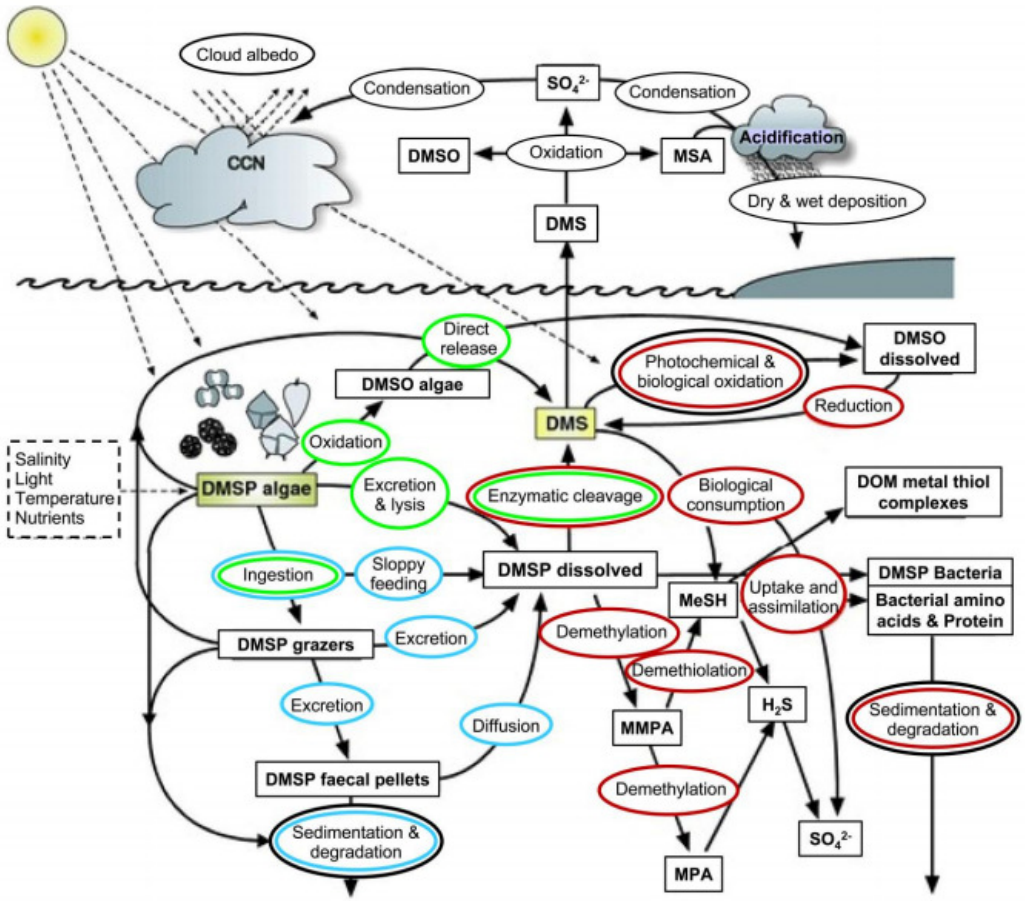

Figure 1.3: *A schematic outlining the current knowledge of the DMS microbial food web. Seawater DMS concentrations are the result of a complex interactions of biotic components indicated by the green ellipses which relate to phytoplankton processes, blue ellipses which relate to zooplankton processes, red ellipses that relate to bacterial processes and abiotic factors which are indicated by black ellipses. Abbreviations: CCN, cloud-condensation nuclei; DOM, dissolved organic material; DMS, dimethyl sulphide; DMSO, dimethyl sulphoxide; DMSP, dimethyl sulphoniopropionate ; MeSH, methanethiol; MPA, mercaptopropionate; MMPA, methylmercaptopropionate; MSA, methanesulphonic acid. Reproduced from Stefels et al. (2007).*

1.3.4.1 DMS sources

The major precursor to DMS within the surface ocean ecosystem is DMSP. DMSP can enter the water column following a number of pathways. A major route for the liberation of DMSPp is cell death with DMSPd concentrations often highest at the

senescence phase of a phytoplankton bloom (Nguyen et al. 1988). Cell death can occur in anumber of ways including autolysis, viral atack or grazing. Nutrient stress at the end of a bloom can increase susceptibility to bacterial and viral attack (Nguyen et al. 1988).

Viral infection has been shown to increase cell lysis and DMSP and DMS concentrations (Evans et al. 2007; Hill et al. 1998; Malin et al. 1998) and can lead to the termination of phytoplankton blooms. Malin et al. (1998) report a 400% increase in DMS production in virus infected cultures of *Phaeocystis pouchetii* compared to control values. However the cultures were not axenic and DMS could have resulted from bacterial conversion of DMSP. Hill et al. (1998) showed increased DMSP concentrations in virally infected, axenic cultures of *Micromonas pusilla* but no DMS in non-axenic cultures. Evans et al. (2007) have however shown elevated DMS concentrations in infected, axenic cultures.

Grazing by zooplankton can also significantly increase DMSPd and DMS concentrations with the size and feeding behaviour of the zooplankton important. Larger meso- and macrozooplankton may liberate DMSP to the water column via sloppy feeding, rupturing cells but not completely assimilating DMSP. Studies on smaller, microzoplankton which engulf their prey suggest that 20-70% of the ingested DMSPp is released to the DMSPd pool (Stefels et al. 2007). Some DMS is also produced by micozooplankton grazing (Wolfe et al. 1997). The proportion of DMS is related to the amount of DMSP-lyse present in the prey indicating that the grazers simply facilitate the mixing of DMSP and DMSP lyase within the prey cell (Wolfe et al. 1997). Some DMSP is also recovered to the DMSPd pool from the faecal pellets of grazers (Yoch 2002).

Some DMSP enters the water following direct exudation by phytoplankton (Stefels et al. 2007). The rate of active exudation of DMSP is species specific with an additional dependence upon abiotic conditions such as temperature, salinity and nutrient status (Stefels et al. 2007). In a modelling study Laroche et al. (1999) suggest a range in the exudation percentage of the DMSP quota per day between different species with 1% for the dinoflagellate *Prorocentrum minimum* to 3-11% for

Phaeocystis sp. There is a lack of experimentally derived rate measurements within the literature (Malin and Kirst 1997).

The fate of DMSPd

Typical dissolved DMSP concentrations are the order of 1-50 nmol l^{-1} but can be an order of magnitude higher at the end of a bloom phase, turnover times are rapid in the order of hours to days (Archer et al. 2002b; Kiene and Linn 2000). DMSP has been shown to play an important role in surface ocean microbial communities (Kiene et al. 2000). DMSP derived sulphur can supply up to 100% of the sulphur demand and DMSP derived carbon up to 15% of the carbon demand of marine bacteria (Kiene et al. 2000; Simó et al. 2002).

Once in the water column DMSPd can either be cleaved to DMS by algal and bacterial DMSP lyase enzymes or it can be catabolised by bacteria via a pathway that does not yield DMS (Curson et al. 2011; Moran et al. 2012; Reisch et al. 2011a). Recent molecular studies have suggested that most DMSP catabolism is undertaken by bacteria despite earlier reports of DMSP lyase activity in coccolithophores (Steinke et al. 1998) and dinoflagellates (Yost and Mitchelmore 2009). The difficulty in obtaining axenic cultures and the lack of molecular descriptions of the enzymes and corresponding genes in phytoplankton has suggested that bacteria are the primary catabolisers (Curson et al. 2011). Figure 1.4 shows the two major known pathways for the catabolism of DMSPd, the dominant demethylation pathway which does not yield DMS and the DMSPd cleavage pathway which can lead to DMS.

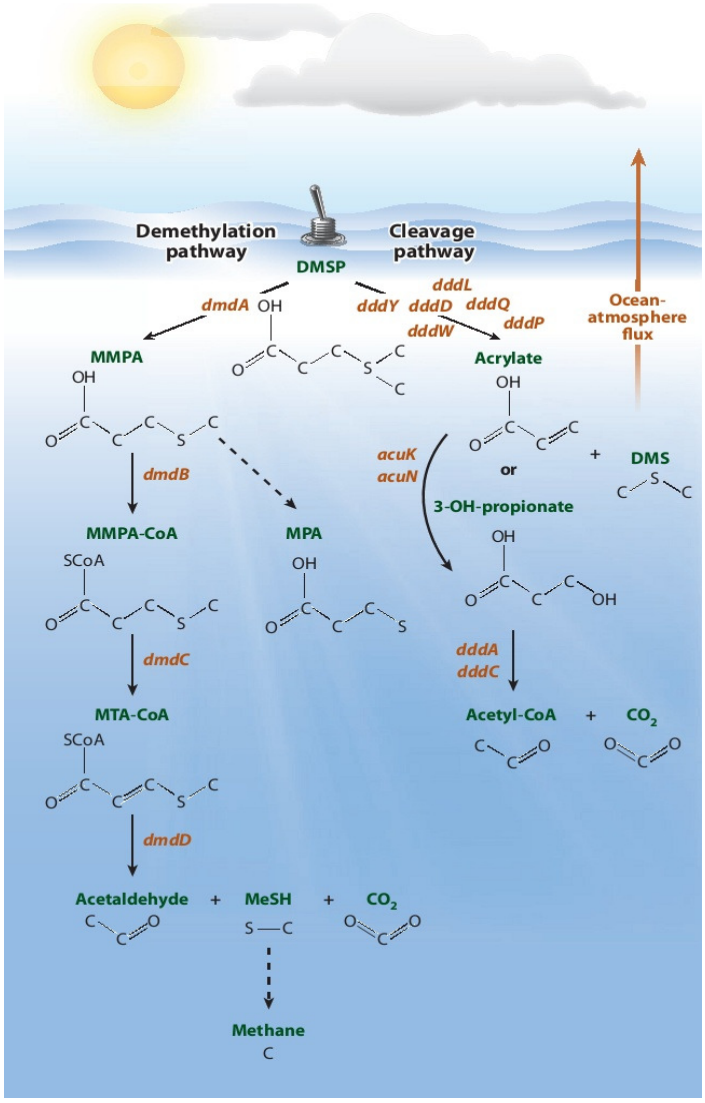

Figure 1.4*: The two major pathways of the catabolism of dimethylsulfoniopropionate (DMSP). Left: the dominant DMSP demethylation pathway which does not yield DMS. The genes dmdA, dmdB, dmdC and dmdD mediate the demethylation of DMSP (Curson et al. 2011; Reisch et al. 2011b) and are widespread in the bacterioplankton genomes and metagenomes . Right: the DMSP cleavage pathway which can lead to dimethyl sulfide (DMS) formation. The first step in the DMSP cleavage pathway can be initiated by the genes dddD, dddL, dddP, dddO and dddW but these genes are less common in the bacterioplankton genomes (Todd et al. 2007; Todd et al. 2009; Todd et al. 2011; Todd et al. 2012). Abbreviations: CoA, coenzyme A; MeSH, methanethiol; MMPA, 3-methiolpropionate; MPA, 3-mercaptopropionate; MTA, methylthioacrylyl. Figure reproduced from Moran et al. (2012).*

Kiene et al. (2000) hypothesised that it is the bacterial sulphur demand relative to the available DMSPd that is critical in determining by which pathway DMSPd is cycled. This has come to be known as the bacterial switch (Howard et al. 2006). When DMSPd concentrations are low bacteria have a preference for the more energy efficient demethylation pathway with DMSP catabolised to methanethiol (MeSH) via several intermediate stages (see figure 1.4). When DMSPd concentrations are high, surplus DMSPd is processed via the cleavage pathway which can yield DMS and acrylate with the acrylate used as a carbon source. If bacterial sulphur demand is diminished the lyase pathway is upregulated increasing the yield of DMS from DMSPd (Kiene et al. 2000; Levine et al. 2012). The bacterial sulphur demand is dependent upon the growth rate and size of the bacterial population and can be reduced by nutrient limitation, high grazing and viral mortality rates, UV induced stress and non-optimal temperatures (Kiene et al. 2000).

As much as 100% of DMSPd can be cycled through the demethylation pathway although there is significant spatial and temporal variation (Kiene & Linn 2000, Kiene et al. 2000). Simó and Pedrós-Alió (1999a) observed a range in the yield of DMS from DMSPd from 5-100% which was correlated to mixed layer depth. A link between shallow mixed layer depths, high UV irradiance and high DMS yield was suggested (Simó and Pedrós-Alió 1999a).

1.3.4.2 DMS sinks

Once free within the water column DMS can be removed by bacteria (Archer 2007; Kiene et al. 2000; Simó et al. 2000), photo-oxidised to DMSO and other breakdown products (Brimblecombe and Shooter 1986; Hatton 2002; Kieber et al. 1996; Toole et al. 2003) or cross the air-sea interface (Elliott 2009; Ho et al. 2006; Liss and Slater 1974).

A major sink for DMS in the surface ocean is bacterial degradation via consumption and oxidation pathways (Kieber et al. 1996; Kiene and Linn 2000). Simó (2004) compiled data from different sites and found that 50-80% of DMS production is lost to bacterial degradation. This sink will be mediated by bacterial growth rates,

population size and speciation (and so potentially by irradiance, nutrients, temperature, bacterial grazing and viral mortality rates) (Simó 2004).

Photooxidation of DMS occurs in response to UV radiation and also at longer, visible wavelengths in the presence of photosensitisers (Brimblecombe and Shooter 1986; Hatton 2002; Kieber et al. 1996) such as chromophoric dissolved organic matter (CDOM) (Brugger et al. 1998; Zepp et al. 1985). DMS photolysis rates have also been shown to be elevated in the presence of nitrate which can photolyse to form reactive oxygen species (Mack and Bolton, 1999; Toole et al. 2004). Thus the DMS photolysis rate at a given depth is dependent upon irradiance intensity and spectral distribution, temperature and the presence of nitrate or photosensitisers (e.g. CDOM). Photolysis rates have been observed to be highly variable with an order of magnitude difference reported between sites with a range of 0.03 – 0.23 h^{-1} from the North Sea to the Antarctic (Hatton 2002; Brugger et al. 1998; Kieber et al. 1996; Toole et al. 2004; Toole et al. 2006). One product of DMS photolysis is DMSO (Hatton 2002; Lee et al. 1999), some of which may be returned to DMS via bacterial reduction pathways (Stefels et al. 2007).

The sea to air transfer of DMS depends primarily upon wind speed, the seawater DMS concentration and temperature (Elliott 2009; Liss and Slater 1974; Wanninkhof 1992). This flux can be parameterised as a function of transfer velocity (k) and the concentration gradient (gas partial pressure difference) (ΔC) of DMS between the atmosphere and the ocean (Liss and Slater 1974; Nightingale et al. 2000) (see equation 1.1). The function of the transfer velocity (k) is generally a power law dependence on wind speed adjusted for temperature although some of the most recent work using eddy covariance suggests this relationship could be linear (Fairall et al. 2011; Huebert et al. 2010). The concentration gradient (ΔC) = $C_{Water} - C_{Atmos}.H^{-1}$, where C_{Water} is the concentration of DMS in seawater, C_{Atmos} is the atmospheric DMS concentration and H is Henry's constant (Dacey et al. 1984; De Bruyn 1995). As C_{Water} is supersaturated with respect to C_{Atmos} so C_{Atmos} assumed to be zero. It is therefore usually assumed that $\Delta C = C_{Water}$ (equation 1.2) (Nightingale et al. 2000).

$$\mathrm{FLUX_{DMS}} = k\Delta\mathrm{C} \qquad (1.1)$$

$$\mathrm{FLUX_{DMS}} = k\Delta\mathrm{C_{Water}} \qquad (1.2)$$

Commonly used parameterisations (e.g. Nightingale et al. 2000; Liss and Merlivat 1986; Wanninkhof and McGillis 1999; Wanninkhof 1992) yield fluxes with a factor of two difference with the parameterisation of Nightingale et al. (2000) an often used intermediate (Stefels et al. 2007) (see Figure 1.5). Recently developed micrometeorological techniques (e.g. Huebert et al. (2004); Zemmelink et al. (2004)) record DMS fluxes that fall within this envelope indicating a relatively well constrained range (Elliott 2009). Sources of uncertainty also include the presence of surfactants (Nightingale et al. 2000), surface roughness, breaking waves, bubble generation (Zappa et al. 2001) and rain effects (Ho et al. 1997). There are greater uncertainties at very low and high wind speeds (Elliott 2009; Ho et al. 2006).

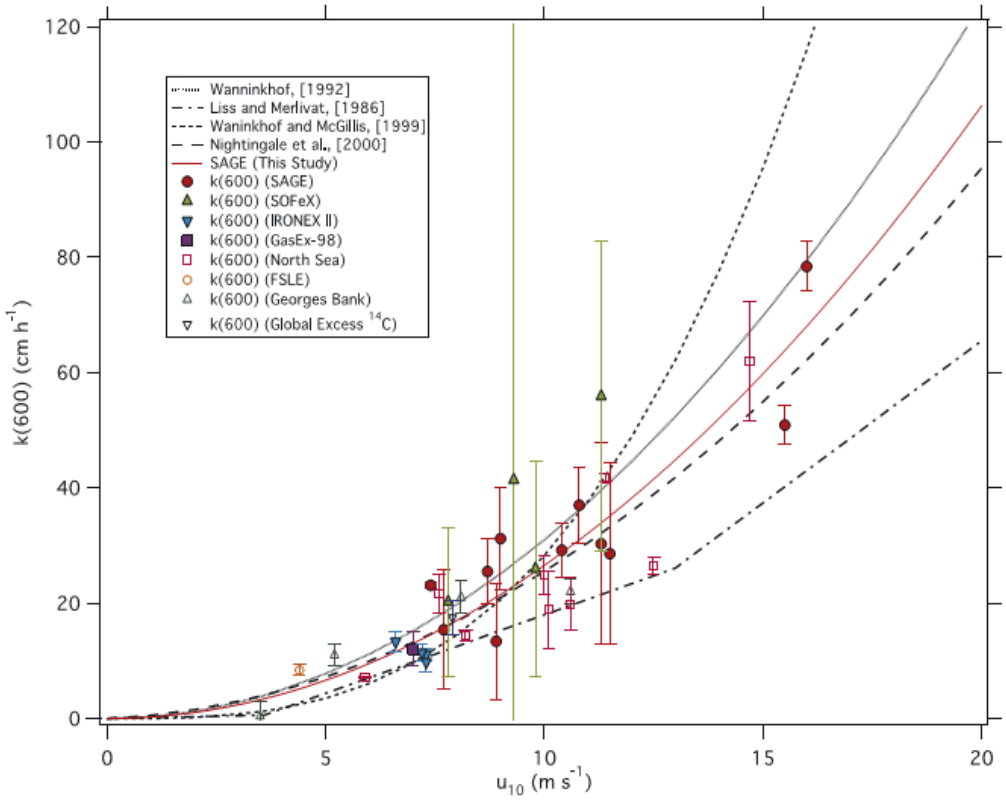

Figure 1.5: *Commonly used short-term wind speed/gas exchange parameterisations. Wanninkhof (1992) and Liss and Merlivat (1986) offer the upper and lower bounds of the approximate factor of two difference with Nightingale et al. (2000) an often used intermediate. Figure reproduced from Ho et al. (2006).*

Figure 1.6 shows the average wind speed for different regions of the ocean. Wind speeds are generally highest at mid to high latitudes between 40^{o}-60^{o} (~8-10 ms^{-1}) and lower within equatorial regions (5-7 ms^{-1}). For a given DMS concentration the flux of DMS will be highest where wind speeds high. However, areas of maximum flux do not generally coincide with regions with the highest wind speed as seawater DMS concentration is also critical in determining the magnitude of the flux (see Lana et al. 2010)

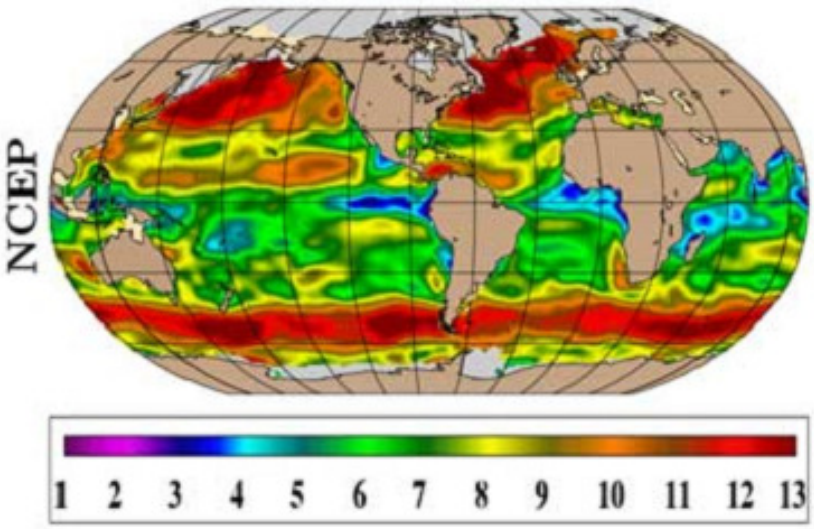

Figure 1.6: *Mean wind speeds (m s^{-1}) at 10 m from National Centres for Environmental Prediction (NCEP) for February 2001. Figure reproduced from Wallcraft et al. (2009).*

The dominant sink for DMS depends on the depth interval considered (Kieber et al. 1996) and the prevailing environmental conditions (Simó and Pedrós-Alió 1999b). Kieber et al. (1996) analysed a series of sampling stations along a transect from the equatorial Pacific. The authors access the relative contribution of biological, photochemical and sea-air flux DMS sinks over three depth intervals, the surface (0-1m), the near surface (0-20m) and the mixed layer (0-60m). Kieber et al. (1996) found that sea-air flux was the largest sink at depths between 0-1m with sea-air flux turnover rates observed between 0.90 – 11.70 d^{-1} relative to biological turnover rates of 0.04 – 0.66 d^{-1} and photolysis turnover rates of 0.16 – 0.47 d^{-1}). For the 0-20m depth interval photolysis and bacterial degradation became more important, with sea-

air flux turnover rates between 0.05 – 0.58 d^{-1}, the biological turnover rate between 0.04 – 0.66 d^{-1} and photolysis turnover rates varied from 0.11 - 0.30 d^{-1}. For the mixed layer depth interval (0-60m), bacterial removal of DMS was the dominant process with biological DMS turnover rates 3 – 11 greater than photolysis rates or sea-air flux rates.

Other studies have also shown that local environmental and meteorological conditions also affect the relative dominance of DMS loss processes. Simó and Pedrós-Alió (1999b) found at a site in the sub-polar North Atlantic that DMS losses due to photolysis dominated in the shallow mixed layer under clear skies (1-10 nmol d^{-1}), the bacterial sink dominated for deeper mixed layers, and cloudy conditions (0-6 nmol d^{-1}), and that the sea-air flux increased to equal bacterial loss rates under high winds (0.03 – 3 nmol d^{-1}).

1.3.5 Controls on seawater DMS concentrations

DMS is an ecosystem product, the sum of sources and sinks to the surface ocean. The surface ocean is a highly dynamic and complex environment. The biotic and abiotic interactions within the surface ocean ecosystem that modulate the various production and loss pathways that ultimately dictate ambient DMS concentrations are equally complex and dynamic. As reviewed in the previous sections, many different abiotic and biotic processes operating at different spatial and temporal scales have been suggested as controls on the various sources and sinks for DMS. The environmental history (on timescales of minutes-hours-days) influenced by such factors as mixing rate and depth, cloud cover, wind speed or predator-prey cycles is important in determining DMS concentrations at a point in space and time (Simó and Pedrós-Alió 1999a; Stefels et al. 2007).

The controls on ambient seawater DMS concentrations have proven difficult to establish, especially at the regional to global scale. It has proven difficult to obtain a strong link between a biological metric such as chlorophyll and DMS (Kettle et al. 1999; Lana et al. 2011a; Leck et al. 1990) although some local studies, especially during blooms dominated by single species from mid to high latitudes have observed stronger correlations (Gibson et al. 1990; Malin et al. 1993; Vallina et al. 2006).

Algorithms which incorporate chlorophyll along with other variables have met with some success (e.g. Anderson et al. 2001; Aumont et al. 2002; Belviso et al. 2004). Aumont et al. (2002) and Belviso et al. (2004) developed algorithms based upon plankton community composition indexes calculated from accessory pigment concentrations (Aumont et al. 2002; Belviso et al. 2004). Anderson et al (2001) parameterise global surface DMS concentrations utilising Chl *a* concentration (C), a mean daily shortwave radiation climatology (J) and a nutrient limitation term based on a climatological nitrogen (Q) to produce a dual equation based on a $\log_{10}(CJQ)$ index. See equations 1.3 and 1.4 where parameter *a* is the baseline DMS value (a = 2.86), parameter *b* is a fitted constant (7.98) and parameter *s* is the breakpoint in the broken stick regression (s = 1.72).

$$\mathrm{DMS} = \mathrm{a} \qquad log(CJQ) < \mathrm{s} \qquad (1.3)$$

$$\mathrm{DMS} = \mathrm{b}(\log(\mathrm{CJQ}) - \mathrm{s}) + \mathrm{a} \qquad log(CJQ) > \mathrm{s} \qquad (1.4)$$

Observations from oligotrophic regions have demonstrated that chlorophyll (algal biomass) can be out of phase with DMS over a seasonal cycle (Belviso et al. 2011; Toole et al. 2003; Vallina et al. 2008). This was first observed at the Bermuda Atlantic Time Series (BATS) site (Dacey et al. 1998) and has become known as the summer paradox (Toole et al. 2003). In these regions DMS is in phase with solar irradiance (Belviso et al. 2011; Toole et al. 2003; Toole and Siegel 2004; Toole et al. 2006). Strong correlations have been reported between the depth of the mixed layer (Simó and Pedrós-Alió 1999a; Simó and Dachs 2002) and the mixed layer averaged irradiance (solar radiation dose: SRD) (Vallina and Simó 2007). Simó and Dachs (2002) build on observations made by Simó and Pedrós-Alió (1999a) to derive a global parameterisation based upon climatological MLD and Chl *a.* (equation 1.5) and data with a Chl/MLD ratio >0.02 a linear regression of DMS against Chl/MLD (see equation 1.6).

$$DMS = 55.8(Chl/MLD) + 0.6 \qquad Chl/MLD < 0.02 \qquad (1.5)$$

$$\mathrm{DMS} = -\ln(\mathrm{MLD}) + 5.7 \qquad Chl/MLD > 0.02 \qquad (1.6)$$

Vallina and Simó (2007) have demonstrated a strong positive relationship between sea surface DMS concentration and the solar radiation dose (SRD) received into the upper mixed layer of the ocean (see equation 1.7).

$$\mathrm{SRD} = \frac{\mathrm{I_0}}{\mathrm{k_d MLD}}\left(1 - \mathrm{e}^{-\mathrm{k_d MLD}}\right) \qquad (1.7)$$

This relationship between SRD and DMS is identified at two fixed locations and at the global level derived using monthly averaged data. This link to irradiance is a step closer to closing a feedback loop proposed by the CLAW hypothesis (Quinn and Bates 2011; Vallina and Simó 2007). A detailed discussion of the theory behind the positive relationship between DMS and irradiance and the SRD-DMS relationship is provided in chapter 2: sections 2.2 and 2.5.

Different parameterisations using different combinations of variables have been met with variable success in different oceanic regions (Bell et al. 2006; Belviso et al. 2004; Hind et al. 2011). Toole and Siegel (2004) suggested that two regimes may be in operation, the first a stress forced regime dominated by irradiance, the second a production mediated regime dominated by algal biomass or production.

What is certain is that DMS is not simply coupled to algal biomass or the production of its biological precursor. It is the balance of sources and sinks of DMS to the surface oceans that dictates the ambient DMS concentrations available for flux to the atmosphere. This balance at a given space and time involves phytoplankton physiology and speciation, the bacterial community, photochemistry and the prevailing meteorological and environmental conditions.

1.4 Thesis objectives and overview

The primary objective of this thesis is to investigate the controls upon seawater DMS concentrations at regional to global scales. The potential role of irradiance is of particular interest because of the relevance to the CLAW hypothesis. This work aims to investigate links between a biological indicator and regional-to global-scale DMS dynamics. A final aim is to identify a set of globally available predictor variables

that can be used to develop a simple parameterisation that can be applied within models or to produce continuous global fields of surface DMS concentrations towards better flux estimates.

To achieve these aims, an analysis of data from a range of spatial and temporal resolutions was undertaken. Chapter 2 details the investigation of the proposed strong positive relationship between the solar radiation dose and surface DMS concentrations that has been reported using monthly averaged, climatological data (Vallina and Simó 2007) using high resolution concurrently sampled *in situ* data from the Atlantic Meridional Transect Programme.

Chapter 3 reports upon the investigation of the roles of primary production and underwater irradiance in determining DMSP and DMS concentrations both at the surface and from all depths of the euphotic zone. The data set compiled for this chapter consists of concurrent, *in situ* data from (i) the Atlantic Meridional Transect program (AMT), (ii) the Barents Sea, (iii) the Atmospheric Chemistry Studies in the Oceanic Environment (ACSOE) research campaign and (iv), the DImethyl Sulphide biogeochemistry within a COccolithophore bloom (DISCO) study. This dataset represents a range of latitudes and biogeochemical and trophic conditions.

Chapter 4 details the investigation of the controls upon surface DMS concentrations at the global scale. In conjunction with the global DMS database (http://saga.pmel.noaa.gov/dms/) this chapter details an investigation into whether the combination of climatological, satellite derived primary production and climatological underwater irradiance can be used to explain and predict global DMS concentrations.

The concluding chapter summarises and synthesises the results, and offers recommendations for future work.

Chapter 2: Testing the relationship between the solar radiation dose and surface DMS concentrations using *in situ* data

This chapter was published in Biogeosciences and is presented in scientific paper format. Co-authors are Tom Bell and Tim Lenton who provided supervision and advice on this work. Minor changes were made following the *viva voce.*

Miles CJ, Bell TG, Lenton TM (2009) Testing the relationship between the solar radiation dose and surface DMS concentrations using in situ data. Biogeosciences 6 (9):1927-1934. doi:10.1029/1999JC000111

2.1 Abstract

The proposed strong positive relationship between dimethylsulphide (DMS) concentration and the solar radiation dose (SRD) received into the surface ocean is tested using data from the Atlantic Meridional Transect (AMT) programme. *In situ*, daily data sampled concurrently with DMS concentrations is used for the component variables of the SRD (mixed layer depth (MLD), surface insolation (I_0) and a light attenuation coefficient (K_d)) to calculate SRD_{insitu}. This is the first time *in situ* data for all of the components, including K_d, has been used to test the SRD-DMS relationship over large spatial scales. We find a significant correlation (ρ = 0.55 n=65 p<0.01) but the slope of this relationship (0.006 nM/W m^{-2}) is less than previously found at the global (0.019 nM/W m^{-2}) and regional scales (Blanes Bay, Mediterranean, 0.028 nM/W m^{-2}; Sargasso Sea 0.017 nM/W m^{-2}). The correlation is improved (ρ = 0.74 n=65 p<0.01) by replacing the *in situ* data with an estimated I_0 (which assumes a constant 50% removal of the top of atmosphere value; I_0est), a MLD climatology and a fixed value for K_d following previous work. Equally strong, but non-linear relationships are also found between DMS and both *in situ* MLD (ρ = 0.61 n=65 p<0.01) and the estimated I_0 (ρ = 0.73 n=65 p<0.01) alone. Using a satellite-retrieved, cloud-adjusted surface UVA irradiance to calculate a UV radiation dose (UVRD) with a climatological MLD also provides an equivalent correlation (ρ = 0.67 n=54 p<0.01) to DMS. With this data, MLD appears the dominant control upon DMS concentrations and remains a useful shorthand to prediction without fully resolving the biological processes involved. However, the implied relationship between the incident solar/ultraviolet radiation (modulated by MLD), and sea surface DMS concentrations, is critical for closing a climate feedback loop.

2.2 Introduction

Dimethylsulphide (DMS) is a climatically important biogenic sulphur compound present in surface ocean waters at sufficient concentrations to sustain a significant flux to the remote marine atmosphere (Bates et al. 1992). There, sulphate aerosols derived from the oxidation of DMS are a major source of cloud condensation nuclei (CCN), promoting cloud formation and increasing cloud albedo (Andreae and Crutzen 1997; Ayers et al. 1991; Ayers and Gillett 2000; Berresheim et al. 1993; Sciare et al. 2001). The resulting impact at the surface is expected to be a reduction in solar insolation and therefore a net cooling. The CLAW hypothesis proposes a feedback loop whereby phytoplankton producing DMS alter their environment by modulating incoming solar radiation, engendering a change in surface ocean conditions whilst simultaneously increasing cloud albedo, with global climatic consequences (Charlson et al. 1987). A prerequisite for the closure of any feedback loop is that environmental variables affected by cloud albedo (e.g. insolation, temperature) can in turn influence seawater DMS concentrations. However, the controls on seawater DMS concentrations (hereafter [DMS]) and its associated biological processes are complex and are yet to be fully resolved (Simó 2001).

Various biogeochemical and physical parameters have been proposed as controls on seawater [DMS] and attempts have been made to incorporate some of the most rigorous into explanatory/predictive algorithms. These include an algorithm using chlorophyll concentration, light and a nutrient term based upon Michaelis-Menten kinetics (Anderson et al. 2001) and algorithms based upon plankton community composition indexes calculated from accessory pigment concentrations (Aumont et al. 2002; Belviso et al. 2004). A proposed relationship between mixed layer depth (MLD) and [DMS] (Simó and Pedrós-Alió 1999a) was adapted and extrapolated to produce global DMS fields derived from MLD and chlorophyll *a* concentration (Simó and Dachs 2002). Aranami and Tsunogai (2004) investigated the MLD-based relationship using regional data and suggested that much of the variance in DMS concentrations could be explained by a simpler relationship with MLD alone based on a dilution effect. Belviso et al. (2004) compared the five aforementioned algorithms utilising a global database of surface seawater [DMS] (http://saga.pmel.noaa.gov/dms/) and found that different algorithms are more skilful

predictors of DMS concentrations in different regions. Bell et al. (2006) analysed data collected as part of the Atlantic Meridional Transect (AMT) programme to test these predictive algorithms and found that a refined version of the Aranami and Tsunogai (2004) algorithm ([DMS] = 40/MLD) was the best fit for the data. The same dataset was used in this work.

Vallina and Simó (2007) have demonstrated a strong positive relationship between sea surface [DMS] and the solar radiation dose (SRD) received into the upper mixed layer of the ocean. This relationship between SRD and DMS is identified at two fixed locations and at the global level utilising monthly averaged data. A further strong positive relationship has been reported between the SRD, atmospheric DMS oxidation and satellite derived CCN over large areas of the global ocean (Vallina et al. 2007). The global SRD methodology combines a climatological mixed layer depth (MLD), the estimated solar radiation incident at the surface (I_0est) derived from a top of atmosphere value (0.5xTOA) and the attenuation of total solar radiation within the water column (K_d, units m^{-1}) represented by a constant fixed value (0.06 m^{-1}). The SRD is essentially a measure of the average light level experienced by the cells confined within the mixed layer in Wm^{-2}. This positive relationship potentially closes a feedback loop between incident solar radiation and marine emissions of DMS, sulphate aerosols, CCN, cloud albedo and climate as postulated by the CLAW hypothesis.

Central to the relationship between the SRD and seawater [DMS] is the proposed interaction between incident surface radiation and MLD. The depth of the mixed layer is expected to have a substantial influence on [DMS] (Simó and Pedrós-Alió 1999a). Stratified waters, although sustaining a lower overall phytoplankton biomass, are characterised by a species assemblage composed of more prolific dimethylsulphoniopropionate (DMSP) producers (Simó and Pedrós-Alió 1999a). DMSP is the dominant biological precursor to DMS as DMSP cleavage by lyase enzymes is a significant DMS production pathway (Steinke et al. 1998; Steinke et al. 2002). In addition, a shallow mixed layer results in elevated exposure to UV irradiance, which inhibits heterotrophic bacterioplankton production as a result of DNA damage caused by UV-B radiation (Slezak et al. 2001; Toole et al. 2006). Reduced bacterioplankton production leads to reduced DMS consumption rates

(Toole et al. 2006). The combination of these factors has been shown to increase [DMS] when surface waters are highly stratified (Simó and Pedrós-Alió 1999a).

Laboratory studies of the diatom *Thalassiosira pseudonana* and the prymnesiophyte *Emiliania huxleyi* have shown that elevated DMS production occurs in response to high UV irradiance with the largest effect under exposure to UV-A wavelengths (320–400 nm) (Sunda et al. 2002). Oxidative stressors (including UV) generate harmful free radicals in the cell, while DMSP, DMS and subsequent DMS oxidation products have been shown to readily scavenge hydroxyl radicals and other reactive oxygen species, relieving oxidative stress (Sunda et al. 2002).This suggests an antioxidant function for DMSP and its breakdown products (including DMS), linking it with UV-induced oxidative stress in marine phytoplankton (Sunda et al. 2002). DMS can also be removed from the water column by photo-oxidation to dimethyl sulfoxide (DMSO) and other breakdown products following exposure to UV-B radiation (Brimblecombe and Shooter 1986), whilst (Kniveton et al. 2003) have demonstrated that extreme changes in UV can cause a reduction in atmospheric DMS on a daily timescale, most likely attributable to photodestruction in the atmosphere. Thus the same shallow MLD and high insolation levels and durations associated with peak summer [DMS] are seemingly ideal for high photochemical loss rates. The photo-oxidation of DMS does not typically dominate as a loss term because it is dependent upon the presence of chromophoric dissolved organic matter (CDOM) which is at lowest concentrations in the summer (Siegel and Michaels 1996). Summer is when the MLD is shallowest and UV irradiance levels are highest and these factors combined (SRD) may help explain the DMS “summer paradox” whereby peak [DMS] occur in the summer despite phytoplankton production, biomass and chlorophyll levels reaching maxima earlier in the year (Toole et al. 2003).

Considering the current state of knowledge, we decided to test the reported relationship between SRD and seawater [DMS] (Vallina and Simó 2007). Belviso and Caniaux (2009) also tested the strength of the SRD-DMS relationship in the North-East Atlantic (using data from the Programme Ocean Multidisciplinaire Meso-Echelle (POMME) experiment). From their data, they conclude that SRD and DMS do not demonstrate a strong correlation (with SRD accounting for only 19% - 24% of

the variance associated with monthly averaged surface DMS concentrations). However, their [DMS] data is not normally distributed and the result from their Spearman's Rank correlation analysis may be more appropriate, suggesting a stronger correlation of $\rho = 0.74$. The authors then conducted a sensitivity analysis using different versions of the SRD equation and suggest that the DMS-SRD relationship is heavily influenced by the choice of fixed irradiance attenuation coefficient (K_d).

In contrast to the global SRD relationship of Vallina and Simó (2007) and the work of Belviso and Caniaux (2009), our study uses *in situ*, daily data from the AMT project sampled concurrently with DMS concentrations for all component variables of the SRD (MLD, I_0 and K_d) to calculate SRD_{insitu}. In particular, this is the first time an *in situ* and thus variable K_d has been used to test the SRD calculation over such a large spatial scale. The AMT [DMS] data is also compared to a SRD calculated using climatological/estimated inputs (SRD_{clim}) using the same methodology and data sources as the global study of Vallina and Simó (2007). The regional studies of Vallina and Simó (2007) and Belviso and Caniaux (2009) are from the coastal northwest Mediterranean (Blanes Bay 41°3N, 2°48E), Sargasso Sea (32°10N, 64°30W) and northeast Atlantic (16°W - 22°W, 38°N - 45°N) respectively. Analysing *in situ* data from different locations is vital to advance understanding of the reported global relationship that has been demonstrated with *in situ* data in these regions. The equatorial/oligotrophic regions covered by our analysis are especially critical as it is here that the decoupling of [DMS] from measures of biomass/chlorophyll (summer paradox) are observed.

Our results broadly support those presented previously (Belviso and Caniaux 2009; Vallina and Simó 2007), but also elaborate upon the importance of K_d and MLD in the SRD equation. We also attempt to directly address UV radiation, adapting the SRD methodology to calculate an ultraviolet radiation dose (UVRD). Sunda et al. (2002) observed that the largest increase in DMSP/cell volume and DMS/cell volume ratios (relative to cultures grown in light environments with no UV radiation) occurred at irradiances filtered for UVB (290-320nm) but included UVA (320-400nm). In addition, Toole et al. (2003) found that wavelength resolved surface photolysis rates from the Sargasso Sea are greatest under UVA wavelengths with

contributions to the total photolysis from UVA (320 - 400 nm) of 67.4 - 77.8% and UVB (280 - 320 nm) of 32.6 - 22.2%. We selected the most appropriate wavelength available within the UVA spectrum (380 nm). Finally, a comparison is made to the work of Bell et al. (2006) who previously found the best fit to the AMT DMS data to be a simple relationship with MLD alone (see equation 2.3 and Bell et al. (2006) for details).

2.3 Methods

The SRD combines the depth of the mixed layer (MLD), the incident solar radiation at the surface (I_0) and its attenuation within the water column (K_d) (Vallina and Simó 2007):

$$\mathrm{SRD} = \frac{I_0}{k_d \mathrm{MLD}} \left(1 - e^{-k_d \mathrm{MLD}}\right) \qquad (2.1)$$

Throughout their global study, Vallina and Simó (2007) use a fixed value of K_d representative of the attenuation of total solar radiation by clear ocean water (0.06 m^{-1}) and estimate I_0 on the assumption that a constant 50% of the solar radiation incident at the top of the atmosphere reaches the surface (0.5xTOA: I_0est). The estimated I_0 is a function of latitude, date and known astronomical constants (Brock 1981; Vallina and Simó 2007). This method of deriving surface irradiance does not account for variable cloud cover or geographical variation in the path length of the irradiance through the atmosphere. MLD is taken from a 2^o x 2^o resolution global climatology (de Boyer Montégut et al. 2004). The mixed layer is characterised by almost vertically uniform salinity, temperature, and density profiles. The MLD is defined as the point at which a departure from this uniform state can be detected based upon an arbitrary choice of criteria such as temperature, salinity or density (de Boyer Montégut et al. 2004). The criterion used to define the climatological MLD is a temperature change of 0.1^oC from a near surface value at 5 m (as used by Vallina and Simó 2007).

In this study we use *in situ* data for the components of the SRD equation (I_0, MLD, K_d) and surface [DMS] sampled concurrently during the AMT programme (24 hour

average values of shipboard surface irradiance (I_0) with MLD and K_d calculated from concurrent *in situ* data to DMS samples (see below)). The AMT program undertakes research cruises between the UK and the Falkland Islands transecting a range of ecosystems but focusing upon the oligotrophic mid-ocean gyres of the North and South Atlantic. This study uses data collected during northern hemisphere spring (cruises AMT-12 in May-June, 2003; and AMT-14 in April-June, 2004) and autumn (AMT-13 in Sept.-Oct., 2003) (Figure 2.1) (see Bell et al. 2006 for more details). To calculate SRD_{insitu} it is necessary to not only have a [DMS] measurement at a sampling point but also concurrent data for the components of the SRD (MLD, I_0 and K_d). Within the AMT dataset, this meant that only 65 DMS data points could be used with concurrent data. Although it would be possible to calculate SRD using climatological data (SRD_{clim}) for more of AMT data points, the analysis was restricted to the same dataset to enable a fair comparison. The same reasoning was applied to the UVRD analysis which used all available UV data in conjunction with the DMS data used for the SRD analysis.

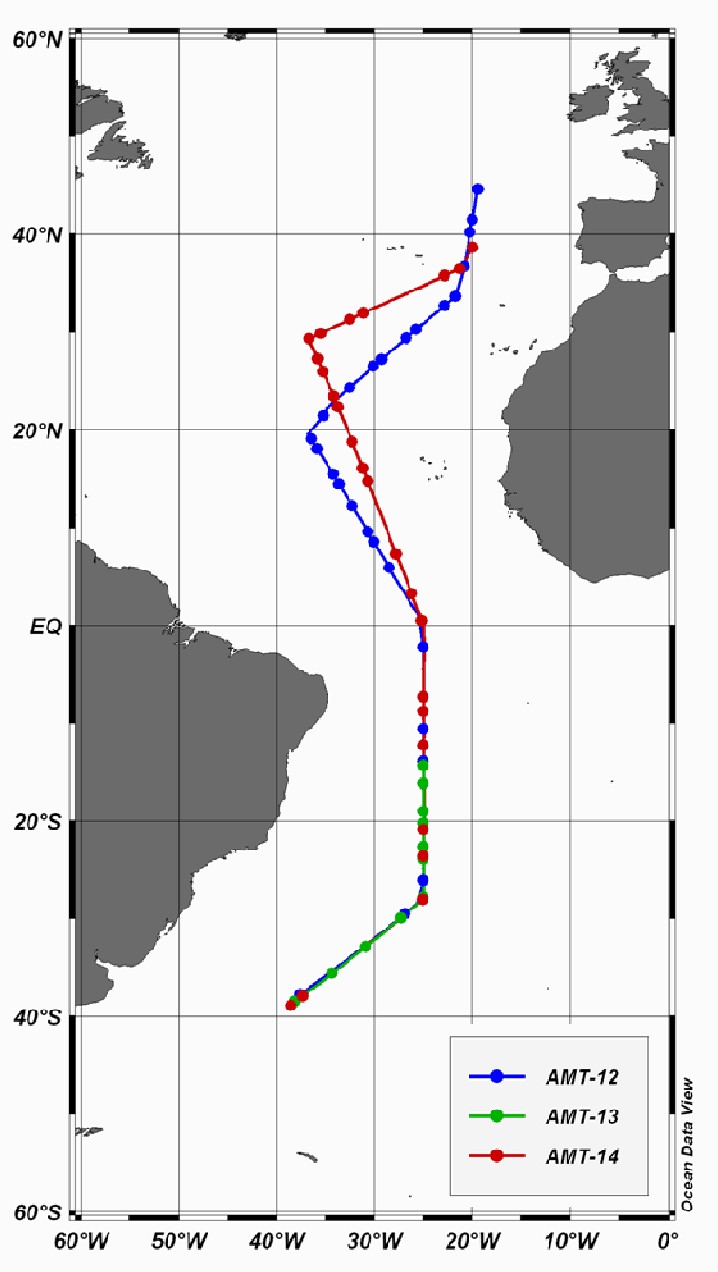

Figure 2.1: *Location of the Atlantic Meridional Transect (AMT) programme cruise tracks (lines) and sampling stations (markers) from which data was available to calculate the SRD (AMT-12, blue; AMT-13, green; AMT-14, red). Plot produced using Ocean Data View (http://odv.awi.de/en/home/).*

For incident solar radiation (I_0), a daily average (24 hours leading up to the point of sampling) of the continuous shipboard measurements of total solar radiation was used. Measurements in Wm^{-2} were made using Kipp & Zonen SP Lite 0339-900 TIR Pyranometers (range 300-3000 nm) that were positioned high up on the ship's

foremast approximately 22 m above sea level. The average of two sensors was used and the same instrumentation used on all cruises. An average value rather than a cumulative total was used to be comparable with the 24 hour average climatological/estimated I_0 value used by V&S07. Similarly, total solar radiation was used for comparability with V&S07 although it should be noted that it is wavelengths within the PAR and UV spectrum that are biologically most important within the water column. Indeed V&S07 state that total solar radiation is intended as a proxy for these biologically relevant wavelengths. The *in situ* MLD is defined using the same criteria as the V&S07 MLD climatology, a temperature departure of 0.1^{o}C from a reference depth of 5 m to avoid the effect of diurnal heating (Bell et al. 2006). The temperature profiles used to calculate the MLD were sampled concurrently with [DMS] along the cruise track at pre-dawn (0300hrs local time) each day. The attenuation coefficient (K_d) used for the SRD_{insitu} was calculated using the sampled 1% light level depth (Z_e) defined as the depth (m) to which 1% of the light incident at the surface penetrated on the previous day's mid-morning (1100hrs local time) cast ($K_{d\,TOT} = ln(0.01)/Z_e$).

We also calculated an ultraviolet radiation dose (UVRD, equation 2.2) based on the SRD equation (equation 2.1) but using a satellite surface UV product from NASA's Total Ozone Mapping Spectrometer (TOMS) in place of *in situ* total solar irradiance (I_o). This was in the form of the noon irradiance for the specific DMS sampling date at the surface of the ocean in mW m^{-2} nm^{-1} at 380 nm (UVA) and at a 1^{o} x 1^{o} degree grid box resolution. This product incorporates the column ozone amount and cloud conditions, taking into account sun-earth distance, solar zenith angle, total ozone amount, tropospheric aerosol optical depth and cloud transmission (Herman and Celarier 1997) and is available at (http://ozoneaq.gsfc.nasa.gov/TOMSUVExposure.md). This product does not account for daylength and as such it should be noted that the methodology differs from the SRD which uses a daily average value. A constant attenuation coefficient appropriate for the attenuation of UV under oligotrophic conditions ($K_{d\,UV} = 0.10$ m^{-1}) was applied (Tedetti and Sempere 2006) as no appropriate *in situ* measurements were available. Tedetti and Sempere (2006) provide a range of Z10% data (the penetration depth for 10% of surface irradiance) for UVA (integration from 315 – 400 nm) from the central subtropical Atlantic for a depth range of 14.5 to 32.5 m

(average depth 23.5 m). Rearranging the Tedetti and Sempere (2006) definition of Z10% (Z10% = 2.3/$K_{d\,UV}$) allows the derivation of K_d from the Z10% depth ($K_{d\,UV}$ = 2.3/Z10%). Utilising the average Z10% value from the central subtropical Atlantic (23.5 m) gives a $K_{d\,UV}$ value of 0.0978 which was rounded up to $K_{d\,UV}$ = 0.01 for use in this chapter.

$$\mathrm{UVRD} = \frac{\mathrm{UV_{380nm}}}{\mathrm{k_d MLD}}\left(1 - \mathrm{e}^{-\mathrm{k_d MLD}}\right) \qquad (2.2)$$

These results are also compared to a simpler relationship between a constant (c) (c = 40 μmol m^{-2}) over MLD and [DMS] (equation 2.3) previously found to be the best fit to this data by Bell et al. (2006) who refitted a simple dilution model proposed by Aranami and Tsunogai (2004) to the AMT data (See Bell et al. (2006) for further details).

$$\mathrm{DMS} = \frac{\mathrm{c}}{\mathrm{MLD}} \qquad (2.3)$$

The non-parametric Spearman's Rank hypothesis was used to evaluate the bivariate correlations to account for the non-normal distribution of the data. All statistical calculations were performed using SPSS™ software.

2.4 Results

2.4.1 SRD

When utilising the SRD methodology in conjunction with the *in situ* AMT data for all of the SRD variables ($K_{d\,TOT}$, I_0, MLD) (SRD_{insitu}) we find a strong and significant correlation (ρ = 0.55, n = 65, p < 0.01) between SRD and [DMS]. The slope of this relationship (0.006 nM/W m^{-2}) is less than that found by Vallina and Simó (2007) at the global (0.019 nM/W m^{-2}) and regional levels (Blanes Bay 0.028 nM/W m^{-2}; Sargasso Sea 0.017 nM/W m^{-2}). As these relationships use monthly averaged values, they are intended to be appropriate for the longer term climatological mean situation (Figure 2.2). Vallina and Simó (2007) demonstrate that the SRD is connected to the seasonal DMS cycle at the global level (10° x 20° grid boxes, ρ = 0.47, n = 545, p < 0.01) and at two fixed locations using monthly averaged data (Blanes Bay ρ = 0.75, n

= 15, $p < 0.01$; Sargasso Sea: $\rho = 0.89$, n = 33, $p < 0.01$). In contrast the AMT data exhibits significant spatial coverage but represents less seasonal variation, covering only a few months of the seasonal cycle (in northern hemisphere spring and autumn). As such, a complete comparison between the two data sets is not possible. However, it is interesting that a strong and significant correlation still exists between SRD and [DMS] when addressing variability on a shorter (daily) timescale in this *in situ* data series.

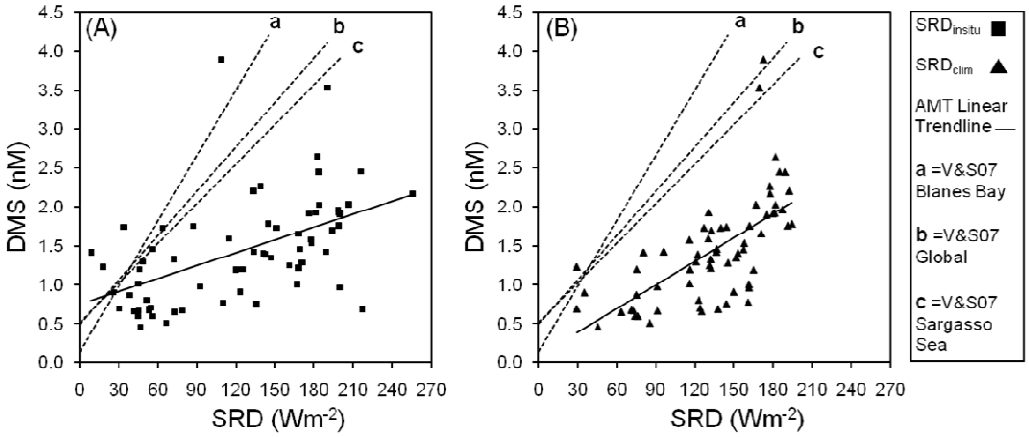

Figure 2.2: *[DMS] (nM) versus SRD (W m^{-2}) calculated using: (A) in situ data (SRD_{insitu}, squares); and (B) climatological data (SRD_{clim}, triangles), for MLD, k and I_0. On both plots, solid line is linear best fit regression of the data ((A) SRD_{insitu}: DMS = 0.755 + 0.006.SRD ($p < 0.01$); (B) SRD_{clim}: DM S= 0.084 + 0.010.SRD ($p < 0.01$)). Dashed lines a – c are the relationships between [DMS] and SRD reported by Vallina and Simó (2007) (a = V&S07 Blanes Bay, DMS = 0.138 + 0.028.SRD; b = V&S07 Global, DMS = 0.492+0.019.SRD; c =V&S07 Sargasso Sea, DMS = 0.51+0.017.SRD).*

The correlation fit to the AMT [DMS] is improved ($\rho = 0.74$, n = 65, $p < 0.01$) when the *in situ* data is replaced with climatological inputs to the SRD calculation (SRD_{clim}) following the methodology used in the global analysis of Vallina and Simó (2007). The slope of this relationship (0.010 nM/W m^{-2}) is also closer to the global relationship reported by Vallina and Simó (2007) (Figure 2.2). An initial motivation of this research was to attempt to improve upon the handling by Vallina and Simó

(2007) of these climatological variables, I_0est (0.5xTOA), MLD (climatology) and $K_{d\,TOT}$ (fixed). A comparison of the AMT *in situ* data with climatological data does yield statistically significant correlations. The climatological and *in situ* MLD compare reasonably well ($\rho = 0.55$, n = 65, $p < 0.01$) although the climatological MLD significantly underestimates the range of MLD and exhibits a shallow bias when compared with the observed, *in situ* MLD data from AMT (*in situ*: range 7 – 144 m, mean 38 m; climatology: range 6 m – 56 m, mean 20 m). The *in situ* and climatological I_0 values compare more favourably ($\rho = 0.78$, n = 65, $p < 0.01$). The climatological I_0 also underestimates the range of solar radiation incident at the surface when compared to the *in situ* data (*in situ*: range 78.2 – 323.4 Wm^{-2}, mean 226.1 Wm^{-2}; climatology: range = 98.9 - 241.9 Wm^{-2}, mean 210.1 Wm^{-2}). This underestimated range can be explained because the estimated I_0 uses a 0.5xTOA value that does not account for varying cloud cover or atmospheric path length. In this shorter, high resolution dataset, variable cloud cover is expected to play an important role especially given the AMT cruise track crossing the equator and the inter-tropical convergence zone (ITCZ). The fixed value of $K_{d\,TOT}$ (0.06 m^{-1}) utilised by Vallina and Simó (2007) falls within the range of *in situ* $K_{d\,TOT}$ values from the AMT dataset (0.03 – 0.11 m^{-1}, mean = 0.05 m^{-1}).

Similar strength correlations to that observed between [DMS] and SRD are also observed between [DMS] and MLD (*in situ* MLD: $\rho = 0.61$, n = 65, $p < 0.01$; climatological MLD: $\rho = 0.70$, n = 65, $p < 0.01$) and climatological I_0 ($\rho = 0.74$, n = 65, $p < 0.01$). To investigate the SRD further we examined the components of the equation to try and determine their respective influences upon the observed correlations between the SRD and [DMS] (Table 2.1).

Table 2.1: *Spearman's rank correlation coefficients (ρ) between [DMS] and the outcome of the 3 equations on test (SRD (Eq. (1)), UVRD (Eq. (2)), 40/MLD (Eq. (3)) with various combinations of the available climatological/in situ data as input variables (I_0/UV_{380nm}, MLD and $K_{d\ TOT}$ or $K_{d\ UV}$).* ***Bold*** *coefficients indicate that an appropriate fixed value for light attenuation (K_d) is used (0.06 m^{-1} for I_0, 0.10 m^{-1} for UVA) (see methods for further details). Plain text indicates that the in situ value for light attenuation (K_d) is used. The simpler DMS = 40/MLD coefficients (italics) does not utilise a light attenuation (K_d) value. All coefficients significant at p<0.01 unless marked with * (in which case, result is not significant at p<0.05). For correlations involving UVA n=54, otherwise n=65).*

	I_0 In situ	I_0 Climatology	I_0 Fixed	UVA (satellite)	40/MLD
MLD In situ	0.55 **0.62**	0.55 **0.61**	0.48 **0.61**	n/a **0.55**	0.61
MLD Climatology	0.53 **0.62**	0.58 **0.74**	0.42 **0.71**	n/a **0.67**	0.70
MLD Fixed	0.46 **0.47**	0.71 **0.73**	n/a n/a	n/a **0.26***	n/a

Replacing the *in situ*, variable light attenuation coefficient ($K_{d\ TOT}$) within the SRD equation with a fixed value (0.06 m^{-1}) uniformly increases the correlation with [DMS] (Table 2.1). This could partly explain the difference in the correlation to [DMS] between SRD_{insitu} and SRD_{clim}. The correlation to [DMS] is almost always increased when the *in situ* I_0 is replaced with the estimated I_0 (0.5xTOA). Fixing the MLD significantly decreases the correlation in conjunction with *in situ* I_0 but a fixed MLD in combination with an estimated I_0 returns a high correlation (Table 2.1). The SRD permutations offer some improvement upon the simpler relationships between [DMS] and MLD (40/ MLD) (MLD climatological: $\rho = 0.70$, n = 65, $p < 0.01$, MLD *in situ*: $\rho = 0.61$, n = 65, $p < 0.01$). Using an I_0 derived from a TOA value that does

not account for cloud (ρ = 0.73, n = 65, p < 0.01) also performs as well as using the optimum SRD formulation (SRD_{clim}).

2.4.2 UVRD

Results from the literature (Toole and Siegel 2004; Toole et al. 2006; Sunda et al. 2002) led us to investigate the SRD equation from the perspective of surface UV irradiance (UVRD, equation 2.2) utilising a cloud-adjusted satellite-retrieved surface UVA irradiance (no direct measurements of UV were available from the AMT) within the SRD methodology (see section 2.3 for details). A fixed value for $K_{d\,UV}$ was adopted as no direct measurements were available from the AMT with an appropriate value for these oligotrophic conditions ($K_{d\,UV}$ = 0.10 m^{-1}) selected from the literature (Tedetti and Sempere 2006). Significant correlations were observed when using UVA (380 nm) in this study and this is consistent with previous work. Toole and Siegel (2004) attribute observed patterns of DMS cycling in the oligotrophic Sargasso Sea to a stress forced mechanism associated with UVA irradiance, while Sunda et al. (2002) noted elevated [DMS] with exposure to UVA wavelengths under laboratory conditions.

The UVRD calculated using a climatological MLD is well correlated to [DMS] from AMT (ρ = 0.67, n = 54, p < 0.01) (Figure 2.3) and is a better fit to the [DMS] data than the SRD_{insitu} with either variable, *in situ* $K_{d\,TOT}$ values (ρ = 0.56, n = 66, p < 0.01) or fixed $K_{d\,TOT}$ values (ρ = 0.63, n = 66, p < 0.01). However, the UVRD does not improve upon the correlation between [DMS] and the SRD_{clim} (ρ = 0.74, n = 66, p < 0.01) although it does use a more appropriate surface irradiance (i.e. cloud adjusted) component. Once again the correlation between UVRD and [DMS] is very similar to the strength of the correlations found between the simpler relationships with [DMS] and MLD alone (40/MLD) or the estimated I_0 derived from the TOA value (0.5xTOA).

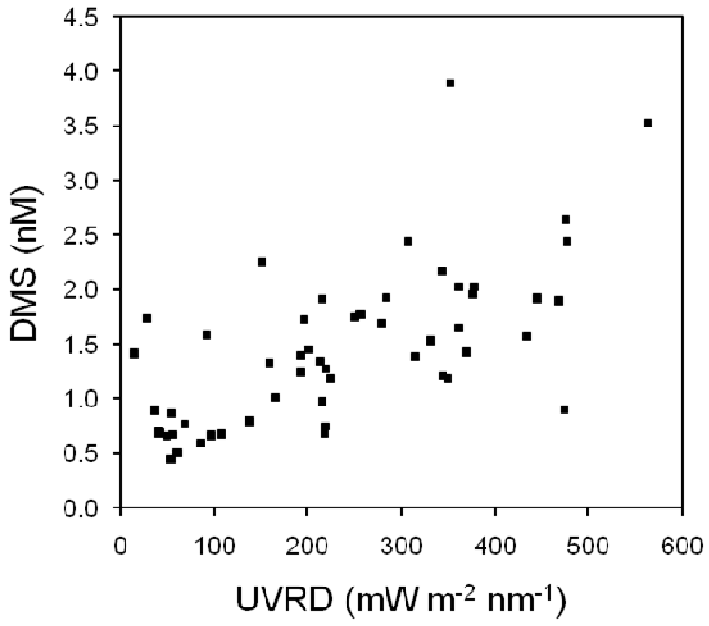

Figure 2.3: *[DMS] (nM) versus UV radiation dose (UVRD, mW m^{-2} nm^{-1}) calculated using a climatological MLD, a constant $K_{d\,UV}$ (0.10 m^{-1}) and satellite-derived UVA (380nm) at the surface (ρ = 0.67. n = 54, $p < 0.01$) (see section 2.3 for further details).*

2.5 Discussion

The SRD calculated using *in situ* components from the AMT (SRD_{insitu}) produces a statistically significant correlation to the concurrently sampled, high resolution [DMS] data. This application is beyond the remit originally proposed. The strength of this correlation is reduced relative to the global and fixed location studies of Vallina and Simó (2007) and the slope of the relationship between SRD and DMS is less. Notably, the correlation fit is improved when *in situ* data is replaced with climatological values as inputs to the SRD (SRD_{clim}), the same approach used to derive the global SRD relationship of Vallina and Simó (2007). This also brings the slope into better agreement with the slopes identified by Vallina and Simó (2007), although variability in slope can be expected given the varying temporal and spatial nature of the cruise track sampling points and the resolution and time period of the data. These results are in agreement with the strength of Spearman's Rank correlation (ρ = 0.74, n = 232, $p < 0.01$) reported between the SRD and [DMS] from the North East Atlantic over a seasonal cycle by Belviso and Caniaux (2009).

A change from a variable, *in situ* light attenuation coefficient ($K_{d\ TOT}$) to a fixed value significantly increased the strength of correlation with [DMS] across the range of SRD equation permutations. Fixing $K_{d\ TOT}$ effectively removes it from the equation in terms of a correlation fit to the data. As Belviso and Caniaux (2009) demonstrate, the value of $K_{d\ TOT}$ can have a substantial impact on the value of SRD. Our data suggests that allowing $K_{d\ TOT}$ to vary significantly reduces the strength of correlation between SRD and [DMS] and implies that the inclusion of a variable $K_{d\ TOT}$ within the SRD equation reduces its effectiveness at predicting surface [DMS]. This was the likely cause of much of the difference between SRD_{insitu} and SRD_{clim} and their strength of correlation with [DMS]. The switch from an *in situ* I_0 to an I_0 derived from a top of the atmosphere value (I_0est) appears to account for the remainder of the difference in the strength of correlation of [DMS] with SRD_{insitu} and SRD_{clim}. Similar strength correlations with [DMS] were also found for climatological I_0 and climatological MLD (40/MLD).

It is important to remember that MLD and I_0 are not completely independent variables and that the two are likely to be coupled over the seasonal cycle with high insolation levels in the summer coinciding with shallow mixed layers (de Boyer Montégut et al. 2004). The advantage of the SRD methodology is that it combines these two interrelated variables, incorporating a physical mechanism to explain why the seasonal coherence of shallow MLD and high insolation combine to produce high DMS concentrations. The problem is that it becomes difficult to isolate the causal effect of insolation beyond a relationship with MLD driven by seasonality in I_0 (i.e. the effect of variable I_0 or SRD given a constant MLD). This is especially apparent when using a non-cloud adjusted, estimated I_0 in place of *in situ* I_0 data. In addition, factors such as CDOM concentration or phytoplankton biomass which determine the attenuation of irradiance are not independent of MLD or I_0.

The main difference between the two measures of surface irradiance is that the *in situ* I_0 represents the variability introduced by cloud cover and geographical differences in the path length of the radiation through the atmosphere whereas the TOA derived, estimated I_0 does not (beyond the assumption that 50% of TOA irradiance is removed). The *in situ,* daily average I_0 values must represent more

faithfully the surface irradiance that is concurrent with the daily sampled [DMS] but the TOA derived I_0est is more successful at providing a correlation fit both in combination with the SRD method and when used in isolation. The estimated, TOA-derived I_0est may be representing the longer-term mean state of the system rather than the snapshot of variability provided by the *in situ* AMT cruise transect data. Within this high resolution *in situ* dataset MLD and I_0 are less likely to be directly coupled and this could explain why the climatological data is more successful at resolving the observed DMS concentrations. The estimated I_0 could also represent seasonality in an unknown variable or combination of variables that combine with shallow summer MLD to produce high [DMS]. Finally, it could represent a smoothed (inverse) version of MLD itself with [DMS] modulated by a dilution effect independent of high resolution changes in insolation. In conjunction with smoothed monthly data the inclusion of an estimated I_0 within the SRD equation may act as a proxy for the seasonality inherent within the DMS cycle, combining latitude and date (seasonality) within one variable. The estimated I_0 could then represent the background potential for exposure to incident surface radiation whilst variations in MLD control the dose.

A motivation of this work was to attempt to improve upon the handling of the climatological and estimated SRD parameters. A dominant role for MLD within the SRD could explain why using *in situ* values for I_0 and $K_{d\,TOT}$ did not yield any improvement in the skill of the SRD equation when applied to this daily data. The combination of a less variable, TOA-derived I_0 and fixed $K_{d\,TOT}$ would also increase the methodological importance of MLD within the SRD calculation. It should be remembered that although MLD seems to be a key variable within the SRD equation (at least in terms of the AMT data) explicit within the SRD reasoning is the implication that shallow MLD allow insolation to influence the dynamics of the DMS(P) food web (Simó and Pedrós-Alió 1999a). This is hinted at in the relationship between [DMS] and UV found in this study.

Prior to the Great Oxidation 2.4 billion years ago, life on Earth evolved without the protection of a stratospheric ozone layer and under much higher UV levels than today (Garcia-Pichel 1998). This evolutionary history may still be reflected in efficient strategies and physiological mechanisms in modern organisms and

ecosystems to prevent UV-induced damage and reduce photo-oxidative stress (Hader et al. 2003). This may be relevant in the context of DMSP and DMS production by marine phytoplankton (Sunda et al. 2002). Addressing UVA directly via the substitution of a cloud adjusted satellite retrieval of surface UVA irradiance (UVRD) did not significantly improve or worsen the correlation to [DMS] relative to the SRD_{clim} , estimated I_0 or 40/MLD relationship. The UVRD equation did improve upon the correlation between [DMS] and SRD_{insitu} but most importantly yields a strong significant correlation in conjunction with a cloud adjusted measure of surface irradiance in a wavelength previously linked to DMS dynamics. This supports the results of Toole and Siegel (2004), who identified a significant correlation between [DMS] and *in situ* UVA (325 nm) within the mixed layer at a fixed location (Hydrostation S) in the Sargasso Sea over the seasonal cycle. It is important to note that as with SRD the strength of correlation between [DMS] and UVRD was likely to be influenced by fixing the value of $K_{d\,UV}$. In the future, utilising direct *in situ* measurements of UVA and UVB coupled with their attenuation within the water column should improve our understanding of UVRD and DMS dynamics.

Within the AMT data, there is little difference between the most highly correlated variation of the SRD equation (SRD_{clim}), the UVRD and the simpler relationships based on *in situ* MLD (40/MLD) or estimated I_0 alone. The notion that MLD could be important in modulating DMS concentrations was introduced by Simó and Pedrós-Alió (1999a) who commented that it was useful shorthand to prediction until the mechanisms controlling DMS concentrations could be resolved. It is questionable from this AMT data whether the inclusion of the variables I_0/UV and K_d via the SRD methodology improves the correlation enough to illuminate causation over this resolution. Recent work by Derevianko et al. (2009) uses the recently-updated global database of surface seawater [DMS] (http://saga.pmel.noaa.gov/dms/) to examine the SRD relationship and comes to similar conclusions.

2.6 Conclusions

A challenge of Earth system science is to decouple the complex inter-relationships and feedbacks between the biosphere and climate. Vallina and Simó (2007) have

demonstrated that a positive relationship may exist between the SRD and surface [DMS] over the seasonal DMS cycle using monthly averaged data. This is a necessary condition for the operation of a negative feedback (Charlson et al. 1987). The SRD methodology asserts that the interrelated seasonal cycles of MLD and surface insolation combine to produce high [DMS] when MLD are shallowest and summer insolation strongest. The SRD method is successful at combining these two relationships into one and provides a plausible bio-physical explanation for the strong correlations observed over the seasonal DMS cycle. The SRD methodology is troubled by the use of an estimated I_0 that does not realistically account for cloud cover or atmospheric path length, especially at this temporal resolution. This has implications for the CLAW hypothesis and the closure of any feedback loop which depends of the modulation of insolation by varying cloud albedo. The UVRD proposed here goes some way to addressing this issue producing a good correlation whilst utilising a cloud adjusted, surface irradiance product at a wavelength (UVA) with an implicated role in DMS(P) dynamics. Whether the SRD (or UVRD) illuminates causation beyond a simpler relationship with MLD or TOA-derived I_0 (i.e. a variable representing seasonality) at this resolution is questionable, at least within this AMT data. The MLD remains a useful shorthand to prediction without fully resolving the biological processes involved. However, it makes it harder to close the CLAW feedback loop. The suggested relationship between incident solar/ultraviolet radiation and sea surface DMS concentrations (modulated by MLD) makes it easier to close that feedback loop.

Chapter 3: Investigating the inter-relationships between water attenuated irradiance, primary production and DMS(P)

This chapter was published in Biogeochemistry and is presented in scientific paper format. Co-authors are Tom Bell and Parv Suntharalingam who provided supervision and advice on this work. Minor changes were made following the *viva voce.*

Miles CJ, Bell TG, Suntharalingam P (2012) Investigating the inter-relationships between water attenuated irradiance, primary production and DMS(P). Biogeochemistry (2012) 110:201–213 DOI 10.1007/s10533-011-9697-5

3.1 Abstract

Both solar irradiance and primary production have been proposed as independent controls on seawater dimethyl sulphide (DMS) and dimethylsulphoniopropionate (DMSP) concentrations. However, irradiance also drives photosynthesis, and thus influences a complex set of inter-related processes that modulate marine DMS. We investigate the potential inter-relationships between the rate of primary production (carbon assimilation), underwater irradiance and DMS/DMSP dynamics by applying correlation analysis to a high resolution, concurrently sampled *in situ* data set from a range of latitudes covering multiple biogeochemical provinces from 3 of the 4 Longhurst biogeochemical domains. The combination of primary production (PP) and underwater irradiance (I_z) within a multivariate regression model is able to explain 55% of the variance in DMS concentrations from all depths within the euphotic zone and 66% of the variance in surface DMS concentrations. Contrary to some previous studies we find a variable representing biological processes is necessary to better account for the variance in DMS. We find that the inclusion of I_z accounts for variance in DMS that is independent from the variance explained by PP. This suggests an important role for solar irradiance (beyond the influence of irradiance upon primary production) in mediating the relationship between the productivity of the ecosystem, DMS/DMSP production and ambient seawater DMS concentrations.

3.2 Introduction

The CLAW hypothesis suggests that DMS could be part of a biologically-mediated biogeochemical-climate feedback loop (Charlson et al. 1987) with global climatic

significance. Seawater DMS concentrations are a critical link in this loop, modulating DMS flux to the atmosphere (Liss and Slater 1974) with a cloud albedo-climate control upon seawater DMS necessary for the operation of a feedback loop. DMS concentrations in the surface ocean are a product of the marine ecosystem and its environmental setting and the result of a complex interaction of sources and sinks (Stefels et al. 2007; Simó 2001). The main DMS precursor, DMSP, is closely associated with algal synthesis with phytoplankton speciation important for determining DMSP production (Keller et al. 1989; Stefels et al. 2007). Once liberated within the water column, DMS can be metabolised by bacteria to dimethylsulphoxide (DMSO) and other non-volatile sulphur species (Kiene et al. 2000; Kieber et al. 1996), photo-oxidised to DMSO and other breakdown products (Brimblecombe and Shooter 1986; Hatton 2002) or, due to its volatile nature, cross the sea/air interface (Liss and Slater 1974).

At the global scale, elevated DMS/DMSP (hereafter referred to as DMS(P)) concentrations are associated with regions of high productivity and biomass (Kettle et al. 1999; Lana et al. 2011a). Underwater irradiance is a major control upon the productivity of marine ecosystems along with nutrients and temperature at regional to global spatial scales and at monthly to seasonal temporal scales (Behrenfeld and Falkowski 1997b; Geider et al. 2001). Consequently, regional to global spatial scale and monthly to annual temporal scale DMS and DMSP distributions may be related to solar radiation via the modulation of productivity by underwater insolation.

At the local scale, underwater irradiances can be highly variable in space and time, inducing a range of physiological states from photoinhibition to light limitation as a result of mixing (depth variations), self shading, and insolation changes due to cloud cover variation or diurnal variation (Macintyre et al. 2000). A mechanism for maintaining photosynthesis at an optimum rate under the stresses of a constantly changing light environment could offer a significant selective advantage over the lifetime of a typical phytoplankton cell (hours to days). DMSP synthesis has been linked to the maintenance of photosynthetic efficiency in some laboratory studies (Archer et al. 2010; Sunda et al. 2002) with DMS and DMSP attributed roles as an antioxidant (Sunda et al. 2002) or as part of an overflow mechanism when growth is

unbalanced (Stefels 2000). This suggests a possible inter-relationship between underwater irradiance, the rate of PP and DMSP synthesis.

Solar radiation also plays a role in modulating two major DMS loss processes; bacterial metabolism and photo-oxidation rates (Simó and Pedrós-Alió 1999a; Toole et al. 2003; Toole and Siegel 2004; Vallina et al. 2007). This offers the potential for an additional direct effect of solar radiation upon ambient DMS concentrations that is independent from the role of solar radiation in modulating PP. A strong positive correlation has been demonstrated between mixed layer irradiance (solar radiation dose, SRD) and monthly averaged surface DMS concentrations at regional and global scales (Vallina and Simó 2007). Chapter 2 reports a strong, significant correlation between DMS and SRD using a higher temporal resolution (daily) sampled dataset from the AMT programme. The mixed layer irradiance framework suggests a simultaneous increase in DMS(P) synthesis (via the antioxidant or overflow hypothesis), a shift in the species assemblage towards high DMSP producers and reduction in bacterial sulphur demand under high irradiances (Simó and Pedrós-Alió 1999a). This provides a plausible biophysical explanation as to why shallow mixed layers coincident with high summer insolation yield elevated DMS concentrations. However, the SRD methodology lacks a direct representation of biology and, although it is successful at explaining temporal DMS concentrations, a large amount of data averaging is required to observe a strong correlation across large spatial scales (Derevianko et al. 2009).

Previous analyses from *in situ* cruise measurements have demonstrated a correlation between PP and total DMSP (DMSPt: the sum of dissolved and particulate DMSP). Using data from the subtropical and equatorial regions of the Atlantic, Bell et al. (2010) report a strong correlation ($\rho = 0.59$, $p < 0.01$, $n = 118$) between DMSPt and PP (per hour, by cells > 2 µm diameter). Using data from higher latitudes, Matrai et al. (2007) report a correlation between depth-integrated values of DMSPt and total PP (per day) over the seasonal cycle from 5 Barents Sea cruises. Bell et al. (2010) demonstrate a correlation between DMSPt and photoprotective pigments but neither of these analyses explored the direct influence of irradiance upon DMSP or DMS concentrations. In this study we apply multivariate correlation analysis to a compiled dataset of concurrently sampled DMS, DMSPt, PP and chlorophyll *a* (Chl

a) data from the ocean surface to the base of the euphotic zone. The dataset covers a range of seasons with data from 8 biogeochemical provinces representing 3 of the 4 biogeochemical domains as defined by Longhurst (1995) with an approximate latitudinal range of 78°N to 40°S. We use this dataset to investigate whether underwater irradiance (I_z) in the marine environment has an independent role in controlling DMSPt and DMS concentrations, beyond its role in modulating PP.

3.3 Methods

Data was collated from (i) the Atlantic Meridional Transect program (AMT), (ii) the Barents Sea (BAR), (iii) Atmospheric Chemistry Studies in the Oceanic Environment (ACSOE) research campaign and (iv) DImethyl Sulphide biogeochemistry within a COccolithophore bloom (DISCO) study (Figure 3.1). Data was sampled from a range of ecosystems, latitudes and seasons from 8 biogeochemical provinces within 3 open ocean biogeochemical domains:

- Polar domain: Boreal Polar Province, BPLR; and Atlantic Subarctic Province, SARC.
- Westerlies domain: North Atlantic Drift Province, NADR; North Atlantic Subtropical Gyral Province West, NAST(W); and North Atlantic Subtropical Gyral Province East, NAST(E);.
- Trade wind domain: North Atlantic Tropical Gyral Province, NATR; Western Tropical Atlantic Province, WTRA; and South Atlantic Gyral Province, SATL (Longhurst 1995).

The 3 cruises from AMT (AMT-12, 12th May – 17th June 2003; AMT-13, 10th September –14th October 2003; and AMT-14, 26th April – 2nd June 2004) were focused on the oligotrophic gyres of the North and South Atlantic, sampling from approximately 40°S to 40°N (see Bell et al. (2010) for further details). The BAR data comprises 5 cruises conducted in high latitude eutrophic waters including some sea ice zone samples during May 1993, March 1998, May 1998, June-July 1999 and July 2001 between approximately 72°N-78°N (see Matrai et al. (2007) for further details). ACSOE and DISCO were both Lagrangian bloom-tracking studies. DISCO tracked the development of a bloom of the coccolithophore, *Emiliania huxleyi* between the 16th and 26th of June 1999 in the northern North Sea at approximately 59°N (see Burkill et al. (2002) for further details). The ACSOE North Atlantic

Experiment tracked an *Emiliania huxleyi* bloom in a eddy south of Iceland between the 10th June and 4th July 1998 at approximately 60°N (see Jickells et al (2008), Simó and Pedrós-Alió (1999b) for more details).

Data were available for analysis from 82 depth profiles of concurrently sampled DMS and DMSPt concentration (nmol l^{-1}), a measurement technique for PP, daily ^{14}C uptake rate (mg C m^{-3} d^{-1}), Chl *a* concentration (mg C m^{-3}), and an estimate of the fraction of surface irradiance available to the sample (I_z) (see discussion below and equation 3.1). For each depth profile, samples were taken from the surface to the base of the euphotic zone (1% of the surface irradiance) and at intermediate depths. Samples were considered concurrent if they were from the same profile and from the same sample depth (z +/- 2m).

All DMS samples were filtered and measured using purge and trap (Turner et al. 1990) coupled with a gas chromatograph (GC) fitted with a flame photometric detector (see Archer et al. (2002b), Bell et al. (2006), Bell et al. (2007), Burkill et al. (2002), Jickells et al. (2008), Matrai et al. (2007), Matrai and Vernet (1997), Matrai and Keller (1993) for details), with the exception of DISCO samples, which were analysed using a mass spectrometer and the analytical protocol of Smith et al. (1999). DMSP samples were typically converted to DMS via cold alkali hydrolysis and, with the exception of some AMT samples that were analysed via headspace analysis (see Bell et al. 2006, 2007), were also analysed using the purge and trap GC technique. Whilst differences have been observed between different analytical techniques, what little data that has been collected on DMS inter-comparability suggests that variability between different techniques is likely to be ≤25% (Bell et al. 2011). Consequently we conclude that this does not present a significant problem for our study. The method of filtration used to separate dissolved DMSP (DMSPd) from particulate DMSP (DMSPp) has been reported to have a more significant influence upon results (Kiene and Slezak 2006). However, we only interpret total DMSP (DMSPp + DMSPd) data in our analysis and thus filtration artefacts were not considered to be such an issue.

Daily ^{14}C uptake rates (mg C m^{-3} d^{-1}) were determined by on-deck incubations for AMT, ACSOE, DISCO and some BAR data using filters to simulate underwater

light levels. PP samples from all sources were determined as the difference between light and dark incubated samples to account for respiration. ACSOE cruises used the standard JGOFS ^{14}C methodology (see Savidge and Gilpin 1999). AMT, BAR and DISCO do not cite primary references for the ^{14}C methods but see Burkill et al. (2002), Poulton et al. (2006), Matrai et al. (2007), Matrai and Vernet (1997) and Simó and Pedrós-Alió (1999b). In common with many other studies, some uncertainty is introduced when water samples are incubated on deck to yield daily PP rates with a potential disparity between simulated and actual abiotic and biotic environments (Marra 2002). Additionally, some BAR PP data were incubated *in situ* at the depths from which the water samples were made (Vernet et al. 1998) rather than on deck but this is not thought to introduce prohibitive differences in the results (Marra 2002). Studies undertaken in the North Atlantic (Joint et al. 1993) and North Sea (Joint and Pomroy 1993) did not find significant differences in the estimates of PP between on deck and *in situ* incubations. Chl *a* concentrations were measured using fluorometric methods: AMT and DISCO publications cite Welschmeyer (1994) as a primary reference while ACSOE and BAR publications do not cite primary references for the methods used (but see Burkill et al. 2002; Matrai 1997 for further information).

Underwater irradiance (I_z) is the estimated 24 hour averaged surface 300-3000 nm irradiance (I_0est) at the sampling depth (z) (see equation 3.1) is a function of latitude, date and known astronomical constants (Brock 1981; Vallina and Simó 2007). I_0est is not an *in situ* measurement and does not take account of cloud variations or the atmospheric path length as it assumes a constant 50% attenuation of top of atmosphere radiation which will dampen some variability in I_z. In common with other studies (Lana et al. 2011a; Vallina and Simó 2007), we used total solar irradiance as a proxy for biologically relevant wavelengths (PAR and UV). It would be ideal to have used *in situ* measurements of PAR and UV from the cruises but these data were not available. Previous authors (Belviso et al. 2011; Jerlov 1974, 1977; Jitts et al. 1976) have used a fixed coefficient to estimate PAR wavelengths from total solar irradiance under clear skies. The application of this fixed coefficient approach would not change the correlation coefficients within our work. Baker and Frouin (1987) used a variable coefficient approach to adjust the clear sky coefficient and found a maximum difference of 0.06 in the ratio of I_0total:I_0PAR depending on

water vapour, aerosol optical thickness and latitude. The variance introduced by cloud cover is larger than variation introduced by variable attenuation of the solar spectrum (Baker and Frouin 1987). We did try using a 10 year cloud adjusted surface PAR climatology derived from SeaWiFS data (http://www.science.oregonstate.edu/ocean.productivity/index.php) to calculate under water irradiance (I_z). This degraded the correlation relationships between I_z and both DMS and DMSP, likely due to the poor spatial and temporal resolution of the climatological data (1/6th degree spatial grid, monthly resolution). This resulted in several profiles from each cruise being assigned the same irradiance value. In addition, the PAR climatology is a noon irradiance value as opposed to a 24 hour average value. We calculated a daily averaged underwater irradiance value so as to be comparable with our daily *in situ* PP rates. Previous authors have suggested that it is the attenuation of irradiance by the water column and its contents that offers the greater uncertainty when determining underwater irradiances (Baker and Frouin 1987; Smith and Baker 1981). We derive our underwater irradiance from *in situ* measures of the fraction of surface irradiance and believe that this greater source of uncertainty has been accounted for more precisely. The fraction (*f*) of surface irradiance at the sample depth z (f_z) which was measured *in situ* and concurrently with the DMSP/DMS/PP water sample was used to calculate I_z (see equation 3.1). In some cases the f_z value from the mid-morning cast of the previous day was used to calculate I_z because the water samples were collected at night (see Poulton et al. 2006). Where no f_z was available data were excluded from the analysis.

$$I_z = I_0 est(f_z) \qquad (3.1)$$

From the Barents Sea data only the May 1993 cruise concurrently sampled DMS as well as DMSPt and PP. This results in a smaller dataset for DMS and PP data (n = 250), in comparison to concurrently measured DMSPt and PP measurements (n = 401). In addition there was no fractional surface irradiance data from the May 1993 cruise so there is no concurrent I_z and DMS data from the Barents Sea.

We applied direct multiple linear regression (MLR) analysis to this dataset. To account for the skewed distribution of the data, we used $\log_{10}$ transformed data in the regression analysis, and a Spearman's Rank test to evaluate bivariate correlations

(Wilcox 2010). We present multiple correlation coefficients (R) and adjusted multiple coefficients of determination (R^2). The adjusted R^2 statistic corrects for the problem of additional explanatory variables increasing the correlation simply due to their inclusion (Weisberg 2005). Equation 3.2 shows calculation of the adjusted R^2 where SS_{err} is the residual sum of squares, SS_{tot} is the total sum of squares, df_t is the total number of degrees of freedom ($n - 1$) and df_e is the total number of degrees of freedom minus the number of fit coefficients/explanatory variables (q) ($n - 1 - q$) (Weisberg 2005).

$$\text{Adjusted } R^2 = \frac{SS_{err}}{SS_{tot}} \frac{df_t}{df_e} \qquad (3.2)$$

We also calculated the tolerance for the predictors to evaluate potential multicolinearity within the MLR. This is calculated as Tolerance = $1\text{-}R^2_n$ where R^2_n is the coefficient of determination of the Independent Explanatory Variable (IEV) n on all other IEV's (Weisberg 2005). Tolerance is the proportion of an IEV's variance that is not accounted for by the other IEV's in the equation. A tolerance level close to 0 indicates multicolinearity (Weisberg 2005). All statistical calculations were performed using SPSS™ software. The Theil-Sen trendlines in Figure 3.2 were derived by finding the median of all slopes for lines between all pairs of points with the intercept calculated for the median slope. This non parametric technique is insensitive to outliers and thus appropriate for non-parametric data (Miller and Miller 2000).

We followed the approach of Bell et al. (2010) to define the criteria for a strong correlation, which reflects the inherent natural variability and relatively dynamic DMS(P) system. A correlation was considered strong if the absolute value of ρ was > 0.5. A correlation was considered statistically significant if it met the threshold criteria of $p < 0.01$. The Hotelling-Williams test (HW test) as described by Steiger (1980) was used to evaluate the significance of any difference between correlation coefficients that share a common variable (e.g. the significance of any difference in the ρ value between DMS:PP and DMS:Chl). The HW test statistic is interpreted as one would a t-statistic with the p value reported as a measure of the error associated

with rejecting the null hypothesis that the two correlation coefficients are equal (H_0: $\rho_{DMS:PP} = \rho_{DMS:Chl}$).

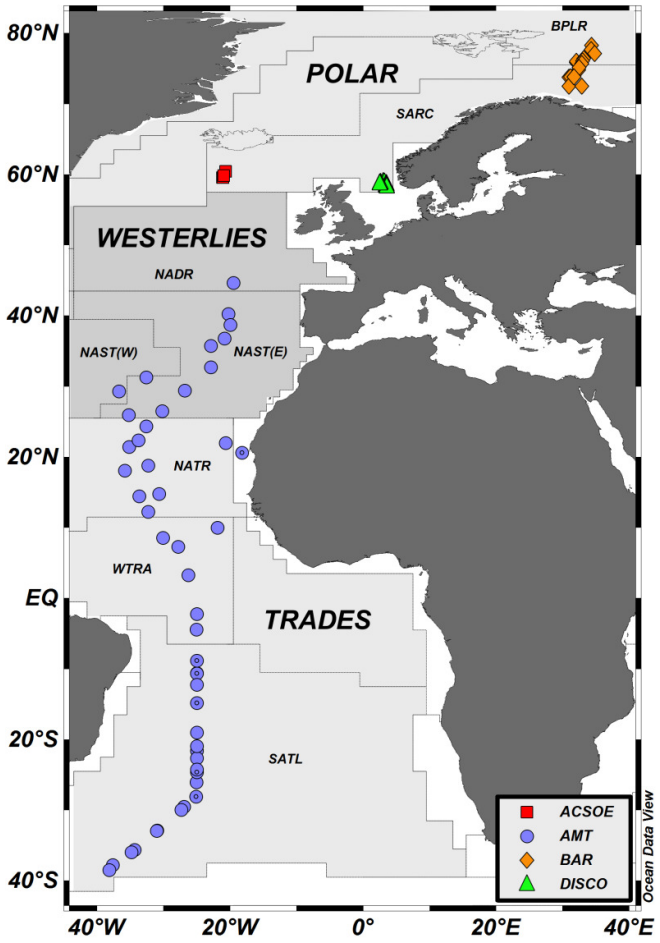

Figure 3.1: *Location of the four data subsets:* ***ACSOE*** *(red squares);* ***AMT*** *(blue circles),* ***BAR*** *(orange diamonds),* ***DISCO*** *(green triangles). Each marker represents a single depth profile, approx 6-8 samples per profile: DMSPt n = 401, AMT n = 169, BAR n = 169, ACSOE n = 11, DISCO n = 52 (approx 48 profiles), DMS n = 250, AMT n = 185, BAR n = 24, ACSOE n = 11, DISCO n = 30 (approx 36 profiles). Grey lines delineate biogeochemical provinces and shaded areas identify biogeochemical domains. One profile from AMT was sampled from the Canary current coastal province (CNRY) which falls within the Coastal domain, this was included in section 3.4.1 but not within section 3.4.2.*

3.4 Results

3.4.1 All data

We analysed the data across all latitudes and found strong, significant correlations between concurrently sampled *in situ* PP and DMSPt ($\rho = 0.55$, $p < 0.01$, $n = 401$) and between concurrently sampled *in situ* PP and DMS ($\rho = 0.66$, $p < 0.01$, $n = 250$) from all depths of the euphotic zone (Figure 3.2a and Figure 3.2c, Table 3.1). Correlations between DMSPt and Chl *a* concentration ($\rho = 0.60$, $p < 0.01$, $n = 409$) are of comparable strength and significance to those between DMSPt and PP. The correlation between DMS and Chl *a* ($\rho = 0.40$, $p < 0.01$, $n = 250$) is weaker than that between DMS and PP. Analysis using the HW statistic (Steiger 1980) shows that the $\rho_{DMS:Chl}$ coefficient value is significantly different (weaker) than the $\rho_{DMS:PP}$ value ($p < 0.001$). There is little correlation between *in situ* DMSPt and estimated average daily water-attenuated irradiance at the sample depth (I_z) ($\rho = 0.12$, $p < 0.05$, $n = 298$). In contrast, the correlation between DMS and I_z is strong, positive and significant ($\rho = 0.55$, $p < 0.01$, $n = 226$) (Figure 3.2b & Figure 3.2d, Table 3.1).

A multiple linear regression (MLR) analysis of the correlation between DMS and the separate variables PP and I_z using the whole dataset yields a multiple correlation coefficient (R) of $R = 0.74$, which is stronger than the correlation between DMS and either explanatory variable in isolation (equation 3.3).

$$\log_{10} \mathrm{DMS} = 0.539\,(\log_{10}\mathrm{PP}) + 0.310(\log_{10} I_z) - 0.279 \qquad (3.3)$$

The adjusted R^2 for equation 3.3 ($R^2 = 0.55$) indicates that 55% of variability in DMS concentrations can be explained by these two variables (Table 3.1). The adjusted R^2 statistic corrects for the problem of additional explanatory variables increasing the correlation simply due to their inclusion (Weisberg 2005) (see section 3.3). The explanatory variables (PP and I_z) for the MLR do not exhibit a strong correlation to each other ($\rho = 0.4$, $p < 0.01$, $n = 345$) and the tolerance is significantly above zero (0.726) indicating that only ~30% of the variance in one explanatory variable is explained by the other and is not indicative of multicolinearity (Weisberg 2005). In addition, both explanatory variables in the MLR are significant ($p < 0.01$). In summary, these statistical tests indicate that the inclusion of PP explains

additional variance in DMS concentrations, independent of the variance explained by I_z.

Table 3.1: *Correlation coefficients are shown in bold whilst sample number (n) is shown in brackets below. All correlations are significant with $p < 0.01$ unless marked*. R^2 is statistically adjusted to account for spurious correlation increases resulting from additional explanatory terms in MLR and/or small sample sizes (Weisberg 2005). MLR uses log_{10} transformed data to account for the non-normal distribution of data (Weisberg 2005).*

	Spearman's Rank correlation coefficient (ρ)			**MLR multiple correlation coefficient (R value)**	**Multiple linear regression (adjusted R^2 value)**
	PP	**Chl *a***	**I_z**	**Input variables: PP & I_z**	**Input variables: PP & I_z**
DMSPt	**0.55** (401)	**0.60** (409)	**0.12*** (298)	**0.67**	**0.45**
DMS	**0.66** (250)	**0.40** (250)	**0.55** (226)	**0.74**	**0.55**

It is important to characterise concentrations of DMS as close to the surface ocean/lower atmosphere interface as possible for two reasons: (i) they are a major control upon DMS flux to the atmosphere (Johnson 2010; Liss and Slater 1974), and (ii) satellites can only typically observe the upper few metres of the surface ocean. We used the approach of Lana et al. (2011a) and Kettle et al. (1999) to select surface DMS samples (i.e. < 10 m) but use only the shallowest depth sample from each discrete CTD profile to capture data that is as close as possible to the sea-air interface. We find strong, significant correlations between surface PP and surface DMS ($\rho = 0.67$, $p < 0.01$, $n = 27$) and between surface DMS and I_z ($\rho = 0.63$, $p < 0.01$, $n = 24$) (Fig. 2c & 2d). Using the same MLR analysis as before yields a multiple correlation coefficient of $R = 0.84$, with an adjusted $R^2 = 0.66$ (see equation

3.4). As before, analysis of the tolerance level statistics does not suggest multicolinearity (tolerance = 0.822).

$$\log_{10} \mathrm{DMS} = 0.507\,(\log_{10}\mathrm{PP}) + 0.240(\log_{10} I_z) - 0.745 \qquad (3.4)$$

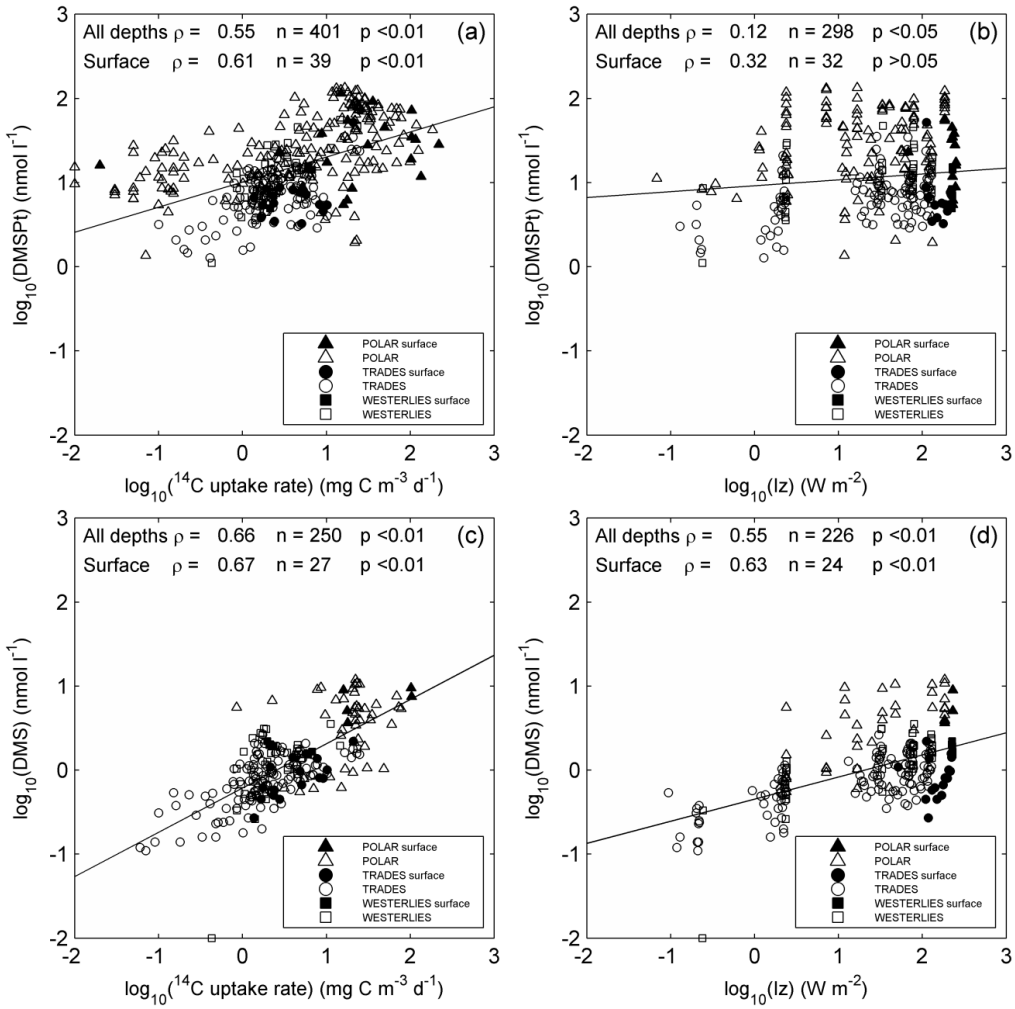

Figure 3.2: *Log-log (base 10) plots of DMSPt concentration (nmol l^{-1}) plotted against:* ***(a)*** *^{14}C uptake rate (mg C m^{-3} d^{-1}); and* ***(b)*** *daily averaged underwater irradiance I_z (W m^{-2}). DMS concentration (nmol l^{-1}) plotted against:* ***(c)*** *^{14}C uptake rate (mg C m^{-3} d^{-1}); and* ***(d)*** *daily average underwater irradiance I_z (W m^{-2}). Data shown from surface (closed symbols) and all other depths (open symbols) for the Polar biogeochemical domain (triangles), Trades biogeochemical domain (circles) and the Westerlies biogeochemical domain (squares) as defined by Longhurst (1995). Also shown are trendlines (solid black line) for data from all depths of the euphotic zone calculated using Theil-Sen (non-parametric) regression (Miller and Miller 2000).*

The PP and I_z data utilised here are representative of a timescale on the order of days. In contrast, reported literature values for the turnover times for DMS and DMSP are of a shorter range from 0.4 to 1.6 days (Archer et al. 2002a; Simó and Pedrós-Alió 1999b). We note that a single sample from a discrete depth represents only a snapshot of the inherent natural variability. Individual concentrations (DMSP, DMS and Chl *a*) from discrete depths are also influenced by the mixing rate and mixing depth of the water body from which they are sampled and its environmental history. The same issue applies to the PP rates that are estimated from incubations either on deck at a constant replicated light level or *in situ* at a stationary depth. Our observed correlations in the discrete data should be interpreted within the context of this variability. To reduce the influence of discrete sampling depths on our results, we integrate data within each depth profile from the surface to the base of the euphotic zone. Applying the same statistical analyses to this data produces similar results to the discrete data; strong and significant correlations can be identified between depth integrated DMSPt and depth integrated PP ($\rho = 0.71$, $p < 0.01$, $n = 74$) and between depth integrated DMS and depth integrated PP ($\rho = 0.67$, $p < 0.01$, $n = 58$). The correlations between depth integrated DMS, DMSPt and I_z are significant but not strong (I_z and DMS, $\rho = 0.47$, $p < 0.01$ $n = 54$; I_z and DMSPt, ($\rho = 0.39$, $p < 0.01$, $n = 65$). MLR analysis indicates that a combination of depth integrated PP and depth integrated I_z can explain 40% of the variance in depth integrated DMS with minimal multicolinearity ($R = 0.64$, $R^2 = 0.40$, tolerance = 0.987).

3.4.2 Biogeochemical domains

So far we have explored relationships across a range of ecological and biogeochemical environments but it is also interesting to examine whether these relationships persist within subdivisions of the data characterised by similar biogeochemical and ecological regimes. This dataset contains data from 8 biogeochemical provinces representing all 3 of the open ocean biogeochemical domains as defined by Longhurst (1995) (see Figure 3.1). BAR, ACSOE and DISCO data come from the Polar domain with the majority located in the Boreal Polar Province (BPLR), which is characterised by eutrophic, high production environments with seasonal phytoplankton blooms. The majority of the AMT data

come from the oligotrophic, gyral provinces of the North and South Atlantic (North Atlantic Subtropical Gyral Province West (NAST(W)), North Atlantic Subtropical Gyral Province East (NAST(E)), North Atlantic Tropical Gyral Province (NATR) and the South Atlantic Gyral Province (SATL)) from the Westerlies and Trades domains (see Figure 3.1). These oligotrophic provinces are characterised by low production and biomass with a lack of strong seasonality (Longhurst 1995). As a result we find it appropriate to show aggregated data for the Westerlies and Trades as a single domain.

Data from within the individual biogeochemical domains displays similar trends as that from the dataset as a whole (Table 3.2) although all of the correlations are generally stronger in the entire dataset in comparison with the domains. Within each biogeochemical domain, the multiple correlation coefficient (R) generated using PP and I_z using MLR are strong and significant (R = 0.66 to 0.76, Table 3.2). These R values are stronger than the bivariate correlations between DMS and either of the explanatory variables within the MLR in isolation. MLR analysis is able to explain 41-56% of the variance in euphotic zone DMS concentrations for each biogeochemical domain using PP and I_z as explanatory variables (see Table 3.2). Multicolinearity analysis demonstrates that the explanatory variables explain independent variance within the MLR.

Table 3.2: *Correlation coefficients for the data separated into Longhurst (1995) biogeochemical domains are shown in bold whilst sample number (n) is shown in brackets. All correlations are significant with $p < 0.01$ unless marked*. R^2 is statistically adjusted to account for spurious correlation increases resulting from additional explanatory terms in MLR and/or small sample sizes (Weisberg 2005). MLR uses log_{10} transformed data to account for the non-normal distribution of data (Weisberg 2005).*

		Spearman's Rank correlation coefficient (ρ)			**MLR R**	**MLR adjusted R^2**
		PP	**Chl *a***	**I_z**	**Input variables: PP & I_z**	**Input variables: PP & I_z**
POLAR DOMAIN	**DMSPt**	**0.56** (220)	**0.33** (237)	**0.10*** (129)	-	-
	DMS	**0.38** (53)	**0.18*** (62)	**0.55** (41)	**0.66**	**0.41**
TRADES DOMAIN	**DMSPt**	**0.34** (126)	**0.01*** (119)	**0.28** (126)	-	-
	DMS	**0.62** (120)	**-0.10*** (135)	**0.53** (142)	**0.72**	**0.50**
WESTERLIES DOMAIN	**DMSPt**	**0.69** (43)	**0.27** (40)	**0.31** (43)	-	-
	DMS	**0.28*** (43)	**-0.42** (40)	**0.62** (43)	**0.76**	**0.56**
WESTERLIES & TRADES DOMAINS	**DMSPt**	**0.41** (169)	**0.14*** (159)	**0.28** (169)	-	-
	DMS	**0.56** (185)	**-0.10*** (175)	**0.58** (185)	**0.70**	**0.49**

3.5 Discussion

We find strong, significant correlations between DMS and PP and DMS and I_z in a compilation of water column measurements from a wide range of oceanic environments (Table 3.1). These correlations are observed in data collected from discrete depths within the euphotic zone, from near-surface waters and within depth profile integrated data. MLR analysis of the dataset as a whole suggests that to explain the maximum amount of variance in DMS concentrations a combination of

PP and I_z is required. This MLR analysis is able to explain 55% of the variance in DMS concentrations from all depths of the euphotic zone, and 66% of the variance in surface DMS concentrations. These relationships are observed in a dataset that represents good latitudinal coverage and contains samples from all 3 of the open ocean biogeochemical domains defined by Longhurst (1995). The AMT cruises were focused on the oligotrophic gyres of the North and South Atlantic. ACSOE and DISCO samples were made during mid to high latitude phytoplankton (summer) blooms and the BAR cruises sampled the eutrophic high latitude Barents Sea with some samples from the sea ice zone. Despite the different trophic regimes, species assemblages, local oceanographic influences and different parts of the seasonal productivity cycle, the correlation is observed in a dataset that spans these temporal and ecological gradients.

An examination of the relative magnitude of the MLR coefficients associated with PP and I_z demonstrates that, of the parameters included, PP is the statistically dominant variable within the MLR both for the surface data and for data from all depths. This indicates that a measure of biological productivity is important for representing DMS concentrations across a gradient of ecological regimes with more productive regions yielding higher DMS concentrations. The correlation between DMS and the rate of PP ($\rho = 0.66$, $p < 0.01$, $n = 250$) is significantly stronger ($p < 0.001$; HW test) than that observed between DMS and Chl *a* ($\rho = 0.40$, $p < 0.01$, $n = 250$). A similar trend is also found within each domain or ecological/oceanographic region. Within each domain the correlation coefficient between DMS and PP is typically greater than between DMS and Chl *a*, especially in oligotrophic environments (Table 3.2). In addition, DMSPt is more strongly correlated to PP than to Chl *a* within the individual domains (Table 3.2). However, DMSPt is as closely associated with biomass (Chl *a* concentration) as it is to the rate of PP across the dataset as a whole (Table 3.1). The rate of PP is related to Chl *a* over larger spatial and temporal scales as high rates of PP allow the accumulation of biomass, which may hamper statistical differentiation between the two variables.

It has been suggested that the intracellular reduced sulphur cycle is involved in the maintenance of an optimal photosynthetic rate, delaying photoinhibition via the scavenging of reactive oxygen species generated under high irradiances (Sunda et al.

2002) or by acting as a sink for excess reduced sulphur or carbon when growth is nutrient limited (Stefels 2000). If so, the rate of PP may give a more instructive indication of DMSP-DMS production in the surface ocean rather than a measure of standing stock biomass such as Chl *a* concentration. The rate of PP may also be more comparable between different environmental conditions as it is possible for cells with different chlorophyll concentrations (due to species differences or variations in environmental conditions/photoacclimation) to photosynthesise at the same rate (Chow et al. 1990; Marra 1997). Chl *a* measurements are unable to distinguish between live, healthy cells and Chl *a* within dead, dying or photosynthetically inactive cells (Marra 1997). Attempts to correlate Chl *a* with DMS over large spatial and temporal scales have typically proved unsuccessful (e.g. Kettle et al. 1999; Kettle and Andreae 2000). Masotti et al. (2010) investigated the relationship between phytoplankton speciation and the Chl:DMS ratio using ship based DMS measurements from the Atlantic, Pacific and Southern oceans in conjunction with satellite retrievals of surface chlorophyll and phytoplankton group dominance using the PHYSAT method. The PHYSAT method (Alvain et al. 2005) uses optical differences between phytoplankton species that, for a given Chl *a* concentration, are manifested in variance in the upwelling radiance just above the seas surface, to determine the dominant phytoplankton group. However, Masotti et al. (2010) concluded that this method could not be used to predict global fields of DMS. Smaller scale Lagrangian studies, where bloom populations are dominated by a single phyla, have demonstrated a correlation between Chl *a* and DMS (e.g. Malin et al. 1993). This is often attributed to the difference in the ratio of carbon:DMSP produced by different species (Keller et al. 1989; Stefels et al. 2007).

Solar radiation plays a potential role in modulating the sources of DMS in the marine ecosystem and two major DMS loss processes; bacterial metabolism and photo-oxidation (Simó and Pedrós-Alió 1999a; Toole and Siegel 2004; Vallina and Simó 2007). Our results suggest an important role for solar radiation (beyond its influence on primary production) in mediating the relationship between DMSP synthesis activity and ambient seawater DMS concentrations. The bivariate correlations observed between DMS and I_z within the whole dataset and within each domain are strong and significant (Table 3.1 and Table 3.2). Although the idea that DMS may be related to I_z in oligotrophic waters is becoming more widely accepted (Toole and

Siegel 2004; Toole et al. 2006; Vallina and Simó 2007; Vallina et al. 2008), it is less well established that I_z may be independently related to DMS in higher production, eutrophic waters. I_z is not statistically as important as PP within the MLR equations, but our analysis indicates that I_z explains additional variance in DMS independent of the variance explained by PP. However, we did not detect a role for the influence of irradiance upon DMSPt beyond its contribution to the rate of PP and found a weak correlation between DMSPt concentrations and I_z across all data and within each biogeochemical domain (Table 3.1 and Table 3.2).

The positive trend in the DMS and I_z data suggests that the suppression of the bacterial sink (Simó and Pedrós-Alió 1999a; Kieber et al. 1996), or the direct release of DMS under light stress (Sunda et al. 2002) is the dominant light-related process in this dataset (i.e. photo-destruction of DMS is a minor process). This is in agreement with other studies of water column DMS(P) dynamics (Kieber et al. 1996; Simó and Pedrós-Alió 1999a; Toole and Siegel 2004). Our results are also in broad agreement with the modelling study of Vallina et al. (2008), which invoked direct exudation of DMS by phytoplankton as the most important explanatory factor in resolving water column DMS concentrations at the oligotrophic Bermuda Atlantic Time-series (BATS) study station. Other global modelling studies also discuss the role of irradiance in driving modelled DMS concentrations beyond the solar forcing already driving the basic ecosystem model (Le Clainche et al. 2010; Vogt et al. 2010). Whilst the positive correlation between DMS and I_z indicates that photo-destruction of DMS is not a dominant process in this dataset, the suppression of DMS concentrations by high irradiance (likely driven by UV) should not be completely discounted as a factor. For example, high surface irradiances are often experienced in the oligotrophic gyres but these regions may have low CDOM and nitrate concentrations which would reduce photooxidation rates. The complexity of these processes are likely to increase the noise observed within the overall identified trends.

Increased intracellular DMSP synthesis has been related to the optimisation and maintenance of photosynthetic efficiency (Stefels 2000; Sunda et al. 2002). Assuming no changes in turnover rates one might expect DMSPt concentrations to be increased under high I_z levels or demonstrate a stronger relationship to the rate of

PP than to Chl *a*. A stronger relationship between PP and DMSPt relative to the correlation between DMSPt and Chl *a* was observed within each domain but not over the whole dataset/larger ecological gradient. A limitation of this work is that the spatial and temporal resolution of this analysis does not allow a full assessment to be made of the possible contribution of I_z and/or PP to DMSP synthesis. A PP rate compared on an equivalent timescale with a rate measurement of DMSP synthesis (rather than a DMSP concentration) would be necessary to resolve these issues.

A limitation of looking for statistical relationships between data from discrete depths is that the *in situ* DMS(P) concentrations and PP rates at each sampling depth reflect the environmental conditions over the range of depths that the water mass has experienced over a given time period due to vertical mixing. As such both the daily rate of PP incubated at a constant simulated light depth and an instantaneous DMS(P) or Chl *a* concentration may not be truly representative ecosystem values. To attempt to account for this issue we integrated each depth profile from the surface to the base of the euphotic zone. This depth integrated data follows similar trends to the data from discrete depths within the euphotic zone, suggesting that DMS and DMSPt concentrations are influenced by the interplay between light and PP anywhere within the euphotic zone. An advantage of collecting such a large dataset is that a general trend can be detected despite the fact that instantaneous DMSP and DMS concentrations from discrete depths may reflect natural variability in space and time in a dynamic and complex system with 1 – 2 day turnover times. The strength of the observed correlations should be interpreted in this context.

The results of our analyses broadly support the proposed biophysical framework where microbial communities experiencing high average mixed layer irradiance exhibit high net surface DMS concentrations (Simó and Pedrós-Alió 1999a; Toole et al. 2003; Toole and Siegel 2004; Toole et al. 2006; Vallina and Simó 2007). The reported positive relationship between mixed layer irradiance (SRD) and monthly surface seawater DMS concentrations (Vallina and Simó 2007) is a necessary condition for the operation of a feedback loop proposed by the CLAW hypothesis (Charlson et al. 1987). However, the SRD equation is constructed solely from abiotic variables and does not contain a term that directly represents the productivity or biomass of the DMS(P)-producing ecosystem. Derevianko et al. (2009)

demonstrated that although the SRD has shown strong correlations to DMS at local scales, the correlation is weaker at the global level without high levels of data aggregation, and that the correlation between SRD and DMS may be largely driven by MLD variability. Derevianko et al. (2009) proposed that seasonal variation in surface DMS concentrations may be controlled by SRD (through physical changes in light and MLD altering mixing, nutrient availability, etc.) whilst spatial variation may be controlled by trophic status. Our multiple correlation analysis suggest that an indicator of biological production (PP) is important for explaining maximal variance in DMS concentrations both across a large latitudinal and ecological gradient and within different biogeochemical/trophic regimes, with an irradiance parameter explaining additional variance.

Our results suggest that when using an explanatory framework it is important to couple biological dynamics (e.g. primary production) with physical forcings such as light and MLD. It is plausible that some environmental changes impact the DMS-relevant biological system without influencing mixed layer irradiances and mixing. For example, decreased carbonate availability arising from future ocean acidification may impact calcareous, high DMSP-producing coccolithophore species such as *Emiliania huxleyi* (Beaufort et al. 2011; Caldeira and Wickett 2005; Hopkins et al. 2010; Kroeker et al. 2010). Elsewhere, changes in atmospheric nutrient deposition (e.g. N, P, Fe, Pb) (Dentener et al. 2006; Fowler et al. 2007; Paytan et al. 2009) may change algal production (Mahowald et al. 2005; Paytan et al. 2009) . Phytoplankton species composition changes may also result from such impacts, which will either favour or inhibit DMSP-producing phytoplankton. Over the last century, Boyce et al. (2010) report a global decline in phytoplankton production of ~1% yr^{-1} and future global productivity is predicted to decline further (Polovina et al., 2008). The balance of drivers affecting the present (and future) marine ecosystem and the subsequent impacts on surface ocean DMS concentrations can only be fully captured in predictive algorithms by improving existing understanding of the relationship between environmental variables and DMSP-DMS dynamics.

3.6 Conclusions

Within a broad ranging and large dataset, we find that a variable representing biological processes (PP) in combination with the calculated underwater irradiance level (I_z) account for maximal variance in DMS concentrations across a range of latitudes and ecosystem types. Furthermore we find that the variance explained by I_z is independent from the variance explained by PP. This confirms previous work, which suggests an important role for solar irradiance (beyond the direct influence on the rate of PP) in mediating the relationship between the productivity of the ecosystem, DMSP-DMS production and ambient seawater DMS concentrations. These results broadly support the proposed biophysical framework where microbial communities that experience higher mixed layer average irradiances may exhibit higher net surface DMS concentrations (Simó and Pedrós-Alió 1999a; Toole et al. 2003; Toole and Siegel 2004; Toole et al. 2006; Vallina and Simó 2007). In addition, whilst previous studies have been unable to identify links between DMS and biological markers such as Chl *a* or other biomarker pigments, our results suggest that a large-scale link exists between the biological community and *in situ* DMS concentrations, which is moderated by processes directly influenced by the *in situ* irradiance. It is important that these inter-relationships are well characterised within the context of global changes in physical parameters such as irradiance and mixing, and future marine ecosystem dynamics and productivity.

Chapter 4: Estimates of Surface DMS Distributions on Regional to Global Scales

4.1 Introduction

The global surface seawater DMS database (http://saga.pmel.noaa.gov/dms/) has recently been updated to become the second largest database of oceanic trace gas measurements (after CO_2) (Bell et al. 2011), and offers a new opportunity to explore the controls upon global DMS concentrations. Despite the recent extensions to this database, it does not yet provide sufficiently high density (spatial and temporal) coverage to enable validation of global chemistry-climate models. These model evaluations require near-continuous coverage, as provided by climatologies, and parameterisations of surface oceanic DMS (Halloran et al. 2010). In order to develop effective large-scale parameterisations it is necessary to derive relationships between surface DMS and a set of predictor variables that are available with close to global coverage.

Matrai et al. (2007) and Bell et al. (2010) identified a link between the primary production rate and DMS(P) concentrations. Chapter 3, utilising high resolution depth profile data found a relationship between DMS and a combination of the concurrently sampled *in situ* primary production rate and underwater irradiance both across and within a range of ecological conditions. The results suggested that a large-scale link exists between the biological community and *in situ* DMS concentrations, which is moderated by processes directly influenced by the *in situ* irradiance. For the first time, this chapter reports upon an investigation into the potential for a climatological primary production rate (derived from satellite data) and climatological underwater irradiance to predict global DMS. The use of climatological variables is necessary because the DMS database does not contain data on concurrent, *in situ* primary production rates or underwater irradiance. It is desirable because the climatological variables provide the global coverage necessary to produce continuous global fields of surface DMS.

The global DMS database consists of many discrete samples that represent snapshots of the highly variable and complex surface DMS ecosystem. The surface DMS concentration at any given point in space and time depends upon the complex interaction between the sources and sinks of DMS to the marine ecosystem (Stefels et al. 2007). Species composition (Stefels et al. 2007; Keller et al. 1989), grazing

(Wolfe et al. 2002), viral attack (Malin et al. 1998; Wolfe et al. 1997; Wolfe et al. 2002), bacterial metabolism (Kiene and Linn 2000; Levine et al. 2012), underwater irradiance (Archer et al. 2010; Galí et al. 2011; Stefels 2000; Sunda et al. 2002; Toole et al. 2006), salinity (Stefels 2000), nutrient stress (Sunda et al. 2002), daily specific growth rate (Stefels et al. 2007), temperature (Van Rijssel and Gieskes 2002), sea-air flux (Liss and Slater 1974) and photo oxidation (Brimblecombe and Shooter 1986; Hatton 2002) have all been implicated as controls on the sources and sinks of DMS(P) identified at different temporal and spatial scales.

In addition the environmental history (minutes-hours-days) of the water mass prior to the DMS sample being taken is an important factor reflecting influences of variations in mixing rate and depth, cloud cover, wind speed or predator-prey cycles etc (Simó and Pedrós-Alió 1999a; Stefels et al. 2007). Variability is also introduced by different sampling strategies (bloom focus vs. transects) and sampling techniques with potential errors (Bell et al. 2011), incomplete spatial and temporal coverage (Lana et al. 2011a) and inter annual variability within the global DMS database. Analysis of the previous global DMS database (Kettle et al. 1999) was unable to identify strong bivariate correlations ($r > 0.5$) between $1^{o}x1^{o}$ gridded DMS data and a range of environmental variables including Chl, nitrate, phosphate, silicate, sea surface temperature, wind speed or dissolved oxygen (Kettle et al. 1999; Kettle and Andreae 2000).

The aim of this chapter is to derive a predictive relationship for surface DMS based on globally available, climatological biological and physical data, which can be applied at the global scale. The chapter starts with an investigation into the relationships between the high resolution DMS database and the climatological primary production rate and underwater irradiance variables. Initially, to assess if the climatological variables and the methods used to derive them are successfully reproducing a set of known *in situ* values, we compare the climatological primary production and underwater irradiance to the *in situ* primary production and underwater irradiance values from chapter 3. We then follow a similar procedure to chapter 3 using multiple linear regression (MLR) to assess whether a single regression model can be successfully developed for high resolution global surface

DMS using a combination of climatological primary production and underwater irradiance.

To identify large scale controls upon ambient surface DMS concentrations it may be necessary to average the raw DMS data to detect any underlying trends above the noise of natural variability in this highly complex and dynamic system. In the second section of this analysis alternative methods of data averaging are investigated. However, care must be taken in how the data is averaged when attempting to identify potential trends. Due to the sparsity of the temporal and spatial coverage within the DMS database, the data must be averaged over a relatively large spatial and temporal unit to generate a statistically valid spatio-temporal average. Within this analysis the biogeochemical provinces defined by Longhurst (1995) are used as spatial units with a monthly temporal resolution. This provides a biologically relevant spatial unit in preference to an arbitrary grid system based upon latitude and longitude. These "province months" are then used to generate a single global MLR model using climatological primary production and underwater irradiance as predictor variables.

In the final section of analysis, the relationship between DMS, primary production and under water irradiance within different regions/biogeochemical provinces is investigated. Evidence from the literature suggests that this relationship may change between provinces. The species composition of both the phytoplankton community and bacterial community will affect the sources and sinks of DMSP and DMS to the surface ocean (Levine et al. 2012; Keller et al. 1989; Kiene and Linn 2000; Stefels et al. 2007). In addition there is an interaction between primary production, biomass and the effectiveness of source and sink process related to irradiance (Bouillon and Miller 2004; Morel et al. 2007; Toole et al. 2003; Toole and Siegel 2004). In response to a lack of correlation between the seasonal peak in biological metrics and the peak in DMS concentrations in oligotrophic regions (the summer paradox) Toole and Siegel (2004) propose that there may be two regimes in operation: a production forced regime and an irradiance forced regime. Developing and applying a new methodology (section 4.3.3), a unique MLR model is derived for each biogeochemical province where sufficient data is available. This allows for both the slope of the relationship between DMS and the individual predictor variables and the relative contribution of two predictor variables to vary between provinces or regions

of the ocean. A single model may not be able to predict DMS in the global domain. A novel composite method to predict DMS is explored where the individual province MLR models are combined to predict global surface DMS concentrations. This method is carried out using the high resolution, "raw" data and province monthly averages. The composite province monthly average method demonstrates the strongest correlation to DMS at the global level in comparison to previous similar analysis that combined biological and physical predictive variables.

The types of questions that can be resolved using this approach must be considered. Detailed process information about specific pathways within the DMSP-DMS ecosystem may be unobtainable at these reduced spatial and temporal scales, these may be better investigated within the laboratory or using local field tests. This global, large scale approach instead may offer insight into the ecosystem level controls that dictate ambient surface DMS concentrations at larger spatial and temporal scales; this may then be applied to understand how surface DMS concentrations may change under future environmental stresses.

4.2 Methods

In this section the DMS database and the climatological data used to derive multivariate statistical models are described.

4.2.1 DMS database

The analysis in this chapter uses the recently updated global surface seawater DMS database (http://saga.pmel.noaa.gov/dms/). This database is the second largest oceanic database of trace gas measurements in terms of number of samples after oceanic CO_2 (Bell et al. 2011) (see Figure 4.1). It contains over 47,000 DMS data points sampled between 03/11/1972 and 06/08/2010. Despite the relatively large size of the database there are still significant gaps in the data in terms of the spatial and temporal coverage in all regions (see Figure 4.1). The database contains DMS concentration data (nmol l^{-1}) sampled from 0 to 21m although ~97% of the measurements are from 0-10m depth. The maximum DMS concentration is 420 nmol l^{-1} with a mean DMS concentration of 4.24 nmol l^{-1} and a standard deviation of

11.62 nmol l^{-1}. The data is strongly positively skewed (Skewness = 12.84) with relatively few high DMS values (see Figure 4.2). Due to the non-normal, skewed distribution it was necessary to transform the DMS data by taking $\log_{10}$ prior to statistical analysis using parametric tests (such as multiple linear regression), or to use non-parametric statistical tests applicable to non-normal distributions such as Spearman's rank hypothesis (Wilcox 2010). The $\log_{10}$ transformation of the DMS data yields a more normal distribution with a skewness of 0.41 (Figure 4.2).

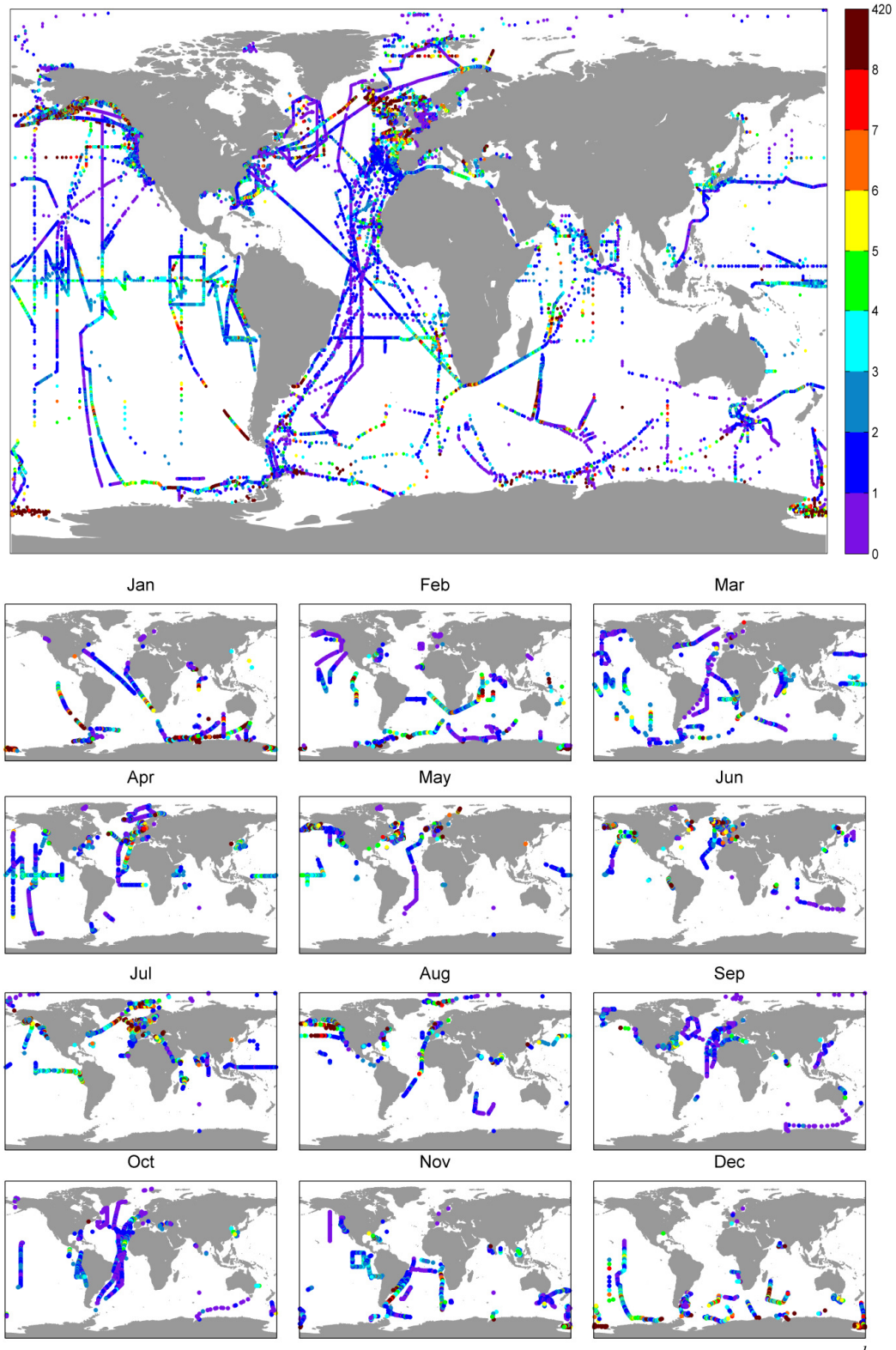

***Figure 4.1**: Top panel shows the global surface dimethyl sulphide (DMS) database (nmol l^{-1}) for all years 1972-2010, n = 47241 (http://saga.pmel.noaa.gov/dms/). Bottom panel shows spatio-temporal coverage with data presented for each month.*

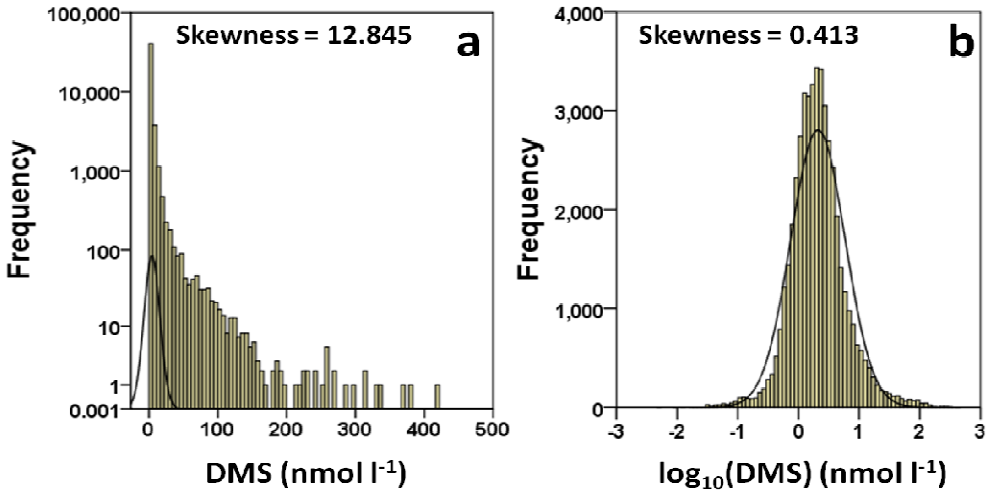

***Figure 4.2**: Histograms of **(a)** DMS data (nmol l^{-1}) with frequency axis shown on a log_{10} scale and **(b)** log_{10} transformed DMS data now indicating a more normal distribution.*

The majority of data in the global DMS database were obtained using purge and trap techniques combined with gas chromatography (Bell et al. 2011). Bell et al. (2011) investigated the inter-comparability of the data within the DMS database and concluded that variability between measurements within the database is likely to be < 25%. The DMS database does not employ formal quality control measures (Bell et al. 2011).

4.2.2 Primary production rate data and model

The primary production rate data used in this chapter is from a global 10 year climatology (1998-2007) of modelled net primary production rate (NPP) data using the Vertically Generalised Production Model (VGPM) (Behrenfeld and Falkowski 1997b). The climatology has a gridded spatial resolution of 1/12th of a degree (~ 9 km at the equator) and a temporal resolution of 8 days. The VGPM model climatology is discussed below and was supplied by the Oregon State University (http://www.science.oregonstate.edu/ocean.productivity/index.php).

Initially the climatology was available as a net primary production value integrated from the base of the euphotic zone to the surface, and with units of mg C m^{-2} d^{-1}. This was converted to an euphotic zone average NPP rate (details below) with units

of mg C m^{-3} d^{-1}. The primary production climatology selected was constructed using data from as long a time period as possible. The DMS database and the primary production climatology do not span the same time period, however, approximately 43% of data within the DMS database (1972 – 2010) falls within the time period covered by the primary production climatology (1998 - 2007).

The VGPM is a "chlorophyll based model" and is a function of satellite retrieved Sea-viewing Wide Field-of-view Sensor (SeaWiFS) surface chlorophyll, the underwater light field, and a temperature dependent description of chlorophyll specific photosynthetic efficiency. The VGPM model climatology is available in two variants based on different satellite retrievals of surface chlorophyll: the SeaWiFS satellite and the Moderate Resolution Imaging Spectroradiometer (MODIS) satellite. The VGPM model using SeaWiFS chlorophyll was selected as SeaWiFS provided the longest continuous record (10 years) (see http://www.science.oregonstate.edu/ocean.productivity/index.php). The VGPM model is formulated as follows:

$$\mathrm{VGPM_{npp}} = \mathrm{Chl} \times \mathrm{pb\_opt} \times \mathrm{daylength} \times \mathrm{f(par)} \times \mathrm{z\_eu} \qquad (4.1)$$

The assumption behind chlorophyll based models is that the NPP rate varies in a predictable way with a standing stock measure of biomass (chlorophyll concentration) (Behrenfeld and Falkowski 1997b, a). The first term in the model is Chl where SeaWiFS surface chlorophyll is used. The derivation of the primary production rate from chlorophyll concentration requires a term that parameterises the chlorophyll specific assimilation efficiency of carbon fixation (Behrenfeld and Falkowski 1997b). VGPM uses the term pb_opt (see equation 4.1) which is a sea-surface temperature dependent, maximum daily net primary production rate (mg C h^{-1}). The pb_opt function is derived from a polynomial fit to observational data, increasing with temperature from -1°C to 20°C and then decreasing above 20°C (Behrenfeld and Falkowski 1997b). The next term, "day length", converts from an hourly to a daily net primary production rate (mg C d^{-1}). Lastly a volume function (f(par)* z_eu) is needed to convert this rate to a water column measurement. Primary production has a light dependency and light penetration is not constant through the

water column so this must be represented within the model. The depth of the euphotic zone (z_eu: 1% surface PAR isolume) defines the vertical extent of the net primary production integral. The light term f(par) parameterises the non-uniform vertical distribution of net primary production due to the exponential decay of light with depth and is derived empirically from field data. The VGPM model was validated using an extensive field data set compiled by Behrenfeld and Falkowski (1997b) (n = 1693) and was found to explain 87% of the variance in observed net primary production measurements ($r^2 = 0.87$) (Behrenfeld and Falkowski 1997b).

Other primary production models are also available. A variant of the VGPM, the Eppley-VGPM is based on an alternative temperature dependent photosynthetic efficiency relationship observed by Eppley (1972) and the carbon based production model (CbPM), a primary production model based upon remotely sensed phytoplankton carbon concentration which replaces chlorophyll as the metric of biomass within the model. The standard VGPM model was selected for this analysis as it is well established, has been widely used and has been successfully and extensively sea truthed. Its application is also well supported by the Oregon State University (http://www.science.oregonstate.edu/ocean.productivity/index.php). Kahru et al. (2009) investigated how well 5 different production models replicated a large *in situ* data set (n = 1862) sampled between 1984 – 2007 representing a range of net primary production rates sampled from oligotrophic to coastal waters and found that an adjusted version of the VGPM model was the best fit to the data.

This euphotic zone integrated net primary production data (VGPM) is generated by first calculating surface NPP and then multiplying the surface value by the depth of the euphotic zone (z_eu) (see equation 4.1). To convert to euphotic zone average net primary production ($VGPM_{avg}$) the VGPM data was divided by z_eu (see equation 4.2) to obtain euphotic zone average net primary production (units of mg C m^{-3} d^{-1}, see Figure 4.3) (pers comm. Robert O'Malley (data manager): http://www.science.oregonstate.edu/ocean.productivity/index.php) . The euphotic zone average NPP ($VGPM_{avg}$) is well correlated to the euphotic zone integrated NPP (VGPM) ($r^2 = 0.98$, $p = <0.01$).

$$\mathrm{VGPM_{avg}} = \frac{\mathrm{VGPM}}{\mathrm{z\_eu}} \qquad (4.2)$$

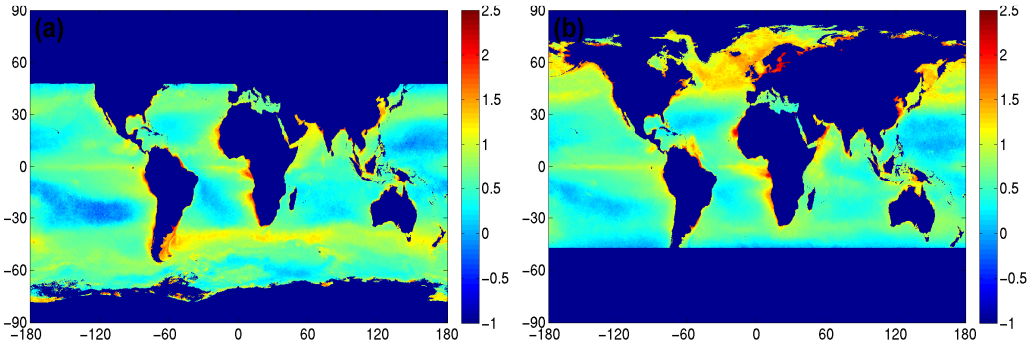

Figure 4.3: *Euphotic zone average net primary production rate (mg C m^{-3} d^{-1}) generated using an adapted version of the vertically generalised production model ($VGPM_{avg}$) for* ***(a)*** *January 1^{st}-8^{th} and* ***(b)*** *July 3^{rd}-10^{th}. Data spatial resolution is a $1/12^{th}$ degree latitude-longitude grid with an 8 day average temporal resolution. Data are converted to a log_{10} scale.*

The depth of the euphotic zone (z_eu) (m) is calculated using the Morel and Berthon (1989) Case I model for Case I waters. Case I waters are generally defined as waters whose inherent optical properties are primarily defined by phytoplankton biomass and the CDOM and detritus degradation products that co vary with the phytoplankton population. Case II waters are defined as "everything else" i.e. those waters where the optical properties are dominated by constituents whose concentrations do not covary with the phytoplankton concentration(Morel 1988). The Case I model used to establish the depth of the euphotic zone in this chapter is the same formulation utilised within the VGPM model (see Figure 4.4 a&b). The Case I model is two empirically fitted equations that estimate z_eu from surface chlorophyll, one for high chlorophyll concentrations and one for low chlorophyll concentration waters. First total water column chlorophyll is parameterised from surface chlorophyll (see equations 4.3– 4.6) and then the euphotic depth is calculated using equation 3.3. If the calculated z_eu is <= 102m then equation 3.4 is used. The equations are based on field observations but essentially describe an inverse relationship between chlorophyll concentration and light penetration (Morel and Berthon 1989). A 10 year climatology of SeaWiFS surface chlorophyll (1998-2007)

at the same spatial and temporal resolution as the $VGPM_{avg}$ net primary production data was utilised for surface chlorophyll and also as a variable within the analysis (see Figure 4.5 a & b).

If surface Chl < 1.0 mg m-3	$\boldsymbol{total\_chl = 38 \,.\, chl^{0.425}}$	*(4.3)*
else	$\boldsymbol{total\_chl = 40.2 \,.\, chl^{0.425}}$	*(4.4)*
	$\boldsymbol{z\_eu = 200 \,.\, total\_chl^{-0.293}}$	*(4.5)*
if z_eu <= 102 m	$\boldsymbol{z\_eu = 568.2 \,.\, total\_chl^{-0.746}}$	*(4.6)*

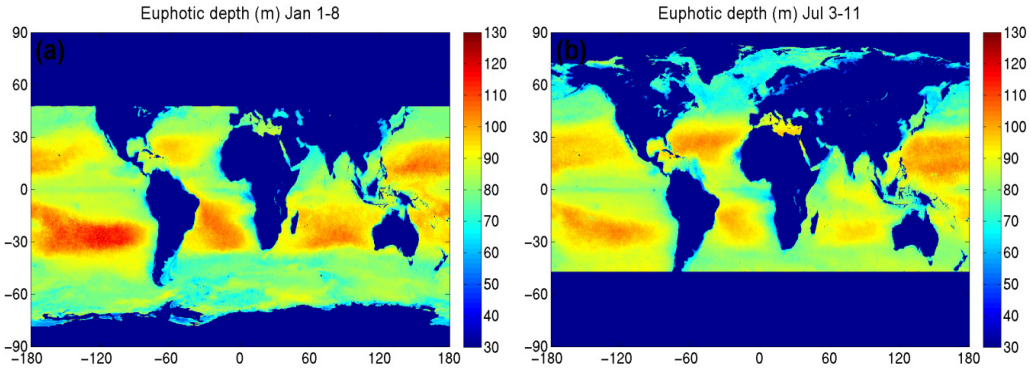

Figure 4.4: *Plots of calculated euphotic depth (z_eu) for* ***(a)*** *January 1st-8th and* ***(b)*** *July 3rd-10th. Euphotic depth is shown in meters (m) and is calculated using the Morel and Berthon (1989) Case I model in conjunction with a 10 year (1998-2007) Sea-viewing Wide Field-of-view Sensor (SeaWiFS) surface chlorophyll climatology (see figure 4.5). Data spatial resolution is a 1/12th degree latitude-longitude grid with an 8 day average temporal resolution.*

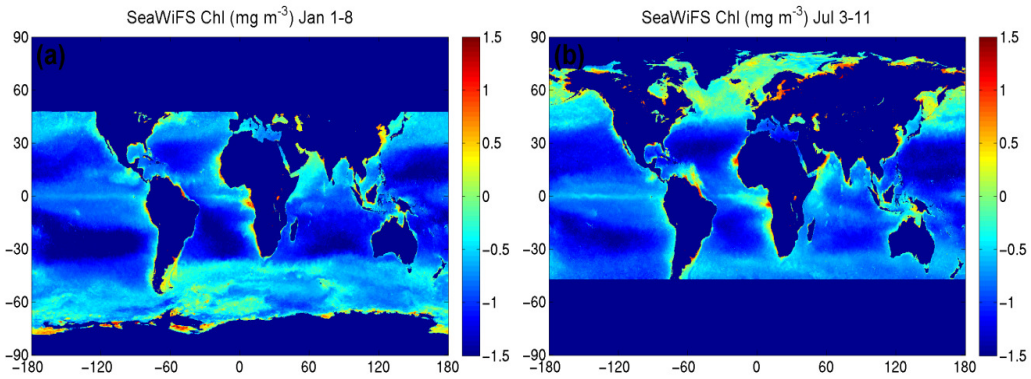

Figure 4.5: *Plots of satellite retrieved surface chlorophyll concentrations (mg m^{-3}) from the Sea-viewing Wide Field-of-view Sensor (SeaWiFS) satellite for* ***(a)*** *January 1^{st}-8^{th} and* ***(b)*** *July 3^{rd}-11^{th}. Data are converted to a log_{10} scale. Data spatial resolution is a $1/12^{th}$ degree latitude-longitude grid with an 8 day average temporal resolution.*

4.2.3 Underwater irradiance ($I_z$sat)

The second variable of interest indentified by chapter 3 as important in surface DMS dynamics is underwater irradiance (I_zsat). I_zsat is defined as the underwater fraction of the 24 hour average total solar surface radiation (I_0) at the DMS sample depth z in W m^{-2} (equation 4.7, Figure 4.6).

$$I_zsat = I_0 e^{-K_d \times z} \qquad (4.7)$$

I_0 is and estimated value and is a function of the latitude, date and geophysical constants. It assumes a 50% attenuation of the estimated top of the atmosphere value for total solar radiation (Brock 1981; Vallina and Simó 2007) (see chapter 3 for a discussion). The light attenuation coefficient (K_d, units m^{-1}, equation 4.8) is calculated following Vallina and Simó (2007) and Miles et al. (2009) where the depth of the euphotic zone (z_eu) is calculated using the Morel and Berthon (1989) case 1 model described above (see equation 4.3 - 4.6) in conjunction with the SeaWiFS chlorophyll climatology.

$$K_d = \frac{\ln(0.01)}{z\_eu} \qquad (4.8)$$

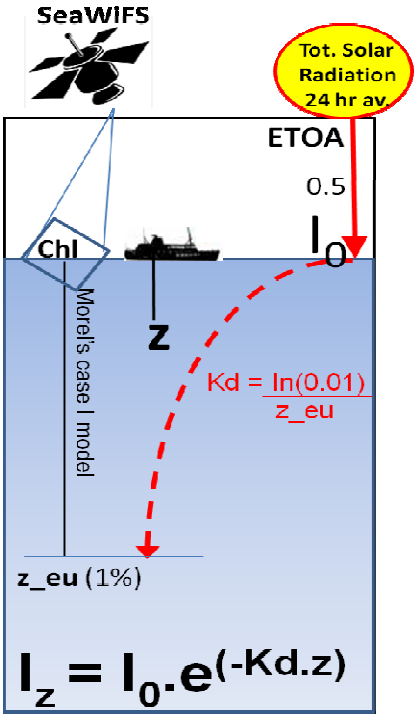

Figure 4.6: *Schematic of the calculation of underwater irradiance ($I_z sat$) where ETOA is the estimated top of the atmosphere radiation, I_0 is the estimated surface irradiance, z is the DMS sample depth, z_eu is the depth of the euphotic zone and Chl is the surface chlorophyll concentration.*

4.2.4 Data allocation method

A climatological primary production and SeaWiFS chlorophyll value is allocated to each individual DMS sample in the global DMS database. This is done using a "nearest neighbour" method whereby the nearest value in time (+/- 8 days max) and space (+/- ~12 km max) ($1/12^{th}$ degree grid: 9km at the equator) is allocated to each DMS sample. The underwater irradiance ($I_z sat$) is calculated for each DMS sample for the depth of the individual sample using the surface irradiance (I_0) at the exact latitude and date of the sample and using the light attenuation coefficient (K_d) derived from the nearest SeaWiFS chlorophyll climatology grid square in space and time (see Figure 4.6).

Not all DMS data within the DMS database was available due to the data availability of $VGPM_{avg}$ or $I_z sat$ data. Most missing data comes from the high latitude winter seasons in both hemispheres. This is because both $VGPM_{avg}$ and $I_z sat$ rely in part

upon SeaWiFS chlorophyll which is dependent upon sufficient surface leaving radiance to obtain ocean colour data. However, 86.4% of the original n = 47241 are included within the analysis. In contrast to other studies (Lana et al. 2011a; Simó and Dachs 2002; Vallina and Simó 2007) no data has been excluded prior to analysis based upon high DMS values or high values within the predictor variables.

4.2.5 Deriving training and validation data subsets

In all sections of the analysis the multivariate statistical models are developed in a randomly assigned training subset of the data and are tested in the remaining validation subset. This allows the strength and utility of any predictive relationships identified to be assessed (Weisberg 2005). In particular this prevents "over-fitted" models or models that have identified apparent relationships within the data but are in fact explaining random error or noise rather than a general trend from being developed (Weisberg 2005). The true test of a regression model is not its ability to maximally explain the variance in the training data but how the model performs within independent, unseen data (Weisberg 2005).

The training and validation subsets were derived using a random number generator to assign each DMS sample to a group. There is a trade off between the size of the training group and the validation group. It is desirable to develop as robust a model as possible (using as much data as possible) whist retaining enough data in the validation to successfully validate the model in a subset that provides a representative spread of the data. In sections 1 and 2 the data is spit 70:30 in favour of the training group. This split is in common with other studies and results in n = 28620 DMS-VGPM$_{avg}$-$I_z sat$ data triplets available for regression analysis within the training group and n = 12179 data triplets for the validation group (see Figure 4.7).

Section 4.3.3 seeks to develop separate MLR models for each biogeochemical province where sufficient data is available. To ensure enough data remains within each province to both develop and test an MLR model using monthly averaged data the database was split randomly 60:40 in favour of the training data on a province by province basis. For the province monthly analysis, a monthly average is defined as the average of all data from a single province for a single month if $n \geq 30$. In

addition, there must be at least $n \geq 4$ months of data from a given province in order to derive monthly MLR model for that province and there must be $n \geq 4$ within the validation subset for that province to test the model. Splitting the data 70:30 as in section 4.3.1and 4.3.2 resulted in too few data points within the province monthly training or validation province subsets (i.e. too few provinces with $n < 4$ monthly averaged data points). Splitting each province 50:50 reduced the skill of the developed MLR models whilst only increasing the number of province monthly averages available from n = 107 (60:40 split) to n = 116 (50:50 split).

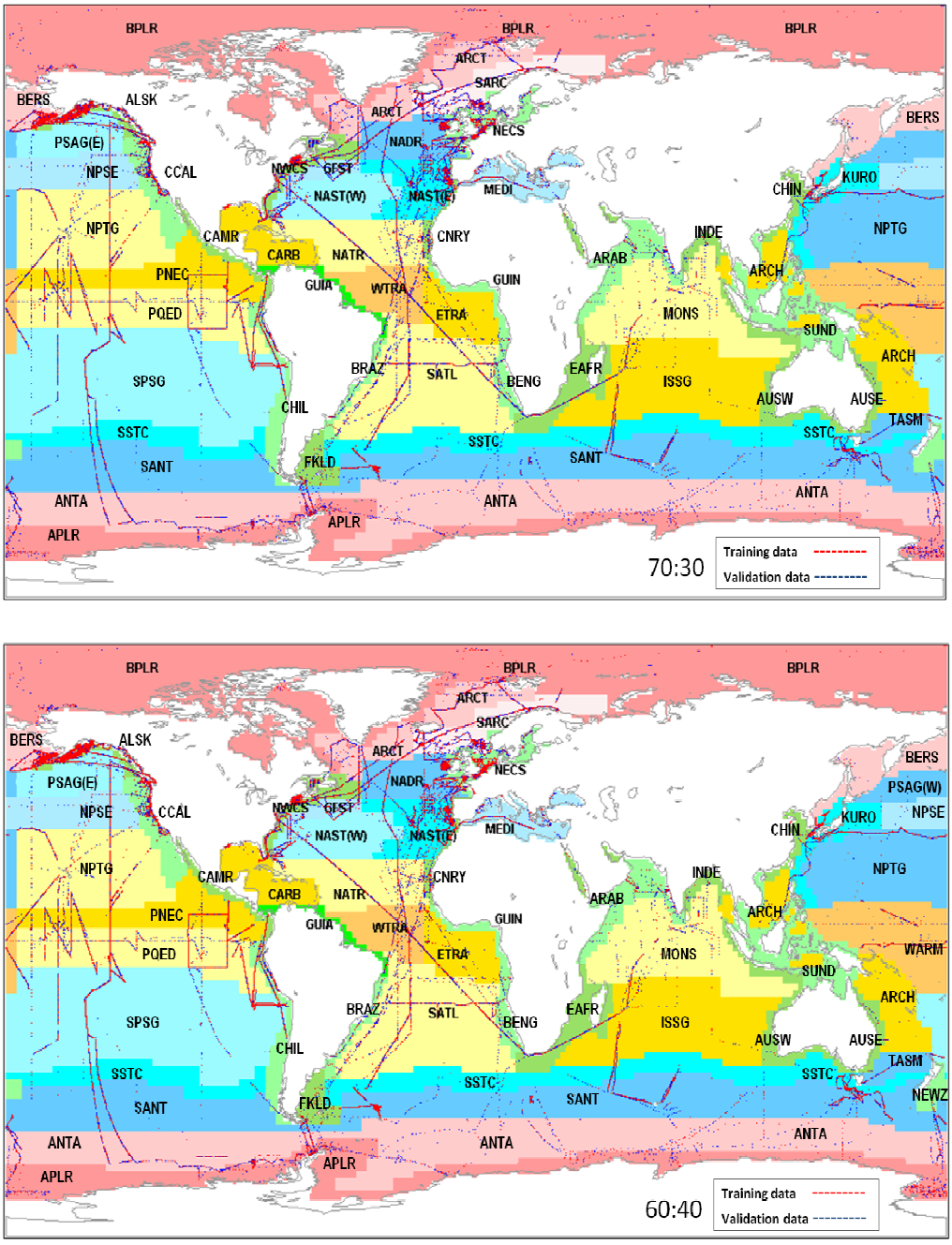

Figure 4.7: *maps showing* ***(top)*** *location of training (70%) and validation (30%) data used in sections 4.3.1 and 4.3.2 and* ***(bottom)*** *location of training (60%) and validation data (40%) split on a province by province basis used in section 4.3.3.In both figures biogeochemical provinces (Longhurst 1995) shaded in red tones belong to the Polar biogeochemical domain, those shaded in blue tones belong to the Westerlies domain, those shaded in yellow tones belong to the Trades domain and those provinces shaded in a green tone belong to the Coastal domain. Each province is labelled with an abbreviation, for the full province names see Table A.0.1 (appendix).*

4.3 Results and discussion

Section 4.3.1 explores the relationship between climatological primary production and climatological underwater irradiance data and the high resolution, un-averaged global surface DMS database. Section 4.3.2 investigates a method of aggregating the data using biologically relevant spatial units to isolate any large scale trends in global DMS above the noise of natural variability, sampling and data issues present within the global DMS database. Section 4.3.3 investigates the relationship between DMS, primary production and water-attenuated irradiance within each biogeochemical province. In response to evidence from the literature (see introduction: section 4.1) that a single model may not be able to successfully predict surface DMS concentrations in all regions, a composite method of predicting DMS is introduced. Separate MLR models are derived for each biogeochemical province which are then combined to predict global DMS. This method is explored using both the high resolution data and province monthly data.

4.3.1 Analysis of the high resolution DMS data

This section utilises data at as high a spatial and temporal resolution as possible without aggregating the DMS data. Initially to establish confidence in the ability of the climatological primary production and underwater irradiance data and the methods used to derive them (see methods section), the climatological variables are compared to the known, *in situ* surface values for primary production and underwater irradiance from chapter 3 (see section 3.3). A similar procedure to chapter 3 is then followed to assess whether a single multiple linear regression model can be successfully developed for the high resolution, global surface DMS data using a combination of climatological primary production and underwater irradiance. The model is derived using a random subset of the data (70%) and its ability to predict DMS is tested in the remaining validation data subset.

4.3.1.1 "Sea truthing" the climatological data using the *in situ* database from chapter 3

The original VGPM model data has been validated by the data providers using an extensive field data set ($r^2 = 0.87$, n = 1693) (Behrenfeld and Falkowski 1997b). The independent validation conducted in this analysis demonstrates that the method used to derive surface primary production from the integrated values (see methods: section 4.2) successfully replicates the *in situ* surface primary production values from chapter 3. The correlation between the *in situ* surface primary production data from chapter 3 and the climatological primary production data ($VGPM_{avg}$) is strong and significant ($\rho = 0.85$, n = 45, $p < 0.01$) (see figure 4.8). This is despite the $VGPM_{avg}$ data describing a euphotic zone average primary production rate whereas the *in situ* primary production data ranges from 0-10m (the definition of the surface used in chapter 3). The $VGPM_{avg}$ primary production rate underestimates the *in situ* primary production rate data at higher production rates. This may be because the *in situ*, surface data is subject to higher irradiance relative to the euphotic zone averaged irradiances.

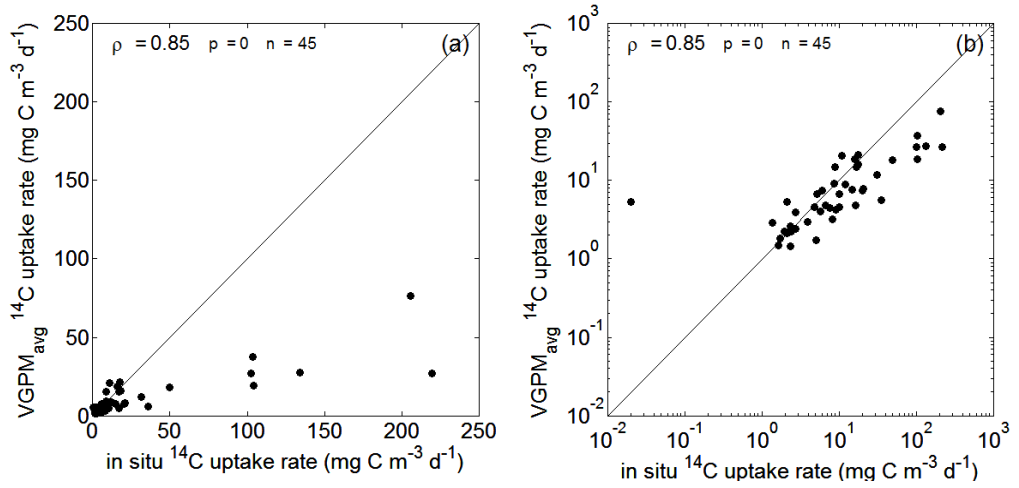

Figure 4.8: (a) *Climatological euphotic zone average daily primary production rate (mg C m^{-3} d^{-1}) using the adapted Vertically Generalised Production Model ($VGPM_{avg}$) (see section 4.2.2) plotted against the surface (0-10m) daily in situ primary production rate data (mg C m^{-3} d^{-1}) from chapter 3 (see section 3.4) and* ***(b)*** *same data plotted on log-log axis. Also shown is a 1:1 line and the Spearman's Rank correlation coefficient ($\rho = 0.85$) p value ($p = 0$) and number of data points ($n = 45$).*

The correlation between the *in situ* surface underwater irradiance data (I_z*insitu*) and climatological underwater irradiance data (I_z*sat*) is also strong and significant (ρ = 0.89, n = 38, p <0.01). This may be partly expected as both I_z*insitu* and I_z*sat* use the same method to calculate the surface radiation (I_0) (see chapter 2 methods for calculation of I_0). The two measures differ in the way that light attenuation to depth z is implemented. The *in situ* I_z uses *in situ*, measured light attenuation data for each DMS sample at depth z. The climatological I_z calculates the attenuated irradiance at depth z using a parameterisation based on surface SeaWiFS Chl data (see methods section 4.2). This strong and significant correlation between I_z*insitu* and I_z*sat* indicates that the I_z*sat* method replicates the conversion of surface irradiance (I_0) to irradiance at depth z (I_z) successfully. Previous authors have suggested that it is the attenuation of surface irradiance that introduces the greater uncertainty when determining underwater irradiances (Baker and Frouin 1987; Smith and Baker 1981; Tedetti and Sempere 2006).

4.3.1.2 Developing a MLR model using the high resolution DMS data

Prior to analysis the global DMS database was randomly divided into two data subsets, a training subset (random 70% of the data) which will be used to develop multivariate statistical model and a validation subset (remaining 30%) which will be use to test the model (see methods section 4.2).

Initially an analysis of the bivariate correlations between DMS, the climatological primary production and underwater irradiance data and other available variables within the test data subset was conducted (see
Table **4.1**). There are significant but relatively weak correlations between DMS and primary production, underwater irradiance and SeaWiFS chlorophyll. The correlations are strong and significant between primary production and SeaWiFS chlorophyll. This is not unexpected as VGPM is a chlorophyll based production model (see methods section 4.2). The correlation between DMS and SST and DMS and salinity are weak. Salinity (dimensionless) and SST (^{o}C) are available from the DMS database and are concurrently sampled with DMS *in situ.*

Table 4.1: *Bivariate correlations using the non parametric Spearman's rank hypothesis (ρ) between the high resolution data within the training data subset (randomly assigned 70% of all available data, see section 4.2.5). Also shown is the two tailed significance value (Sig.) and number or data points (n). Correlations marked with a single asterisk* are significant at the 0.05 level, correlations marked with a double asterisk** are significant at the 0.01. Correlations without an asterisk fall below the 0.05 significance level.*

		DMS	Water attenuated irradiance ($I_z sat$)	Chlorophyll (SeaWiFS)	Primary Production ($VGPM_{avg}$)	Sea Surface Temperature	Salinity
DMS	ρ	1.000	**.30****	**.24****	**.35****	**.07****	**-.07****
	Sig. (2-tailed)	.	.000	.000	.000	.000	.000
	n	33148	29321	31749	30776	29220	23823
Water attenuated irradiance ($I_z sat$)	ρ		1.000	**-.30****	**-.03****	**.45****	**.31****
	Sig. (2-tailed)		.	.000	.000	.000	.000
	n		29321	29321	28620	26136	21697
Chlorophyll (SeaWiFS)	ρ			1.000	**.87****	**-.56****	**-.65****
	Sig. (2-tailed)			.	.000	.000	.000
	n			31749	30776	28080	22940
Primary Production ($VGPM_{avg}$)	ρ				1.000	**-.28****	**-.40****
	Sig. (2-tailed)				.	.000	.000
	n				30776	27323	22220
Sea Surface Temperature	ρ					1.000	**.47****
	Sig. (2-tailed)					.	.000
	n					29220	23748
Salinity	ρ						1.000
	Sig. (2-tailed)						.
	n						23823

A multiple linear regression model was constructed using the climatological primary production and underwater irradiance to predict and explain the variance in high resolution global surface DMS. Using the training data subset to develop the model, the combination of $I_z sat$ and $VGPM_{avg}$ within a MLR analysis yields a multiple correlation coefficient of R = 0.47, with the adjusted R^2 = 0.23 (non-adjusted is also

R^2 = 0.23) (n = 28620, p <0.01) (see equation 4.9). The variables are $\log_{10}$ transformed to account for the non-normal distribution of the data (see methods section 4.2). The Spearman's rank correlation between the MLR predicted vs. observed DMS (ρ = 0.47, p < 0.01, n = 28620) within the training data is the same as the R indicating that the distribution of the data is close to normal and not biasing the result. This multiple correlation is stronger than the bivariate correlations between DMS and the independent explanatory variables within the MLR which are significant but relatively weak (see
Table **4.1**) The tolerance statistic is significantly greater than zero (0.987) indicating that the MLR does not suffer from high multicolinearity and that only 1.3 % of the explained variance is shared between the explanatory variables within the MLR. The R^2 is statistically adjusted to account for the possible spurious increases in correlation due to additional explanatory variables being added to the model (Weisberg 2005)(see chapter 3 methods for discussion). The adjusted and non adjusted R^2 are the same indicating that the model does not suffer from this spurious increase (Weisberg 2005). In addition the multiple correlation coefficient is stronger than the bivariate correlations between DMS and SeaWiFS chlorophyll, sea surface temperature (SST) or salinity (see
Table **4.1**).

$$\log_{10} \mathrm{DMS} = -1.850 + 0.326\left(\log_{10} \mathrm{VGPM}_{\mathrm{avg}}\right) + 0.874(\log_{10} I_z sat) \qquad (4.9)$$

This model derived using MLR within the training data (randomly assigned 70%) is then tested within the validation subset (remaining 30%). Figure 4.9 shows a plot of the predicted DMS (using equation 4.9) vs. the observed DMS within the validation subset. Predicted DMS is significantly correlated to the observed DMS but this correlation is not strong (ρ = 0.48, r = 0.49, p <0.01, n = 12179) and is only able to explain 24% of the variance in observed DMS concentrations (r^2 = 0.24). The model is able to explain a similar amount of variance within the validation data (24%) as was explicable within the training data (22%). This suggests that the model is not "over-fitted" (Weisberg 2005; Wilcox 2010) (see methods section 4.2).

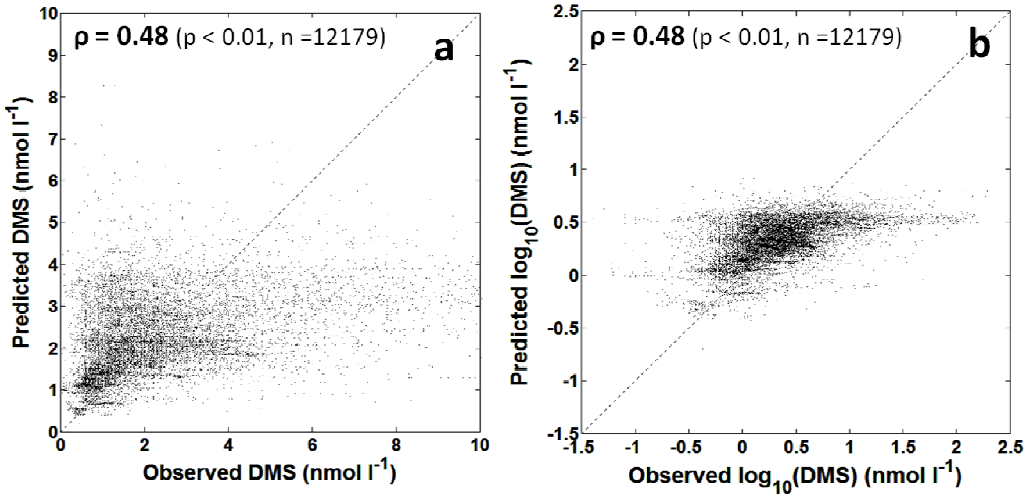

Figure 4.9: *Predicted high resolution DMS (nmol l^{-1}) plotted against observed high resolution DMS data (nmol l^{-1}) within the validation data subset of the global DMS database (http://saga.pmel.noaa.gov/dms/). Predicted DMS is calculated using the multiple linear regression model developed within the high resolution training data subset $log_{10}(DMS) = -1.850 + 0.326*log_{10}(VGPM_{avg}) + 0.874*log_{10}(I_z sat)$ (see section 4.3.1.2). For details of the derivation of the training and validation subsets see section 4.2.5. Panel* ***(a)*** *shows the data with the axis limited to 10 nmol l^{-1} and panel* ***(b)*** *shows the same data on a log_{10} scale with no axis limitation. Also shown is the Spearman's rank correlation coefficient (ρ), the significance value (p) and the number of data points (n). Dashed line is a 1:1 tend line.*

This regression model does not explain enough variance within training data or the validation data to be useful as a predictive tool at this resolution. As in other work (Kettle et al. 1999; Kettle and Andreae 2000; Lana et al. 2011a), the bivariate correlations between the high resolution DMS and biotic or abiotic variables are not strong ($\rho < 0.5$). However, the strength of these correlations must be viewed within the context of the data within the DMS database.

As discussed in the introduction the global DMS database consists of many discrete samples that represent brief snapshots of the highly variable and dynamic surface DMS ecosystem. The ambient surface DMS concentration at any given point in space and time depends upon the complex interaction between the sources and sinks of DMS to the marine ecosystem (Stefels et al 2007). The relative importance of

these sources and sinks will change in space and time and will be affected by the environmental history of the sampled water column (Kieber et al. 1996). This natural variability is combined with potential noise from the different sampling strategies (e.g. bloom focus vs. transects) and sampling and analysis techniques (e.g. gas chromatography vs. mass spectrometry (Bell et al. 2011)). This is also coupled with incomplete spatial and temporal coverage with unknown inter-annual variability within the global DMS database. Furthermore correlations are sought with climatological variables which are disconnected in time space from the DMS samples (e.g. $VGPM_{avg}$ 10 year average with a $1/12^{th}$ degree grid by 8 day temporal resolution). For example the climatological values will not be able to capture the transient high chlorophyll concentrations or primary production rates observed in localised phytoplankton blooms.

It may therefore be impossible to observe strong correlations between environmental variables and the raw, "noisy" data. In order to identify the larger scale properties and drivers of the DMS ecosystem it is necessary to average the data to distil these features above the noise within the global DMS database. An approach to averaging the data using biologically coherent spatial units is explored in the next section.

4.3.2 Data aggregation based on biologically coherent spatial units

This section investigates whether any large scale trends in global DMS can be isolated above the noise of natural variability found in such a complex and dynamic system and the potential noise introduced by sampling and data issues present in a large global database constructed from many sources over a long time period. Monthly averages using a biologically relevant spatial unit, the biogeochemical provinces defined by Longhurst (1995) are calculated. These "province monthly averages" are then used to derive a single multivariate regression model for surface DMS. Again the model is derived using the training data subset (70%) and validated in the remaining data.

4.3.2.1 Aggregation method

The DMS database contains a large number of samples but the data is not uniform in its spatial and temporal coverage (see Figure 4.1). This is further complicated when the dataset is reduced in size by splitting the data in to training and validation subsets (70:30). This dictates that a relatively large box size is required to capture enough data to generate a representative monthly average.

In this analysis, we are interested to see whether the biological characteristics of the data and the environmental setting (e.g. the rate of primary production and the underwater irradiance conditions) are correlated with, and are able to predict, the concentration of DMS in the global surface ocean. When designing a spatial-temporal unit over which to aggregate there is therefore a trade off between capturing enough data to generate a representative average, generating enough spatial-temporal units to generate a reliable statistical model that also provides globally representative coverage, and not having the spatial-temporal unit so large that the data becomes over smoothed so that the characteristics of interest contained within the data become lost.

Previous analyses have used arbitrary grids based upon latitude and longitude as spatial units (e.g. Lana et al. 2011b; Vallina and Simó 2007; Simó and Dachs 2002). Due to the limited data coverage the use of too small a grid (e.g. a 1^{o} x 1^{o} grid) does not allow enough data in each grid to provide a representative average. Once the grid becomes too large (e.g. a 10^{o} x 20^{o} grid) the aggregation unit does not respect the characteristics of the data so that data from disparate biologically regimes are arbitrarily grouped together. Therefore a relatively large but biologically coherent spatial unit is required. In this analysis we use the biogeochemical province defined by Longhurst (1995) with a temporal resolution of a month. The number of samples required to before a province monthly average is calculated is $n \geq 30$.

55 out of 57 provinces defined by Longhurst (1995) contain some DMS data (n>=1). Using this aggregation method, 180 monthly province averages are available within the training data subset with 44 out of 55 (80%) provinces represented by at least one "province month" of data (see Figure 4.10). Within the validation data 114 province months are available with 36 out of 55 (~65%) of provinces represented by at least

one “province month”. Both the training data and validation data subsets include provinces months from all 4 biogeochemical domains as defined by Longhurst (1995) representing a range of latitudes and trophic regimes from eutrophic to oligotrophic regions.

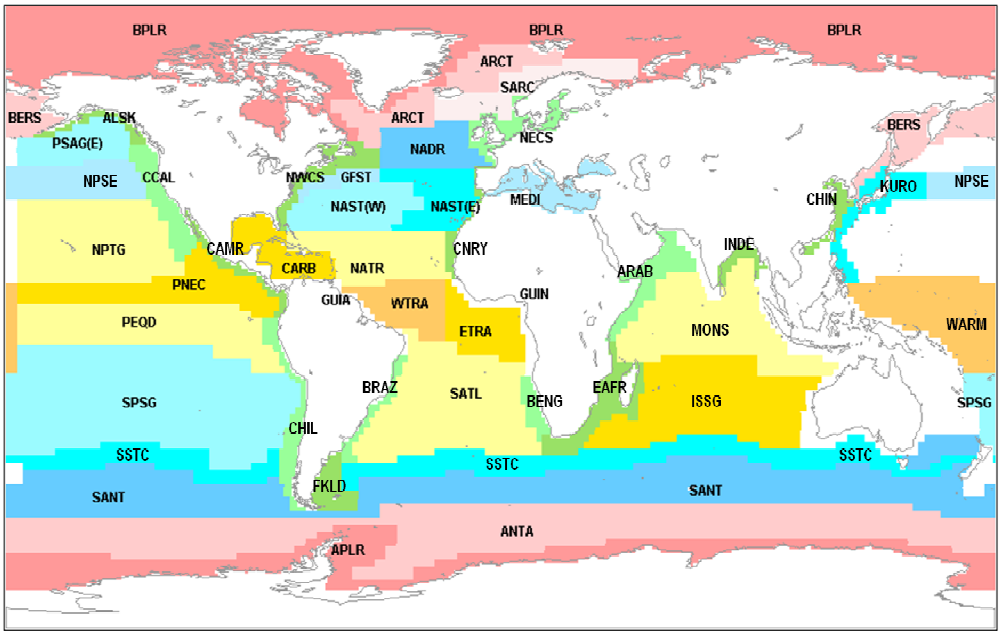

Figure 4.10: *Shaded areas represent the location of the 44 out of the 57 provinces defined by Longhurst (1995) where at least one month of data is included within the MLR model. Areas shaded in red tones belong to the Polar domain, those shaded in blue tones belong to the Westerlies domain, those shaded in yellow tones belong to the Trades domain and those provinces shaded in a green tone belong to the Coastal domain. Each province is labelled with an abbreviation, for the full province names see Table A.0.1 (appendix).*

4.3.2.2 Model development and validation

Initially an analysis of the bivariate correlations between the province monthly averaged variables was conducted (see Table 4.2). The correlations between province monthly DMS and primary production rate and underwater irradiance are strong and significant. The correlation between primary production rate and DMS is stronger than the correlation between DMS and SeaWiFS chlorophyll which is significant but not strong. The primary production rate and chlorophyll are correlated

because VGPM is a chlorophyll based model (see methods section 4.2). Water attenuated irradiance is not strongly correlated with SeaWiFS chlorophyll.

Table 4.2: *Bivariate correlations using the non parametric Spearman's rank hypothesis (ρ) between the province monthly averaged data within the training data subset (randomly assigned 70% of all available data, see section 4.2.5). Also shown is the two tailed significance value (Sig.) and number or data points (n). Correlations marked with a single asterisk* are significant at the 0.05 level, correlations marked with a double asterisk** are significant at the 0.01. Correlations without an asterisk fall below the 0.05 significance level.*

		DMS	Primary Production ($VGPM_{avg}$)	Chlorophyll (SeaWiFS)	Water attenuated irradiance ($I_z sat$)
DMS	*P*	1.000	.47**	.33**	.60**
	Sig. (2-tailed)	.	.000	.000	.000
	N	182	182	182	180
Primary Production ($VGPM_{avg}$)	*P*		1.000	.88**	.16*
	Sig. (2-tailed)		.	.000	.037
	N		182	182	180
Chlorophyll (SeaWiFS)	*P*			1.000	-.08
	Sig. (2-tailed)			.	.289
	N			182	180
Water attenuated irradiance ($I_z sat$)	*P*				1.000
	Sig. (2-tailed)				.
	N				180

**. Correlation is significant at the 0.01 level (2-tailed).

*. Correlation is significant at the 0.05 level (2-tailed).

A MLR model is developed using province monthly averaged data with climatological primary production ($VGPM_{avg}$) and climatological underwater irradiance ($I_z sat$) as explanatory variables (equation 4.10). This model is developed within the same training data subset defined in section 4.3.1. The variables are $\log_{10}$ transformed to correct for the non-normal distribution of the data (see methods section 4.2).

$$\log_{10} \mathrm{DMS} = -2.847 + 0.310\left(\log_{10} \mathrm{VGPM}_{\mathrm{avg}}\right) + 1.381\left(\log_{10} I_z sat\right) \qquad (4.10)$$

The correlation between the MLR modelled DMS and observed DMS within the training data is strong and significant ($\rho = 0.70$, $R = 0.74$, adjusted $R^2 = 0.53$ (unadjusted $R^2 = 0.54$) ($p < 0.01$, $n = 180$)) and is able to explain 53% of the variance in the training data province monthly DMS values. The R^2 is statistically adjusted to correct for additional terms in the model artificially increasing the correlation ((Weisberg 2005) see chapter 3, section 3.3). The adjusted and non adjusted R^2 are very similar indicating that the explicable variance is not due to spurious increases due to additional model terms (Weisberg 2005). The tolerance statistic is significantly greater than zero (0.952) indicating that the MLR does not suffer from high multicolinearity (Weisberg 2005). Supporting this, $VGPM_{avg}$ and $I_z sat$ are not strongly correlated $\rho = 0.16$ ($p = 0.37$, $n = 180$). These diagnostic statistics indicate that the two separate explanatory variables within the MLR are explaining different parts of the explicable variance in DMS and that this is not an artefact of the number of terms in the regression model.

This model developed within the training data (equation 4.10) is then tested using the validation subset. Figure 4.11 shows a predicted vs. observed plot using the equation 4.10 and applied to the validation dataset. Each data point represents an average of a single months data ($n >= 30$) from a single biogeochemical province (province month). The correlation between province monthly predicted and observed DMS is strong and significant ($\rho = 0.70$, $r = 0.73$, $p < 0.01$, $n = 114$) with the predicted DMS able to explain 53% of the observed DMS ($r^2 = 0.53$). The model is able to explain the same amount of variance within the validation data (53%) as was explicable within the training data (53%). This suggests that the model is not "over-fitted" (Weisberg 2005).

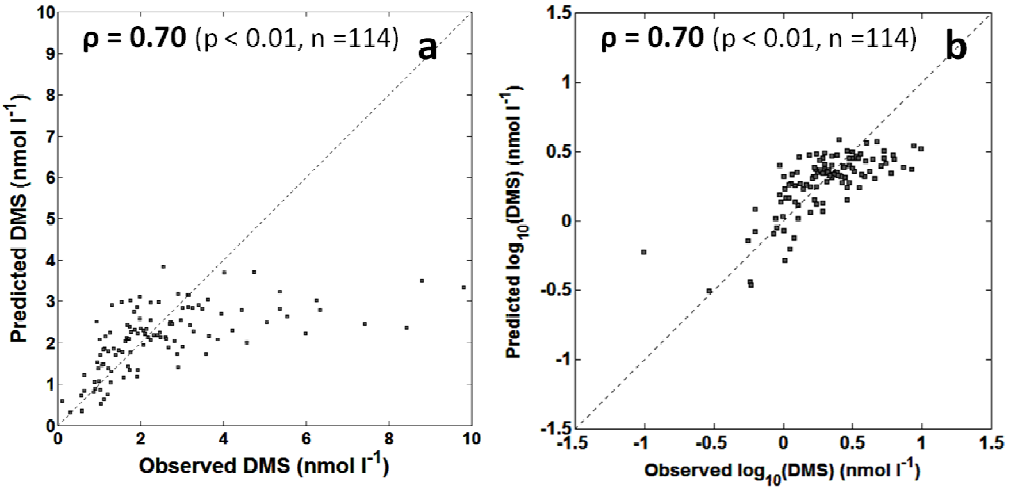

Figure 4.11 *Predicted province monthly averaged DMS (nmol l^{-1}) plotted against observed province monthly averaged DMS data (nmol l^{-1}) within the validation data subset of the global DMS database (http://saga.pmel.noaa.gov/dms/). Predicted DMS is calculated using the multiple linear regression model developed within the province monthly training data subset $log_{10}(DMS) = -2.847 + 0.310.log_{10}(VGPM_{avg}) + 1.381.log_{10}(I_z sat)$ (see section 4.3.2.2). For details of the derivation of the training and validation subsets see section 4.2.5 and for details of the derivation of the province monthly averages see section 4.3.2.1. Panel* ***(a)*** *shows the data with the axis limited to 10 nmol l^{-1} and panel* ***(b)*** *shows the same data on a log_{10} scale with no axis limitation. Also shown is the Spearman's rank correlation coefficient (ρ), the significance value (p) and the number of data points (n). Dashed line is a 1:1 trend line.*

This model using province monthly data is able to explain more of the variance in DMS concentrations (53%) than the model derived and tested using the high resolution DMS data in section 4.3.1.2 (24%). Upon examination, Figure 4.10 shows the model performs best at predicting low to approximately average DMS concentrations (average DMS = 4.24 nmol l^{-1}). This is not an insignificant result as ~80.5% (38009/47241) of the DMS samples in the global database are below the 4.24 nmol l^{-1} average value. DMS concentrations >~4.24 nmol l^{-1} are subject to more variance about the 1:1 line with the model underestimating high DMS concentrations. This may be due to the smoothed, climatological nature of the predictor variables used within the MLR models as compared to the global DMS

database which is comprised of *in situ* non-smoothed samples. The high DMS concentrations observed within localised blooms within the *in situ* data from the DMS database will not be replicated by similar peaks in production/biomass within the smoothed climatological predictor variables. Although the averaging of the DMS by province month will reduce the impact of high DMS values it may still be influencing them.

An approach using the province monthly median value was investigated but this did not improve upon or produce significantly different results however. The analysis was also re-run with high DMS (DMS > 99.9th percentile of 148.44 nmol l^{-1} where max = 420 nmol l^{-1}) values excluded prior to analysis. There were no significant changes in the strengths of the bivariate correlations or the amount of variance explained by the MLR models observed. This would suggest that although the climatological nature of the predictor variables may be affecting the skill of the model to predict higher DMS concentrations, it may also be likely that other factors are important. Species composition of the phytoplankton and bacterial community, the rate of grazing, cell lysis, autolysis and interactions between the rate of primary production/biomass and irradiance driven processes may affect the slope of the relationship between the individual predictor variables and DMS. To try and account for this the next section explores using a composite method to predict global surface DMS.

4.3.3 A composite method for the prediction of surface DMS

In response to evidence from the literature (see introduction), this section aims to investigate if allowing relative magnitude and slope of the predictor variables (primary production and underwater irradiance) to vary between provinces improves the explanatory power. A method of deriving a separate MLR model for each of the biogeochemical provinces that contains sufficient DMS data is developed. These MLR models are then combined to predict surface DMS. The MLR models use the same two explanatory variables ($VGPM_{avg}$ and $I_z sat$) to predict surface DMS concentrations but the relative contribution of the variables (magnitude of the coefficients) is derived separately for each province. A MLR model is developed for both the high resolution "raw" data and for province monthly data.

4.3.3.1 Composite methodology

The MLR models are again developed using a training subset and tested using a validation subset. This process was slightly different from the split in sections 4.3.1 and 4.3.2 (see methods section 4.2). To ensure enough data remains within each province to both develop and test an MLR model the data was split randomly 60:40 in favour of the training data on a province by province basis. As in section 2 a criteria of n≥ 30 data points from a single province month are required to calculate an average. In addition there must be n ≥ 4 months from a single province to develop a MLR model and n ≥ 4 months from that province to test the model.

For the province monthly analysis the criteria described above reduced the number of provinces for which a MLR model could be developed and validated to 20 out of 57 provinces with a total of n = 180 province monthly averages included within the training subset and n = 107 included in the validation subset. Table 4.3 shows the provinces that are included in the province monthly composite analysis. The table details which biogeochemical domain the provinces are from and for which months data is available within both the training data and validation data subsets for each province. Figure 4.12 shows the geographic location of the provinces. There are no provinces where 12 months of monthly data (averages of n ≥30) are available. Within the training data the maximum number of months in a single province is 9 (with a median value of 6 months per province). Within the validation data subset the maximum number of months in a single province is 8 (with the median value of 5 months per province). The DMS database has a sampling bias with some provinces particular poorly represented. For example, Figure 4.1 shows that the high latitude winters are relatively under sampled. This introduces potential statistical bias into any analysis of the global DMS database. It would be ideal to have the full seasonal cycle of 12 months of data from each province to develop and validate the MLR models but this is not possible. The minimum number of months from a single province used to develop a model in this analysis is 4 with the potential for these to be 4 consecutive months (e.g. 4 summer months) although this is often not the case (see Table 4.3). An MLR model developed for a province under this scenario is likely to be less reliable at predicting data outside the range of months from which

they were developed (e.g. winter data) than models developed from data which includes a greater seasonal span of months. Table 4.3 indicates the number of months used for each model which can be used to infer the potential predictive capacity of the individual province models.

All 6 provinces from the polar biogeochemical domain are included, 6 provinces out of 16 from the Westerlies domain are included, 4 out of 12 provinces from the Trade winds domain are represented and 4 out of the 23 Coastal domain provinces are included within the analysis. A large number of unrepresented provinces come from the coastal domain as DMS research tends to focus on open ocean environments where DMS emissions are most climatically relevant (Bates et al. 1992; Twomey 1991). 16 out of 33 of all open ocean provinces (~49%) are included. In total the provinces for which there is data cover ~66% of the global oceans by area. These provinces include data from all four Longhurst (1995) biogeochemical domains and span eutrophic, mesotrophic and oligotrophic regions from a range of latitudes.

Table 4.3: *Details of the provinces included in the monthly composite analysis including: province key, full province name, the trophic status of the province based upon province average SeaWiFS chlorophyll concentration (E = Eutrophic > 1.0 mg l^{-1}, M = Mesotrophic 0.18-1.0 mg l^{-1},O = Oligotrophic < 0.18 mg l^{-1}) following Belviso et al. (2011) (after Morel (2010)), the biogeochemical domain (BGCD) to which the province belongs (Longhurst 1995) (P = Polar, C = Coastal, W = Westerlies, T = Trades) and the monthly averages available within each province within the training and validation subsets.*

Province Key	**Full province name**	**Tropic Status**	**BGCD**	**Months available in training subset**													**Months available in validation subset**											
				N	J	F	M	A	M	J	J	A	S	O	N	D	**N**	J	F	M	A	M	J	J	A	S	O	N	D
BPLR	Boreal Polar Province	E	P	**5**				x			x	x	x	x			**4**				x			x	x	x			
ARCT	Atlantic Arctic Province	E	P	**6**			x	x	x		x		x	x			**4**			x	x			x			x		
SARC	Atlantic Subarctic Province	E	P	**5**			x	x	x	x	x						**4**				x	x	x	x					
BERS	N. Pacific Epicontinental Province	E	P	**4**			x		x	x		x					**4**			x		x	x		x				
ANTA	Antarctic Province	E	P	**6**	x	x	x	x							x	x	**6**	x	x	x	x							x	x
APLR	Austral Polar Province	E	P	**5**	x	x	x								x	x	**4**	x	x									x	x
NECS	NE Atlantic Shelves Province	E	C	**9**	x	x	x	x	x	x	x	x	x				**8**	x		x	x	x	x	x	x	x			
NWCS	NW Atlantic Shelves Province	E	C	**8**		x	x	x	x		x	x	x	x			**8**		x	x	x	x		x	x	x	x		
ALSK	Alaska Down-welling Coastal Province	E	C	**6**		x	x		x	x	x	x					**6**		x	x		x	x	x	x				
CCAL	California Upwelling Coastal Province	E	C	**6**		x		x	x	x		x			x		**5**				x	x	x		x			x	
NADR	N. Atlantic Drift Province	M	W	**7**			x	x	x	x	x		x	x			**7**			x	x	x	x	x		x	x		
PSAG(E)	Pacific Subarctic Gyre Province East	M	W	**5**		x	x		x	x	x						**5**		x	x		x	x	x					
SANT	Sub-Antarctic Province	M	W	**7**	x	x	x	x				x			x	x	**6**	x		x	x				x			x	x
PNEC	N. Pacific Equatorial Counter-current Prov	M	T	**5**		x	x	x						x	x		**5**		x	x	x						x	x	
PEQD	Pacific Equatorial Divergence Province	M	T	**8**		x	x	x	x		x			x	x	x	**7**		x	x	x			x			x	x	x
NAST(W)	N. Atlantic Subtropical Gyre Prov West	O	W	**6**	x	x	x				x		x	x			**5**	x	x					x		x	x		
NAST(E)	N. Atlantic Subtropical Gyre Province East	O	W	**6**		x		x		x	x		x	x			**5**				x		x	x		x	x		
SPSG	S. Pacific Subtropical Gyre Province	O	W	**7**	x	x	x	x						x	x	x	**6**		x	x	x						x	x	x
SATL	South Atlantic Gyre Province	O	T	**4**		x	x							x	x		**4**		x	x							x	x	
NPTG	N. Pacific Tropical Gyre Province	O	T	6		x	x	x						x	x	x	**4**		x	x	x								x

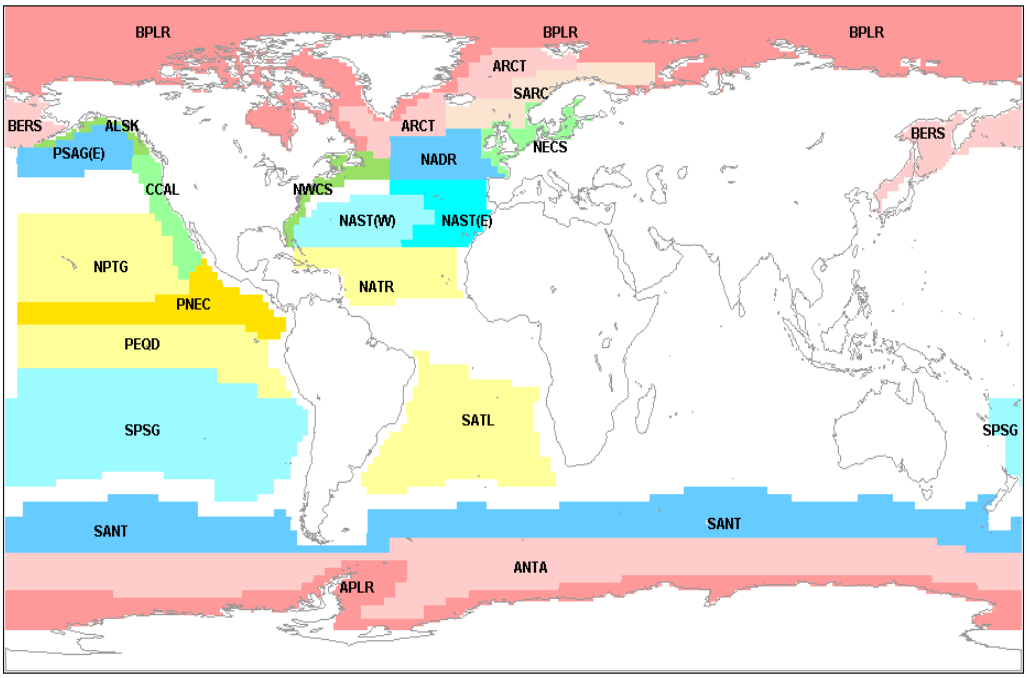

Figure 4.12: *Location of biogeochemical provinces defined by Longhurst (1995) included within the monthly composite analysis (shaded and labelled provinces). Provinces shaded in red tones belong to the Polar domain, those shaded in blue tones belong to the Westerlies domain, those shaded in yellow tones belong to the Trades domain and those provinces shaded in a green tone belong to the Coastal domain. Each province is labelled with an abbreviation, for the full province names see Table 4.3.*

4.3.3.2 Composite method monthly data results

Figure 4.13 shows predicted vs. observed province monthly averages of DMS within the validation subset using the composite method of combining the MLR models developed within the 20 available provinces. The correlation between the composite predicted and observed DMS using the province monthly approach within the validation subset is strong and significant ($\rho = 0.93$, $p = 0$, $n = 107$). This composite method also provides strong and significant correlations within the four biogeochemical domains and within the regions defined by trophic status (see Table 4.4).

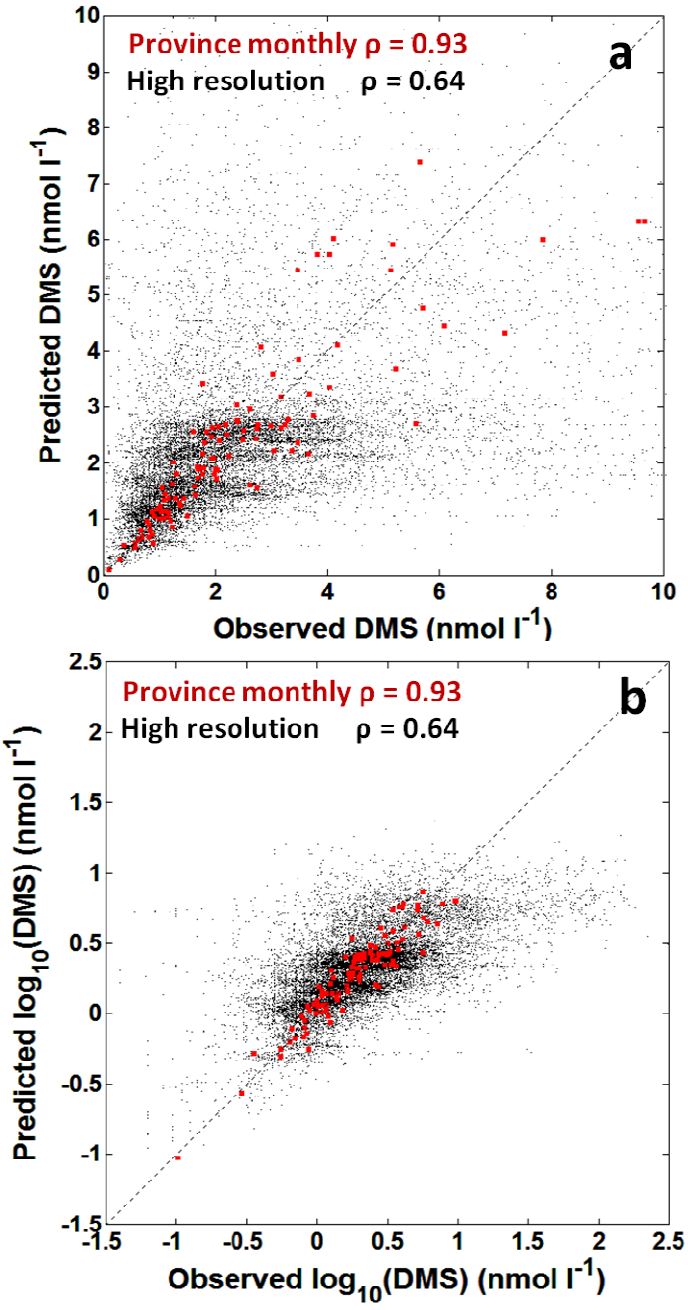

Figure 4.13: *Predicted DMS (nmol l^{-1}) plotted against observed DMS data (nmol l^{-1}) within the validation data subset of the global DMS database (http://saga.pmel.noaa.gov/dms/). Predicted DMS is calculated using the "composite method" (see section 4.3.3.1 for details on composite method). Panel* ***(a)*** *shows the data with the axis limited to 10 nmol l^{-1} and panel, large red markers represent province monthly averaged data and smaller black markers represent the high resolution (non averaged) data. Panel* ***(b)*** *shows the same data on a log_{10} scale with no axis limitation. Also shown is the Spearman's rank correlation coefficient (ρ), the significance value (p) and the number of data points (n). Dashed line is a 1:1 trend line.*

Table 4.4: *Regional predicted vs. observed correlations (Spearman's rank hypothesis (ρ)) within the validation data using the composite method. Regions are groups of Longhurst (1995) biogeochemical provinces assigned a trophic status based on province average chlorophyll concentration (Eutrophic > 1.0 mg l^{-1}, Mesotrophic 0.18-1.0 mg l^{-1}, Oligotrophic < 0.18 mg l^{-1}) following Belviso et al. (2011) (after Morel et al. (2010). All correlations are significant at p < 0.01 level.*

Region	***ρ***	**n**
Eutrophic provinces	0.94	53
Mesotrophic provinces	0.91	24
Oligotrophic provinces	0.88	24
Polar domain provinces	0.97	31
Coastal domain provinces	0.90	38
Westerlies domain provinces	0.91	23
Trades domain provinces	0.90	29

This correlation is stronger than correlation obtained using a single model for province monthly data ($\rho = 0.70$, $r = 0.73$, $p < 0.01$, $n = 114$). There is also an improvement in the ability of the method to predict high DMS concentrations. Although the scatter about the 1:1 line is still higher at high observed DMS concentrations, the composite method does not consistently underestimate high DMS. The smoothed nature of the climatological variables may be partly responsible for the decreased skill at predicting high DMS in the composite approach but the increase in correlation relative to the single model suggests that the relative importance or the slope of the relationship between the individual predictors is changing between provinces.

There is evidence from the literature that the strength and slope of the relationship between individual environmental variables (e.g. primary production rate and underwater irradiance) will be different within different regions of the global ocean. The rate of DMSPp production per unit of carbon is not constant in all species ranging from 0.0000015 in Prochlorophytes/Cyanophytes and 0.00086 in diatom species to 0.022 in Dinoflagellates (mol:mol) (Keller et al. 1989; Stefels et al. 2007). Species composition has been identified as the most important factor in determining

DMSP concentrations with a dependence upon abiotic conditions (Stefels et al. 2007).The rate of active exudation of DMSP, a source of DMSPd and so DMS, is also species specific with an additional dependence upon environmental conditions such as temperature, salinity and nutrient limitation (Stefels et al. 2007). Laroche et al. (1999) in a modelling study suggest a range in the exudation percentage of the DMSP quota per day between different species with 1% for the dinoflagellate *Prorocentrum minimum* to 3-11% for Phaeocystis species however there is limited experimental data on DMSP exudation rates. This model study would suggest that slope or strength of the relationship between primary production and DMSPd may be different for regions dominated by different species. Although Kiene and Slezak (2006) suggest that the concentration of DMSPd is always <2.8 nmol l^{-1}, it is the rate of conversion and the relative pathway that is relevant.

Once free within the water column the fraction of DMSPd that is converted to DMS by bacterial degradation is dependent upon the biomass, composition and production rate of the bacterial community (Stefels et al. 2007). This in turn is partially dependent on the rate of primary production as the biomass of bacterial community is related to the biomass of the phytoplankton community (Geider et al. 2001). DMSPd may be utilised by the bacterial community via two major pathways, the cleavage pathway which can lead to DMS (plus acrylate) and demethylation which does not yield DMS (Curson et al. 2011; Kiene and Linn 2000; Moran et al. 2012; Reisch et al. 2011b). Kiene and Linn (2000) proposed that when ambient DMSPd concentrations are low, bacteria have a preference for the more energy efficient demethylation pathway. When DMSPd concentrations are high, the DMSPd that is not assimilated is processed via the catabolic pathway that can (but not always) yield DMS and acrylate with the acrylate used as a carbon source (Howard et al. 2006; Todd et al. 2010) (see Figure 1.4). However it is the bacterial sulphur demand relative to the available DMSPd that is critical (Kiene et al. 2000; Moran et al. 2012), therefore if bacterial sulphur demand is reduced because of UV stress or nutrient limitation then the demethylation pathway is reduced and the cleavage pathway upregulated increasing the yield of DMS from DMSPd (Curson et al. 2011). The yield of DMS from DMSPd had been observed to range from 5-100% and was correlated to mixed layer depth with a link between shallow mixed layer depths, high UV stress and high DMS yields suggested (Simó and Pedrós-Alió 1999a). It is

therefore possible that the slope of the relationship between underwater irradiance and DMS concentrations will be different for different regions depending upon the state and composition of the bacterial community which in turn is partially determined by the primary production rate.

Photooxidation is a sink for DMS in the surface ocean. Photooxidation rates have a temperature dependence doubling with an increase of 20^{o}C (Toole et al 2003). Additionally nitrate concentrations also play a role in the modulation photolysis rates (Toole and Siegel 2004; Toole et al. 2004). The depth interval over which photolysis is effective is related to light attenuation and the presence of CDOM (Bouillon and Miller 2004; Tedetti and Sempere 2006) which are in turn related to algal biomass and the rate of primary production (Bouillon and Miller 2004). Thus there is the potential for both the rate of photooxidation and the slope of the relationship between underwater irradiance and DMS to differ between regions and for the relative contribution of the DMS loss term due to photooxidation to be partially dependent upon the rate of primary production (biomass). Other processes thought to be important within the DMS ecosystem that are linked to irradiance such as the direct exudation of DMS following oxidative stress (Sunda et al. 2002) will also have this partial dependence upon production via the rate of light attenuation.

There is also evidence to suggest that the relative importance of biological/environmental variables via their impact on the balance between sources and sinks of DMS is likely to change between locations in space and time. Belviso et al. (2004), Bell et al. (2006) and Hind et al. (2011) found that different algorithms using different combinations of variables were more successful in explaining the variance in DMS within different regions. An ecosystem model developed for the southern ocean by Gabric et al. (1993) had to be reparameterised to successfully simulate DMS in the Barents Sea and the North Atlantic. Vallina and Simó (2007), Belviso and Caniaux (2009) and chapter 2 found different slopes in the relationship between SRD and DMS at different sites (see chapter 2).

Investigations from oligotrophic waters have identified a lack of correlation between seasonal peaks in biomass and DMS (Belviso et al. 2011; Toole and Siegel 2004; Vallina et al. 2008) with stronger correlations between DMS and underwater

irradiance; this is known as the "summer paradox" (Toole and Siegel 2004). Toole and Siegel (2004) proposed that there may be two regimes in operation responsible for this phenomenon. The first is a production regime where DMS concentrations are coupled to biomass or production. Some studies from mid-high latitude eutrophic regions have found correlations between biomass/chlorophyll and DMSP or DMS during blooms of high DMSP producing species (e.g. Gibson et al. 1990; Malin et al. 1998). However, other studies from similar regions have not (Leck et al. 1990; Kettle et al. 1999; Simo et al. 1995). The second is a stress regime where the balance of DMS production and loss processes are controlled by irradiance driven processes such as the antioxidant hypothesis (Sunda et al. 2002), the overflow hypothesis (Stefels 2000), bacterial metabolism (Kieber et al. 1996; Kiene and Linn 2000) and photo-oxidation (Brimblecombe and Shooter 1986; Hatton 2002).

The literature outlined above suggests irradiance may dominate DMS dynamics in oligotrophic environments. If this is true underwater irradiance (I_z) may be the dominant variable within the MLR models (largest coefficient) developed within oligotrophic environments or provinces. Belviso et al. (2011) following Morel et al. (2010) identified 9 provinces where the most oligotrophic waters are found using SeaWiFS chlorophyll. These provinces come from both the Westerlies and Trades domains and are dominated by the mid ocean gyres. Monthly province data is available for 5 of these provinces which cover 16.7% of the global ocean (NAST(W), NAST(E), SATL, NPTG, SPSG: see Table 4.5 and Figure 4.12 for full province names and locations)). The average SeaWiFS Chl that is paired to the high resolution DMS data from within each province is 0.09 – 0.17 mg l^{-1}. As expected, within the 5 MLR models $I_z sat$ is the dominant variable (see Table 4.5). The predicted vs. observed correlation within the validation data for the 5 provinces are NAST(W) ρ = 0.98 (n = 6) , NAST(E) ρ = 0.66 (n = 6), SATL ρ = 0.60 (n = 4), NPTG ρ = 0.89 (n = 6), SPSG ρ = 0.07 (n = 7)) (see Table 4.6).The Spearman's correlation is low for SPSG but the Pearson's coefficient is relatively strong (r = 0.68). Using the composite method for all of the oligotrophic provinces generates a predicted vs. observed correlation of $\rho = 0.88$ ($p < 0.01$, n = 24).

It is difficult to assess the operation of the summer paradox within the oligotrophic provinces because only part of the seasonal cycle within each province is available.

There is a positive bivariate correlation between the monthly averaged primary production rate and DMS in most oligotrophic provinces ($\rho = 0.32$-0.60) and the primary production coefficients within the MLR models are small relative to the irradiance coefficients (see Table 4.5). The exceptions are NAST(W) where the correlation is negative ($\rho = -0.66$, $n = 6$) reflected in a negative MLR coefficient and SATL where the correlation is very weak ($\rho = 0.01$, $n = 4$) with a small, non-significant negative coefficient within the MLR for this province. The relatively weak and sometimes negative correlations to primary production rate within the oligotrophic provinces may reflect the summer paradox. Some parts of the seasonal cycle would generate a negative relationship between biomarkers and DMS as summer biomass declines after the spring bloom whilst DMS concentrations continue to rise to their summer peak. Alternatively photooxidation may be dominant in these provinces, in these months. Belviso et al. (2011) found the summer paradox operating in these provinces (DMS relative to chlorophyll) using the DMS climatology (Lana et al. 2011a). However primary production rates have been found to be much more variable than chlorophyll concentrations. Marañón et al. (2003) found a 20-fold variation in integrated primary production rates relative to a 3-fold variation in chlorophyll in a study of 34 stations in the North and South Atlantic subtropical gyre.

The pattern within the coefficients of the MLR models from eutrophic waters where primary production may be expected to be the dominant variable (Toole and Siegel 2004) is less clear (see Table 4.5). Eutrophic waters are found within provinces belonging to the Coastal and Polar Domains (province average SeaWiFS chlorophyll is 1.65 – 2.67 mg l^{-1}). The composite method does successfully predict DMS for the eutrophic provinces with a strong predicted vs. observed correlation within the validation data ($\rho = 0.94$, $p < 0.01$, $n = 53$). Data is available for all 6 polar provinces and 4 out of 24 Coastal provinces covering 32.1% and 1.8% of the global ocean respectively. The MLR models developed within the training data for the Polar provinces are all strong ($R^2 = 0.79$-0.96, $\rho = 0.90$-0.99) and there are strong bivariate correlations between DMS and both underwater irradiance ($\rho = 0.70$-0.94) and primary production rate ($\rho = 0.71$-0.99), with the exception of BPLR ($\rho = -0.30$). These models also successfully predict Polar monthly province DMS within the validation data ($\rho = 0.80$-0.99) in provinces from both the southern and northern

hemispheres with the exception of BPLR (ρ = 0.4). This poor prediction probably arises from the poor correlation between primary production rate and DMS (and so poorly developed coefficients within the MLR) for that province. This also demonstrates the importance of rigorously testing the models in separate unseen data. For the Polar province monthly data, primary production is the dominant variable (largest coefficient) within the MLR models in only 3 of the 6 the Polar provinces (ARCT, SARC, ANTA), although the difference in magnitude between the coefficients is less pronounced than in the oligotrophic provinces (see Table 4.5). This may be because irradiance and primary production are more closely correlated within Polar provinces as primary production tends to be limited by irradiance in these regions (Longhurst 1995). As the temporal resolution has been reduced (monthly averages) there is less statistical distinction between the primary production rate and irradiance within the MLR and so the coefficients are more similar with no pattern in the dominance of one over the other.

Within the 4 Coastal provinces for which there is province monthly data available, primary production is the dominant coefficient in 3 out of 4 provinces (NECS, ALSK, CCAL) (see Table 4.5). The MLR models developed within the training data for the Coastal provinces are all strong (R^2 = 0.69-0.98, ρ = 0.77-0.90) and there are strong correlations between DMS and both underwater irradiance (ρ = 0.75-0.83) and primary production (ρ = 0.66-0.94), with the exception of NWCS (PP ρ = 0.43, I_z ρ = 0.36). These models successfully predict coastal monthly province DMS within the validation data (ρ = 0.50-0.98) with the exception of NWCS (ρ = 0.36).

The remaining 5 provinces for which province monthly DMS data is available may be thought of as mesotrophic with a province average SeaWiFS chlorophyll of 0.18 – 0.78 mg l^{-1} (NADR , PSAG(E) , SANT , PNEC and PEQD). These provinces cover ~15.4% of the global ocean. The MLR models developed within the training data for these mesotrophic provinces are all strong (R^2 = 0.61-0.99), with the exception of PEQD (R^2 = 0.02) (see Table 4.5). The models also successfully predict province monthly DMS (predicted vs. observed ρ = 0.79-0.94) with the exception of PEQD (ρ = 0.34) (see Table 4.6). The coefficient acting upon primary production is dominant within the 4 successful MLR models developed for these mesotrophic provinces (Table 4.5). PEQD is located in the ENSO affected region of the Pacific where

potentially large inter-annual variability in primary production rates may not be reflected in the smoothed climatological $VGPM_{avg}$ rates. Using the composite method for all of the mesotrophic provinces generates a strong predicted vs. observed correlation of $\rho = 0.91$ ($p < 0.01$, $n = 24$).

Table 4.5: *Statistics related to MLR model development within the training subset for each province (multiple correlation coefficient R and R^2, the p value and the number of province monthly averages used to derive the model (n).The coefficients for each model in the form DMS = $b_1 + b_2(VGPM) + b_3(I_z sat)$ are shown. Also shown is the trophic status of the province defined using SeaWiFS chlorophyll following Belviso et al. (2011) after Morel et al. (2010) (Eut = Eutrophic, Mes = Mesotrophic and Oli = oligotrophic). Also shown is the Longhurst (1995) biogeochemical domain to which the province belongs.*

Province	Trophic status	BGCD	R	R^2	p	n	b_1 (constant)	b_2 (VGPM)	b_3 (IzSat)
BPLR Boreal Polar Province	Eut	P	0.98	**0.96**	0.02	5	-1.373	-0.810	1.045
ARCT Atlantic Arctic Province	Eut	P	0.93	**0.86**	0.02	6	-2.273	1.053	0.682
SARC Atlantic Subarctic Province	Eut	P	0.96	**0.93**	0.08	5	-0.010	1.403	-0.493
BERS N. Pacific Epicontinental Province	Eut	P	0.92	**0.85**	0.08	4	2.255	1.437	-1.674
ANTA Antarctic Province	Eut	P	0.89	**0.79**	0.02	6	-0.356	0.395	0.217
APLR Austral Polar Province	Eut	P	0.89	**0.8**	0.08	5	-2.322	0.151	1.293
NECS NE Atlantic Shelves Province	Eut	C	0.99	**0.98**	0	9	-5.299	0.924	1.907
NWCS NW Atlantic Shelves Province	Eut	C	0.65	**0.42**	0.33	8	-1.466	0.245	0.683
ALSK Alaska Downwelling Coastal Prov	Eut	C	0.99	**0.97**	0.06	6	0.286	1.517	-0.842
CCAL California Upwelling Coastal Prov	Eut	C	0.83	**0.69**	0.1	6	-1.311	0.728	0.271
NADR N. Atlantic Drift Province	Mes	W	0.83	**0.68**	0.05	7	-1.317	1.006	0.253
PSAG(E) Pacific Subarctic Gyre Prov (East)	Mes	W	0.94	**0.89**	0.08	5	-1.241	1.192	0.145
SANT Subantarctic Province	Mes	W	0.78	**0.61**	0.02	7	-1.310	0.861	0.403
PNEC N. Pacific Equatorial Counter current	Mes	T	0.99	**0.99**	0.02	5	-4.765	2.294	1.611
PEQD Pacific Equatorial Divergence	Mes	T	0.13	**0.02**	0.75	8	-0.350	-0.063	0.372
NAST(W) N. Atlantic Subtropical Gyre Prov(West)	Oli	W	0.99	**0.98**	0.02	6	-2.952	-0.548	1.647
NAST(E) N. Atlantic Subtropical Gyre (East)	Oli	W	0.62	**0.39**	0.18	6	-1.871	0.210	0.853
SATL South Atlantic Gyral Province	Oli	T	0.90	**0.81**	0.42	4	-10.686	-0.101	4.943
SPSG S. Pacific Subtropical Gyre Prov	Oli	W	0.68	**0.46**	0.91	7	-4.615	0.361	2.133
NPTG N. Pacific Tropical Gyre Province	Oli	T	0.94	**0.88**	0.03	6	-3.530	0.371	1.549

***Table 4.6**: Predicted vs. observed statistics (Spearman's rank hypothesis (ρ)) for each province using the models developed within the training data (see Table 4.5)*

Province	ρ	p	n
BPLR Boreal Polar Province	**0.40**	0.75	4
ARCT Atlantic Arctic Province	**0.99**	0.08	4
SARC Atlantic Subarctic Province	**0.80**	0.33	4
BERS N. Pacific Epicontinental Province	**0.99**	0.08	4
ANTA Antarctic Province	**0.99**	0	6
APLR Austral Polar Province	**0.99**	0.08	4
NADR N. Atlantic Drift Province	**0.79**	0.05	7
NAST(W) N. Atlantic Subtropical Gyral Province (West)	**0.99**	0.02	5
NAST(E) N. Atlantic Subtropical Gyral Province (East)	**0.60**	0.35	5
PSAG(E) Pacific Subarctic Gyres Province (East)	**0.90**	0.08	5
SPSG S. Pacific Subtropical Gyre Province	**0.09**	0.92	6
SANT Subantarctic Province	**0.94**	0.02	6
SATL South Atlantic Gyral Province	**0.99**	0.08	4
NPTG N. Pacific Tropical Gyre Province	**0.80**	0.33	4
PNEC N. Pacific Equatorial Countercurrent Province	**0.80**	0.13	5
PEQD Pacific Equatorial Divergence Province	**0.32**	0.5	7
NECS NE Atlantic Shelves Province	**0.98**	0	8
NWCS NW Atlantic Shelves Province	**0.36**	0.39	8
ALSK Alaska Downwelling Coastal Province	**0.77**	0.10	6
CCAL California Upwelling Coastal Province	**0.50**	0.45	5

In contrast to some other studies these strong correlations to monthly DMS are observed in data which are averaged using biologically relevant spatial units, the data is only averaged once and not grouped by the predictor variable, no high DMS data has been excluded and the models have been validated using data that has not been used to develop the model. These methods also explain DMS for the entire range of the DMS within the global database.

Anderson et al (2001) derive a global parameterisation for surface DMS concentration using a combination of concurrently sampled Chl *a* concentration (C) from the Kettle and Andreae (2000) climatology, a mean daily shortwave radiation climatology (J) and a nutrient limitation term based on a climatological nitrogen (Q) to produce a $\log_{10}$(CJQ) index (see section 1.3.5: equations 1.3 and 1.4). This method reduced the number of data cases to 2622 which were then sequentially grouped by ascending $\log_{10}$(CJQ) and then averaged to produce 114 data points. Using a broken stick linear least squares regression on these average points produced a positive correlation between high $\log_{10}$(CJQ) and DMS was found (>2.3 nmol l^{-1}) but was unable to resolve low DMS concentrations (<2.3 nmol l^{-1}) applying a constant DMS concentration to these areas. Belviso et al. (2004) note that this is a significant weakness as it represents approximately half of the DMS data within Kettle and Andreae (2000) climatology from large regions of the global open ocean including the southern hemisphere high to mid latitudes and the subtropical gyres. It is difficult to compare the results from this chapter with Anderson et al. (2001) as they did not provide any comparable statistics regarding the broken stick regression. Anderson et al. (2001) do not validate their relationship within unseen data.

Simó and Dachs (2002) building on observations made by Simó and Pedrós-Alió (1999a) derive a global parameterisation based upon the ratio of climatological MLD (1^o x 1^o x month resolution) and Chl *a* concurrent to the Kettle et al. (1999) global DMS database (see section 1.3.5: equations 1.5 and 1.6). After filtering for extreme values (removing data pairs with DMS > 100 nmol l^{-1} and/or Chl > 15 mg m^{-3}) this reduced the number of data cases to 2385. The data was then further binned into 43 groups according to cruise origin or groups based on latitude bands (~10^o) or changes in MLD (>~20 m), and then averaged (Simó and Dachs 2002). This resulted in a double algorithm (lower limit for the regression set at 1.5 nmol l-1) where low

Chl/MLD ratio (< 0.02) are represented by a non-linear relationship with MLD alone (~80% of the cases) and data with a Chl/MLD ratio >0.02 a linear regression of DMS against Chl/MLD.

Care must also be taken not to over average the data. Vallina and Simó (2007) investigated the relationship between mixed layer irradiance (solar radiation dose: SRD) and global surface DMS (see section 1.3.5: equation 1.7). DMS from the Kettle et al (1999) global database was averaged into monthly 10^o latitude by 20^o longitude bins (n=545). These bin averages were then grouped by 15 Wm^{-2} intervals of SRD and again averaged together (n=14). The highest 5% of the bin means were excluded (upper limit ~10 nmol l^{-1}). Linear regression was then conducted using the 14 data points. Although a strong relationship was found after grouping monthly 10^ox20^o box means (r^2=0.95, n=14), prior to grouping they observed a correlation of $\rho = 0.47$ ($p << 0.01$, $n = 545$).

Derivienko et al. (2009) re-analysed the global SRD-DMS relationship. They found a weak correlation between DMS and SRD when averaging the data using a 2.5^o x 2.5^o grid ($r^2 = 0.14$) and a similarly weak correlation when averaging using the 10^o x 20^o grid used by Vallina and Simó (2007). Only after binning the averaged data by intervals of SRD (following Vallina and Simó (2007)) did the strong correlation exist ($r^2 = 0.94$). Derivienko et al. (2009) conclude the strong positive relationship observed at the global level is an artefact of the binning procedure. Derivienko et al. (2009) also find a similar pattern in the correlation relationships between DMS and MLD alone (although DMS is inversely related to MLD). Within the analysis in this chapter, the data is averaged only once and is not grouped by a predictor variable. In addition Vallina and Simó (2007) do not validate their relationship using unseen data although it is not intended to be a predictive algorithm. In our analysis no DMS data are excluded based upon extreme values in either the DMS data or the predictor variables.

The correlation between SRD and DMS observed prior to grouping by intervals of SRD by Vallina and Simó (2007) ($\rho = 0.47$) is significantly weaker than the correlations observed between the predicted and observed DMS in this chapter using similar levels of averaging (e.g. the single algorithm developed from province

monthly data in section 4.3.2 (ρ = 0.70) and the composite method outlined in this section (ρ = 0.93)). Indeed even in conjunction with the high resolution data the correction is comparable (ρ = 0.48), and higher using the composite approach with the high resolution data (ρ = 0.64). This suggests that this combination of primary production and underwater irradiance offers a significant improvement in the prediction of global surface DMS concentrations.

4.3.3.3 High resolution data composite approach

Within the high resolution DMS data there must be n >= 30 data points from a single province to derive a MLR model for that province, and n >= 30 data points in the same province within the validation data to test the model. This resulted in the development and validation of MLR models for 45 out of 55 or ~80% of provinces (only 45 out of 57 provinces contain n >= 30 data points in both the data subsets). This includes all 6 provinces from the Polar domain, 14 out of 16 from the Westerlies domain, 11 out of 12 provinces from the Trades domain and 14 out of 23 from the Coastal domain. Most provinces for which there is insufficient data come from the coastal domain. Those open ocean provinces, for which there is data, represent 31 out of 33 or ~94% of all the open ocean provinces defined by Longhurst (1995).

The correlation between composite predicted and observed DMS within the validation subset for the high resolution data using a combination of 45 MLR models is strong and significant (ρ = 0.64, p = 0, n = 16219) (see Figure 4.12). This is stronger than the correlation between predicted and observed DMS obtained when using a single MLR model trained using all of the high resolution data within the training subset (ρ = 0.48, r = 0.49, p <0.01, n = 12179) (section 4.3.1.2). This composite method also provides strong and significant correlations within the four biogeochemical domains (Polar domain: high resolution (ρ = 0.66, p = 0, n = 2323), Westerlies domain: high resolution (ρ = 0.59, p = 0, n = 5884), Trades domain: high resolution (ρ = 0.64, p = 0, n = 3382) and the Coastal domain: high resolution (ρ = 0.64, p = 0, n = 4636). However there are no clear trends within the relative magnitude of the predictor variables within the separate MLR models developed for each province (see Table A0.2 and Table A0.3 in the appendix). This highlights the

problem of seeking correlation relationships within the high resolution data subject to high natural and sampling/methodologically imposed variability.

The improvement of the high resolution composite approach over the single model mirrors the increase in predictive power between the monthly single MLR and composite approach. This highlights the value of deriving separate models to account for differences in the relationships between DMS and primary production and irradiance in different provinces.

4.4 Summary

A climatological, satellite retrieved primary production rate in combination with a climatological underwater irradiance term explains a significant fraction of the variance in province monthly averaged DMS data using a province-by-province composite method. The provinces that are included in this analysis cover ~66% of the global ocean representing all 4 biogeochemical domains and spanning a large range of trophic regimes, latitudes and seasons. This has been achieved by utilising biologically relevant spatial units. The amount of variance explained improves upon the variance explained by other global relationships using similar levels of data averaging. This method outperforms the single MLR model derived in section 4.3.2 from province monthly average values suggesting that the relative importance of primary production and underwater irradiance in determining ambient DMS concentrations in the surface ocean changes between different trophic regions or biogeochemical domains. A comparison of the relative magnitude of the coefficients between the province MLR models from different trophic regimes suggests that primary production (a biological indicator) is dominant in the eutrophic regions found at the high latitudes and coastal regions whilst underwater irradiance may be dominant in oligotrophic regions. This broadly supports the proposal by Toole et al. (2004) that a production forced regime and a stress forced regime may be in operation at the global scale. The differences in the MLR models between the provinces may also be partly attributable to the observed differences in the ratio of C:DMS(P) (Stefels et al 2007) between algal species as the species assemblages change between provinces

The analysis of the higher resolution data did not yield such strong correlations but given the complex and dynamic nature of the DMS marine ecosystem and the potential error within the DMS database this is not unexpected. If surface DMS was simply and strongly coupled to algal biomass in all regions of the ocean, detectable above the noise of natural variability, then many of the questions that still persist regarding the global scale controls on seawater DMS concentration would be closer to a resolution. Despite these issues it has been possible to identify two potential large scale ecosystem controls, the rate of primary production and underwater irradiance, that are detectable from space that interact to modulate average DMS concentrations on regional to global spatial scales over monthly-seasonal timescales.

Chapter 5: Conclusions

This concluding chapter draws together the findings of the preceding chapters before discussing how future work should progress.

5.1 Summary

Chapter 2 tested the strong positive relationship observed between surface DMS and the SRD at (i) the monthly global scale and (ii) using monthly averaged time series data (Vallina and Simó 2007) using high resolution, daily, concurrently sampled *in situ* data from the AMT programme.A significant correlation was observed between DMS and SRD using *in situ* data for all of the components of the SRD calculation (SRD_{insitu}) but the SRD calculated using climatological data (SRD_{clim}) yielded higher correlations. It may be that the *in situ* data is subject to too much natural variance and noise.

Chapter 2 demonstrated that the slope and strength of the correlation relationship between SRD and DMS was found to be different between data from different sites: the AMT programme (Chapter 2), monthly time series data from Hydrostation-S in the Sargasso Sea (Vallina and Simó 2007) and Blanes Bay (coastal Northwest Mediterranean) (Vallina and Simó 2007), data from the Northeast Atlantic (Belviso and Caniaux 2009), and at the global level using monthly averaged data (Vallina and Simó 2007). This was probably partly due to the different formulations and data used to derive the SRD equation and the different spatial and temporal resolution of the data. It could also indicate that the processes determining DMS concentrations are different between sites and operate at different spatial and temporal scales. It is quite likely that the contribution of the biological factors is introducing variability in slopes. The SRD or MLD based approach may require additional variables that directly parameterise the biology of the DMS ecosystem.

Using satellite-retrieved, cloud-adjusted surface UVA irradiance to calculate a UV radiation dose (UVRD) with a climatological MLD provides a correlation to DMS that is equivalent to SRD_{clim}. Although adjusting for cloud and irradiance wavelength is theoretically more satisfactory it does not improve the correlation to the AMT DMS data. This may be because the natural variability in the system at this daily

resolution is larger than the variability introduced by cloud and/or the spectral differences between total irradiance and UVA (380nm).

The incident surface radiation and the depth of the mixed layer are related and it is difficult to disentangle a role for irradiance beyond MLD within the SRD framework. As noted by Simó and Pedrós-Alió (1999), the MLD offers a useful shorthand to prediction without fully resolving the biological processes involved. Within the AMT data, MLD appears to be the dominant variable in terms of a correlation to DMS concentrations. Derevianko et al. (2009) re-examined the global relationship reported by Vallina and Simó (2007) and suggest that dilution via changes in MLD is the dominant term within the SRD formulation. They also suggest that the strong correlation may result from the averaging procedure (see chapter 4, section 4.3.3.2 for a detailed discussion).

The SRD explanatory framework does not include a direct measure of the biology. The incorporation of a biological indicator would be advantageous. Future environmental changes may affect the biology of the DMSP-DMS web without influencing MLD or irradiance (e.g. ocean acidification, increased deposition of nutrients or toxic metals). Phytoplankton species composition changes may also result from such impacts, which will either favour or inhibit DMS(P)-producing phytoplankton.

Chapter 3 identified that within a broad ranging and large dataset the rate of primary production in combination with the calculated underwater irradiance level accounted for maximal variance in DMS concentrations. These correlations are observed in data collected from discrete depths within the euphotic zone, from near-surface waters and within depth profile integrated data that spans multiple biogeochemical domains, latitudes and trophic conditions. Significant correlations are also observed within biogeochemical domains which display similar biogeochemical properties. The *in situ* dataset utilised in chapter 3 was too small to allow meaningful analysis of data at the smaller biogeochemical province level.

Whilst previous studies have been unable to identify a strong link between ambient DMS concentrations and indicators of the biological community (e.g. chlorophyll) at

larger spatial scales, the results of chapter 3 indicate that a link between the productivity of the ecosystem and the concentration of DMS may exist. Chapter 3 also identifies that additional variance that is statistically independent from the rate of primary production is explained by the amount of underwater irradiance. This suggests that DMS concentrations are at least partly moderated by processes that are directly influenced by solar radiation. These processes may include the upregulation of the production of DMSPp as part of an antioxidant or overflow mechanism (Stefels 2000; Sunda et al. 2002), the suppression of bacterial sulphur demand by UV radiation which in turn may switch the route by which DMSPd is catabolised to a pathway that yields DMS (Kiene et al. 2000), the suppression of the bacterial metabolism of DMS by high irradiances (Simó 2004) and the photochemical oxidation of DMS (Brimblecombe and Shooter 1986; Hatton 2002).

Chapter 4 sought to investigate if the rate of primary production and underwater irradiance could explain global surface DMS concentrations using the global surface DMS database. Climatological data were used as predictor variables. Utilising a novel, province-by-province composite approach, a combination of a climatological primary production rate and a climatological underwater irradiance explained a significant proportion of the variance in province monthly DMS concentrations. The provinces included within this approach covered approximately two-thirds of the global ocean and included data from a range of biogeochemical domains, trophic states, latitudes and seasons. In addition this chapter reports that a single MLR model, derived using province monthly averages, also explains significant variance in global DMS.

The analysis of the higher resolution data did not yield such strong correlations. Given the complexities and inherent natural variability of the DMS marine ecosystem and the inherent variability within the DMS database this is not unexpected. The inherent variability within the DMS database will come from sampling errors due to instrument calibration and different techniques (e.g. gas chromatography vs. mass spectrometry (Bell et al. 2011) and sampling strategies (e.g. bloom focused vs. transects). Other sources of error include the under sampling of some regions over certain parts of the seasonal cycle such as high latitude winter

and interannual variability within regions. Due the variability in the data, DMS may need to be smoothed to distil the signal from the noise.

The amount of variance in DMS explained by the composite method and single province monthly MLR model demonstrated a significant improvement relative to the analysis of the high resolution data. These approaches also offered an improvement upon other global relationships when utilising similar levels of data averaging (e.g. SRD). This suggests that this combination of variables offers a significant improvement in the prediction of global surface DMS concentrations.

The results suggested that the relative importance of primary production and underwater irradiance in determining ambient DMS concentrations in the surface ocean changes between different trophic regions/biogeochemical domains. A potential driver of these differences could be algal and bacterial speciation. Primary production (a biological indicator) was dominant in the eutrophic regions found at the high latitudes and coastal regions whilst underwater irradiance was dominant in oligotrophic regions. This broadly supports the proposal by Toole and Siegel (2004) that two regimes (a production forced regime and a stress forced regime) may be in operation at the global scale.

The results broadly support the proposal that microbial communities exposed to higher mixed layer average irradiances may yield higher net surface DMS concentrations (Simó and Pedrós-Alió 1999a; Toole et al. 2003; Toole and Siegel 2004; Toole et al. 2006; Vallina and Simó 2007). However, these results suggest that it is important to couple a biological indicator (primary production) with physical forcings such as irradiance or MLD.

It has been possible to identify two potential large scale ecosystem controls that are detectable from space that interact to modulate average DMS concentrations on regional to global spatial scales over monthly-seasonal timescales.

5.2 Future work

The SRD offers a compelling explanation of temporal DMS dynamics in oligotrophic regions and has been invoked to explain the decoupling of biomass from peak DMS concentrations in these regions (the summer paradox). Formulations of the SRD have also been able to explain significant variance in DMS from the AMT programme in Chapter 2 (which has an oligotrophic focus). However, recently planktonic succession from low to high DMSP producers has also been invoked to explain the summer paradox (Polimene et al. 2012). Doubt has been cast over the strength of the SRD-DMS relationship at the global scale (Derevianko et al. 2009). To further evaluate the SRD-DMS relationship more data from higher latitudes and different trophic regimes is required.

High resolution (hourly) time series data on DMS, MLD and wavelength specific incident irradiance and its attenuation would improve understanding of the effect of mixed layer irradiance on DMS dynamics although at present this type of data series has not been measured. This would allow the effect of the environmental history prior to the DMS sample to be evaluated. It may be that an integral of the SRD/UVRD received 1, 2 or 3 hours prior to the sample explains more variance in DMS concentrations. In addition, data on the mixing rate would be interesting. It may be possible to estimate how often an average phytoplankton cell is mixed in and out of a "stress zone" defined as the depth to which different spectral bands of irradiance penetrate (e.g. UVB, UVA) The UV model developed by Smyth (2011) could be used to establish surface UV irradiance. Archer et al. (2010) demonstrated that higher rates of DMSP synthesis occurred when low light acclimated cells were exposed to acute doses (1 hour) of PAR+UV irradiance. The relationship between MLD, the mixing rate and the depth to which stress-inducing levels of UV are able to penetrate could be informative. This may also be investigated using a simple 1D ecosystem model. In addition, concurrent data on bacterial and algal production rates and photolysis rates would be useful to test some of the suppositions of the SRD theory.

Chapter 4 identified that primary production and underwater irradiance can explain significant variance in global DMS. As within the SRD methodology, it would be

interesting to try using cloud adjusted, wavelength specific irradiances (e.g. UVA, UVB, PAR). The model of UV model of Smyth (2011) could be utilised for this. A more sophisticated, wavelength specific light attenuation parameterisation involving *in situ* or satellite retrievals of CDOM may also improve the results.

The averaging procedure in chapter 4 may mask the differences in the spectral composition of the irradiance. It may be necessary to increase the resolution of the data studied to resolve this issue rather than decrease it (i.e. lab studies) to get to the process related detail.

Chapter 4 utilised a chlorophyll based production model (VGPM) to generate the climatological primary production data. The standard VGPM model was selected for this analysis as it is well established, widely used, has been successfully and extensively sea truthed and is well supported by the Oregon State University. It would be interesting to compare other production models including more complex, carbon based models (e.g. Behrenfeld et al. 2005; Carr et al. 2006). A variant of the VGPM is available based on an alternative temperature dependent photosynthetic efficiency relationship observed by Eppley (1972), the Eppley-VGPM. Also available are more complex models such as the carbon based production model (CbPM) which uses satellite-derived carbon to Chl-a ratio to predict phytoplankton growth rate (Behrenfeld et al. 2005). However, Kahru et al. (2009) investigated how well 5 different production models replicated a large *in situ* data set (n = 1862) sampled between 1984 – 2007 representing a range of net primary production rates sampled from oligotrophic to coastal waters and found that an adjusted version of the VGPM model was the best fit to the data.

The MLR models in chapter 4 struggle to predict high DMS values (> average DMS value), potentially because the predictor variables are smoothed, climatological values (although ~80.5% of the data falls below the average value). An improvement in the correlations and predictive ability of the MLR models may result from using the nearest SeaWiFS chlorophyll datum in space and time to each DMS sample to calculate the $VGPM_{surf}$ primary production data and the attenuation coefficient for the surface irradiance (rather than use a 10 year climatology).

Chapter 4 used the biogeochemical provinces defined by Longhurst (1995) as biologically relevant spatial units to average the data. A problem with the delineation of the oceans using static boundaries, as acknowledged by Longhurst (1995), is that ocean circulation and so water mass location changes in space and time, over a seasonal cycle, in response to inter-annual variability (e.g. ENSO) and due to extreme atmospheric events (Platt and Sathyendranath 1993). Recently, dynamic methods of defining biogeochemical provinces have been developed (e.g. Devred et al. 2007; Vichi et al. 2011) that use remotely sensed data to delineate the ocean. Using this method may improve the correlations obtained in chapter 4.

Some of the differences observed between the coefficients within the MLR models developed on a province-by-province basis may be attributable to differences in the ratio of C:DMSP between algal species (Stefels et al 2007). It may be possible to further explore these ideas by determining phytoplankton size classes (PSC's) or phytoplankton functional types (PFT's) using remotely sensed chlorophyll (e.g. Masotti et al. 2010; Hirata et al. 2011) or remotely sensing size fractionated primary production rates (e.g. Brewin et al. 2010).

PFTs and PSCs are conceptual groupings of phytoplankton species, based upon a shared ecological functionality, for example calcifiers (e.g. coccolithophores) and silicifiers (e.g., diatoms), or other characteristics, such as cell size (pico, nano and micro-phytoplankton). PFTs and PFCs can be derived from ocean-colour remote sensing via direct effects (phytoplankton community composition determines the absorption and backscattering of incident irradiance, affecting the reflectance spectra) and indirect effects (the composition of the particles and dissolved substances that accompany the phytoplankton community influences the reflectance spectra). These relationships between water leaving irradiance spectra and dominant PFTS/PSCs must be well established (sea truthed) using empirical data before they can be used to aid DMS research (Alvain et al. 2005; Ciotti and Bricaud 2006; Devred et al. 2006; Hirata et al. 2011; Uitz et al. 2008).

Brewin et al. (2010) developed a size fractionated primary production model by integrating a community model (Sathyendranath et al. 2001) used to estimate

respective phytoplankton size classes (PSC's) in this case, microplankton >20 μm and combined nano- and picoplankton <20 μm, into a primary production model. Regions with similar PFTs, PSCs or size fractionated production rates could be analysed to improve the composite approach. Ultimately this may help to derive a more powerful single MLR model for global surface DMS concentrations. A first step may be to calculate non-diatom production rates as diatoms are known to be low producers of DMS(P) (Stefels et al 2007).

It may also be that other variables are important for capturing additional variance in DMS concentrations. Simó and Pedrós-Alió (1999), Simó & Dachs (2002) and Vallina and Simó (2007) found that the depth of the mixed layer was important in explain surface DMS concentrations although this is disputed by Derevianko et al. (2009). Anderson et al. (2001) found that a function of chlorophyll, irradiance and a nitrate limitation term accounted for high DMS concentrations but could not explain areas of low DMS concentrations. Phosphate limitation may be important within DMS dynamics in oligotrophic regions (Belviso et al. 2011) and iron limitation may be important in modulating DMS, especially in high nutrient low chlorophyll (HNLC) regions such as the Southern Ocean (Turner et al. 2004).

Over the last century, Boyce et al. (2010) report a global decline in phytoplankton production of ~1% yr^{-1} and future global productivity may decline further as low latitude, stratified, low production zones expand (Polovina et al. 2008). The increased deposition of nutrient (N, P, Fe) may increase regional primary production rates. This may be especially relevant within the iron limited HNLC waters of the southern ocean (Jickells et al. 2005; Turner et al. 2004) while increased deposition of some toxic metals (e.g. lead) may have the opposite impact (Paytan et al. 2009). An assessment of how these changes might affect DMS concentrations in the context of the findings of chapter 3 and 4 would be warranted.

Finally, the use of a simple 1D ecosystem model (e.g. DMOS; Vallina et al. (2008), PhEcoM-DMS; Jodwalis et al.(2000), CMOC2-DMS; Monahan and Denman (2004)) in conjunction with a DMS time series such as the BATS data to test the sensitivity of DMS concentrations to different forcings (e.g. irradiance, algal production and bacterial processes) in different provinces or regions could be used to

evaluate the findings of this thesis. However, what is needed for modelling DMS dynamics is additional time series data, especially from eutrophic and high latitude regions. The Southern Ocean would be an ideal location for a DMS time series or a location close to the Cape Grim baseline air pollution research station (http://www.csiro.au/en/Organisation-Structure/Divisions/Marine--Atmospheric-Research/Cape-Grim.aspx) where a long term record of meteorological variables and atmospheric trace gasses exists, including DMS and some of its oxidation products. Ideally these time series should be high resolution (daily samples) and include concurrent measurements of biotic and abiotic factors such as irradiance, mixed layer depth, wind speed, algal and bacterial production, chlorophyll and CDOM. Finally, a more complex 3D model (e.g. Archer et al. 2004; Bopp et al. 2008; Buitenhuis et al. 2006; Elliott 2009; Le Clainche et al. 2004; Six and Maier-Reimer 2006; Vogt et al. 2010) could be used to evaluate the findings at a larger global scale.

Appendix

Table A.0.1 *List of provinces included in the training data subset/model development in section 4.3*

	Province Code	Full Province Name
1	BPLR	Boreal Polar Province
2	ARCT	Atlantic Arctic Province
3	SARC	Atlantic Subarctic Province
4	NADR	N. Atlantic Drift Province
5	GFST	Gulf Stream Province
6	NAST(W)	N. Atlantic Subtropical Gyral Province (West)
7	NATR	N. Atlantic Tropical Gyral Province
8	WTRA	Western Tropical Atlantic Province
9	ETRA	Eastern Tropical Atlantic Province
10	SATL	South Atlantic Gyral Province
11	NECS	NE Atlantic Shelves Province
12	CNRY	Canary Coastal Province
13	NWCS	NW Atlantic Shelves Province
14	MEDI	Mediterranean Sea, Black Sea Province
15	CARB	Caribbean Province
16	NAST(E)	N. Atlantic Subtropical Gyral Province (East)
17	BRAZ	Brazil Current Coastal Province
18	FKLD	SW Atlantic Shelves Province
19	BENG	Benguela Current Coastal Province
20	MONS	Indian Monsoon Gyres Province
21	ISSG	Indian S. Subtropical Gyre Province
22	EAFR	E. Africa Coastal Province
23	ARAB	NW Arabian Upwelling Province
24	INDE	E. India Coastal Province
25	BERS	N. Pacific Epicontinental Province
26	PSAG(E)	Pacific Subarctic Gyres Province (East)
27	KURO	Kuroshio Current Province
28	NPPF	N. Pacific Polar Front Province
29	NPST(E)	N. Pacific Subtropical Gyre Province (East)
30	TASM	Tasman Sea Province
31	SPSG	S. Pacific Subtropical Gyre Province
32	NPTG	N. Pacific Tropical Gyre Province
33	PNEC	N. Pacific Equatorial Countercurrent Province
34	PEQD	Pacific Equatorial Divergence Province
35	WARM	W. Pacific Warm Pool Province
36	ALSK	Alaska Downwelling Coastal Province
37	CCAL	California Upwelling Coastal Province
38	CAMR	Central American Coastal Province
39	CHIL	Chile-Peru Current Coastal Province
40	CHIN	China Sea Coastal Province
41	SSTC	S. Subtropical Convergence Province
42	SANT	Subantarctic Province
43	ANTA	Antarctic Province
44	APLR	Austral Polar Province

Table A0.2: *Statistics related to MLR model development within the training subset for each province using high resolution data (multiple correlation coefficient R and R2, the p value and the number of province monthly averages used to derive the model (n).The coefficients of the model in the form DMS = b1 + b2(VGPM) + b3($I_z$sat) are shown.*

Province	**R**	**R^2**	**ρ**	**p**	**n**	**b_1**	**b_2**	**b_3**
BPLR Boreal Polar Province	0.10	0.01	0.23	0	204	-0.035	-0.142	0.193
ARCT Atlantic Arctic Province	0.83	0.69	0.82	0	446	-2.541	0.951	0.914
SARC Atlantic Subarctic Province	0.72	0.52	0.7	0	629	-1.859	0.834	0.706
NADR N. Atlantic Drift Province	0.62	0.39	0.62	0	619	-1.689	0.936	0.436
GFST Gulf Stream Province	0.42	0.18	0.48	0	115	-2.138	0.036	0.997
NAST(W) N. Atlantic Subtropical Gyral (West) P.	0.60	0.36	0.61	0	605	-0.263	-0.713	0.419
NATR N. Atlantic Tropical Gyral P.	0.09	0.01	0.14	0.04	196	-0.047	-0.062	0.080
WTRA Western Tropical Atlantic P.	0.47	0.22	0.45	0	211	-1.400	0.833	0.427
ETRA Eastern Tropical Atlantic P.	0.74	0.54	0.8	0	65	4.925	0.443	-2.224
SATL South Atlantic Gyral Province	0.43	0.19	0.6	0	602	-4.616	0.244	2.119
NECS NE Atlantic Shelves Province	0.56	0.32	0.5	0	780	-4.609	0.216	2.074
CNRY Canary Coastal Province	0.57	0.32	0.59	0	365	-2.286	0.597	0.867
NWCS NW Atlantic Shelves Province	0.21	0.04	0.15	0	1300	-1.246	0.152	0.622
MEDI Mediterranean Sea, Black Sea P	0.20	0.04	0.34	0	285	0.317	-0.206	0.114
CARB Caribbean Province	0.37	0.14	0.26	0	302	-1.131	0.240	0.526
NAST(E) N. Atlantic Subtropical Gyral (East)	0.45	0.20	0.4	0	508	-1.505	0.142	0.701
FKLD SW Atlantic Shelves Province	0.53	0.28	0.52	0	71	-3.594	-0.103	1.721
BENG Benguela Current Coastal P.	0.49	0.24	0.59	0	93	7.172	-0.071	-2.938
MONS Indian Monsoon Gyres P.	0.47	0.22	0.45	0	159	4.561	0.240	-1.947
ISSG Indian S. Subtropical Gyre P.	0.50	0.25	0.49	0	212	-2.607	0.203	1.365
EAFR E. Africa Coastal Province	0.65	0.42	0.57	0	118	27.492	-0.322	-12.163
ARAB NW Arabian Upwelling P.	0.50	0.25	0.48	0.01	32	-5.524	-0.060	2.712
INDE E. India Coastal Province	0.45	0.20	0.44	0	56	2.106	0.513	-0.913
INDW W. India Coastal Province	0.60	0.35	0.65	0	54	5.928	0.729	-2.797

BERS N. Pacific Epicontinental P	0.54	0.30	0.52	0	1450	1.531	1.333	-1.220
PSAG(E) Pacific Subarctic Gyres (East)	0.60	0.36	0.61	0	437	-0.967	0.885	0.197
PSAG(W) Pacific Subarctic Gyres (West)	0.54	0.29	0.67	0	36	-1.893	1.528	0.142
KURO Kuroshio Current Province	0.52	0.27	0.57	0	631	-1.561	0.791	0.454
NPPF N. Pacific Polar Front Province	0.64	0.41	0.68	0	196	-2.138	0.472	0.906
NPST(W) N. Pacific Subtropical Gyre (West)	0.19	0.03	0.08	0.25	197	-0.164	-0.151	0.182
TASM Tasman Sea Province	0.63	0.39	0.64	0	62	-180.85	2.172	78.679
SPSG S. Pacific Subtropical Gyre P.	0.47	0.22	0.28	0	2321	-4.167	0.337	1.928
NPTG N. Pacific Tropical Gyre Province	0.71	0.50	0.69	0	551	-3.613	0.577	1.538
PNEC N. Pacific Equatorial Countercurrent P	0.50	0.25	0.42	0	673	0.151	0.672	-0.127
PEQD Pacific Equatorial Divergence P	0.12	0.01	0.13	0	1534	0.451	-0.122	0.021
WARM W. Pacific Warm Pool Province	0.35	0.12	0.31	0	579	-8.950	0.202	4.091
ALSK Alaska Downwelling Coastal P.	0.69	0.48	0.61	0	2518	-1.717	0.733	0.630
CCAL California Upwelling Coastal P.	0.49	0.24	0.48	0	1165	-1.178	0.410	0.427
CAMR Central American Coastal P.	0.62	0.38	0.29	0.04	52	12.194	0.328	-5.617
CHIL Chile-Peru Current Coastal P.	0.19	0.04	0.22	0	343	0.986	0.373	-0.465
CHIN China Sea Coastal Province	0.21	0.04	0.08	0.52	60	1.666	0.237	-0.701
SSTC S. Subtropical Convergence P.	0.56	0.31	0.52	0	467	-2.546	-0.191	1.369
SANT Subantarctic Province	0.43	0.18	0.4	0	2484	-1.416	0.517	0.592
ANTA Antarctic Province	0.46	0.21	0.48	0	383	-0.199	0.629	0.112
APLR Austral Polar Province	0.53	0.28	0.54	0	352	-0.295	0.741	0.150

Table A0.3: *Predicted vs. observed statistics (Spearman's rank hypothesis (ρ)) for high resolution data, for each province using the models developed within the training data*

Province	ρ	p	n
BPLR Boreal Polar Province	0.18	0.03	136
ARCT Atlantic Arctic Province	0.81	0	322
SARC Atlantic Subarctic Province	0.73	0	414
NADR N. Atlantic Drift Province	0.56	0	400
GFST Gulf Stream Province	0.34	0	83
NAST(W) N. Atlantic Subtropical Gyral (West) P.	0.64	0	371
NATR N. Atlantic Tropical Gyral P.	0.06	0.51	140
WTRA Western Tropical Atlantic P.	0.56	0	134
ETRA Eastern Tropical Atlantic P.	0.76	0	47
SATL South Atlantic Gyral Province	0.65	0	375
NECS NE Atlantic Shelves Province	0.50	0	526
CNRY Canary Coastal Province	0.64	0	270
NWCS NW Atlantic Shelves Province	0.09	0.01	861
MEDI Mediterranean Sea, Black Sea P	0.31	0	183
CARB Caribbean Province	0.31	0	189
NAST(E) N. Atlantic Subtropical Gyral (East)	0.45	0	372
FKLD SW Atlantic Shelves Province	0.21	0.12	58
BENG Benguela Current Coastal P.	0.31	0.01	63
MONS Indian Monsoon Gyres P.	0.33	0	93
ISSG Indian S. Subtropical Gyre P.	0.55	0	152
EAFR E. Africa Coastal Province	0.55	0	74
ARAB NW Arabian Upwelling P.	0.24	0.3	21
INDE E. India Coastal Province	-0.12	0.52	32
INDW W. India Coastal Province	0.28	0.09	39
BERS N. Pacific Epicontinental P	0.47	0	954
PSAG(E) Pacific Subarctic Gyres (East)	0.61	0	248
PSAG(W) Pacific Subarctic Gyres (West)	0.34	0.15	19
KURO Kuroshio Current Province	0.50	0	400

NPPF N. Pacific Polar Front Province	0.69	0	132
NPST(W) N. Pacific Subtropical Gyre (West)	0.11	0.22	139
TASM Tasman Sea Province	0.65	0	54
SPSG S. Pacific Subtropical Gyre P.	0.31	0	1570
NPTG N. Pacific Tropical Gyre Province	0.63	0	387
PNEC N. Pacific Equatorial Countercurrent P	0.41	0	442
PEQD Pacific Equatorial Divergence P	0.14	0	1015
WARM W. Pacific Warm Pool Province	0.27	0	403
ALSK Alaska Downwelling Coastal P.	0.59	0	1635
CCAL California Upwelling Coastal P.	0.52	0	750
CAMR Central American Coastal P.	0.30	0.05	44
CHIL Chile-Peru Current Coastal P.	0.26	0	196
CHIN China Sea Coastal Province	0.44	0	39
SSTC S. Subtropical Convergence P.	0.49	0	322
SANT Subantarctic Province	0.40	0	1591
ANTA Antarctic Province	0.47	0	262
APLR Austral Polar Province	0.64	0	235

References

Albrecht BA (1989) Aerosols, cloud microphysics, and fractional cloudiness. Science 245 (4923):1227-1230

Alvain S, Moulin C, Dandonneau Y, Bréon FM (2005) Remote sensing of phytoplankton groups in case 1 waters from global SeaWiFS imagery. Deep-Sea Research Part I: Oceanographic Research Papers 52 (11):1989-2004. doi:10.1016/j.dsr.2005.06.015

Anderson TR, Spall SA, Yool A, Cipollini P, Challenor PG, Fasham MJR (2001) Global fields of sea surface dimethylsulfide predicted from chlorophyll, nutrients and light. Journal of Marine Systems 30 (1-2):1-20

Andreae MO, Crutzen PJ (1997) Atmospheric aerosols: Biogeochemical sources and role in atmospheric chemistry. Science 276 (5315):1052-1058

Andreae MO, Rosenfeld D (2008) Aerosol-cloud-precipitation interactions. Part 1. The nature and sources of cloud-active aerosols. Earth-Science Reviews 89 (1-2):13-41

Aranami K, Tsunogai S (2004) Seasonal and regional comparison of oceanic and atmospheric dimethylsulfide in the northern North Pacific: Dilution effects on its concentration during winter. Journal of Geophysical Research-Atmospheres 109 (D12):15. doi:D1230310.1029/2003jd004288

Archer S (2007) Crucial uncertainties in predicting biological control of DMS emission. Environmental Chemistry 4 (6):404-405

Archer SD, Gilbert FJ, Allen JI, Blackford J, Nightingale PD (2004) Modelling of the seasonal patterns of dimethylsulphide production and fate during 1989 at a site in the North Sea. Canadian Journal of Fisheries and Aquatic Sciences 61 (5):765-787. doi:10.1139/f04-028

Archer SD, Gilbert FJ, Nightingale PD, Zubkov MV, Taylor AH, Smith GC, Burkill PH (2002a) Transformation of dimethylsulphoniopropionate to dimethyl sulphide during summer in the North Sea with an examination of key processes via a modelling approach. Deep-Sea Research Part II: Topical Studies in Oceanography 49 (15):3067-3101. doi:10.1016/s0967-0645(02)00072-3

Archer SD, Ragni M, Webster R, Airs RL, Geider RJ (2010) Dimethyl sulfoniopropionate and dimethyl sulfide production in response to photoinhibition in Emiliania huxleyi. Limnology and Oceanography 55 (4):1579-1589. doi:10.4319/lo.2010.55.4.1579

Archer SD, Smith GC, Nightingale PD, Widdicombe CE, Tarran GA, Rees AP, Burkill PH (2002b) Dynamics of particulate dimethylsulphoniopropionate during a Lagrangian experiment in the northern North Sea. Deep-Sea Research Part II: Topical Studies in Oceanography 49 (15):2979-2999. doi:10.1016/s0967-0645(02)00067-x

Archer SD, Stelfox-Widdicombe CE, Burkill PH, Malin G (2001) A dilution approach to quantify the production of dissolved dimethylsulphoniopropionate and dimethyl sulphide due to microzooplankton herbivory. Aquatic Microbial Ecology 23 (2):131-145

Aumont O, Belviso S, Monfray P (2002) Dimethylsulfoniopropionate (DMSP) and dimethylsulfide (DMS) sea surface distributions simulated from a global three-dimensional ocean carbon cycle model. Journal of Geophysical Research-Oceans 107 (C4):19. doi:302910.1029/1999jc000111

Ayers GP, Cainey JM (2007) The CLAW hypothesis: A review of the major developments. Environmental Chemistry 4 (6):366-374
Ayers GP, Cainey JM, Gillett RW, Ivey JP (1997) Atmospheric sulphur and cloud condensation nuclei in marine air in the Southern Hemisphere. Philosophical Transactions of the Royal Society B: Biological Sciences 352 (1350):203-211. doi:10.1098/rstb.1997.0015
Ayers GP, Gillett RW (2000) DMS and its oxidation products in the remote marine atmosphere: implications for climate and atmospheric chemistry. Journal of Sea Research 43 (3-4):275-286
Ayers GP, Gras JL (1991) Seasonal relationship between cloud condensation nuclei and aerosol methanesulphonate in marine air. Nature 353 (6347):834-835
Ayers GP, Ivey JP, Gillett RW (1991) Coherence between seasonal cycles of dimthyl sulphide, methansulphonate and sulphate in marine air. Nature 349 (6308):404-406
Baker KS, Frouin R (1987) Relation between photosynthetically available radiation and total insolation at the ocean surface under clear skies. Limnology and Oceanography 32 (6):1370-1377
Barnes I, Becker KH, Patroescu I (1994) The tropospheric oxidation of dimethyl sulfide: a new source of carbonyl sulfide. Geophysical Research Letters 21 (22):2389-2392
Bates TS, Lamb BK, Guenther A, Dignon J, Stoiber RE (1992) Sulphur emissions to the atmosphere from natural sources Journal of Atmospheric Chemistry 14 (1-4):315-337
Beaufort L, Probert I, De Garidel-Thoron T, Bendif EM, Ruiz-Pino D, Metzl N, Goyet C, Buchet N, Coupel P, Grelaud M, Rost B, Rickaby REM, De Vargas C (2011) Sensitivity of coccolithophores to carbonate chemistry and ocean acidification. Nature 476 (7358):80-83. doi:10.1038/nature10295
Behrenfeld MJ, Boss E, Siegel DA, Shea DM (2005) Carbon-based ocean productivity and phytoplankton physiology from space. Global Biogeochemical Cycles 19 (1):1-14. doi:10.1029/2004gb002299
Behrenfeld MJ, Falkowski PG (1997a) A consumer's guide to phytoplankton primary productivity models. Limnology and Oceanography 42 (7):1479-1491
Behrenfeld MJ, Falkowski PG (1997b) Photosynthetic rates derived from satellite-based chlorophyll concentration. Limnology and Oceanography 42 (1):1-20
Bell TG, Malin G, Kim YN, Steinke M (2007) Spatial variability in DMSP-lyase activity along an Atlantic meridional transect. Aquatic Sciences 69 (3):320-329. doi:10.1007/s00027-007-0894-1
Bell TG, Malin G, Lee GA, Stefels J, Archer S, Steinke M, Matrai P (2011) Global oceanic DMS data inter-comparability. Biogeochemistry (this issue)
Bell TG, Malin G, McKee CM, Liss PS (2006) A comparison of dimethylsulphide (DMS) data from the Atlantic Meridional Transect (AMT) programme with proposed algorithms for global surface DMS concentrations. Deep-Sea Research Part II: Topical Studies in Oceanography 53 (14-16):1720-1735. doi:10.1016/j.dsr2.2006.05.013
Bell TG, Poulton AJ, Malin G (2010) Strong linkages between dimethylsulphoniopropionate (DMSP) and phytoplankton community physiology in a large subtropical and tropical Atlantic Ocean data set. Global Biogeochemical Cycles 24 (3). doi:10.1029/2009gb003617
Belviso S, Bopp L, Moulin C, Orr JC, Anderson TR, Aumont O, Chu S, Elliott S, Maltrud ME, Simo R (2004) Comparison of global climatological maps of

sea surface dimethyl sulfide. Global Biogeochemical Cycles 18 (3). doi:10.1029/2003gb002193
Belviso S, Caniaux G (2009) A new assessment in North Atlantic waters of the relationship between DMS concentration and the upper mixed layer solar radiation dose. Global Biogeochemical Cycles 23 (1). doi:10.1029/2008gb003382
Belviso S, Masotti I, Tagliabue A, Bopp L, Brockmann P, Fichot C, Caniaux G, Prieur L, Ras J, J. U, Loisel H, Dessailly D, Alvain S, Kasamatsu N, Fukuchi M (2011) DMS dynamics in the most oligotrophic subtropical zones of the global ocean. Biogeochemistry (this issue). doi:DOI 10.1007/s10533-011-9648-1
Berresheim H, Eisele FL, Tanner DJ, McInnes LM, Ramseybell DC, Covert DS (1993) Atmospheric sulpur chemistry and cloud condensation nuclei (CCN) concentrations over the Northeastern pacific coast. Journal of Geophysical Research-Atmospheres 98 (D7):12701-12711
Bigg EK (2007) Sources, nature and influence on climate of marine airborne particles. Environmental Chemistry 4 (3):155-161. doi:10.1071/en07001
Boers R, Ayers GP, Gras JL (1994) Coherence between seasonal variation in satellite-derived cloud optical depth and boundary layer CCN concentrations at a mid- latitude Southern Hemisphere station. Tellus, Series B 46 B (2):123-131
Bonadonna F, Caro S, Jouventin P, Nevitt GA (2006) Evidence that blue petrel, Halobaena caerulea, fledglings can detect and orient to dimethyl sulfide. Journal of Experimental Biology 209 (11):2165-2169
Bopp L, Aumont O, Belviso S, Blain S (2008) Modeling the effect of iron fertilization on dimethylsulfide emissions in the Southern Ocean. Deep Sea Res Part II:55
Bouillon RC, Miller WL (2004) Determination of apparent quantum yield spectra of DMS photodegradation in an in situ iron-induced Northeast Pacific Ocean bloom. Geophysical Research Letters 31 (6):L06310 06311-06314
Boyce DG, Lewis MR, Worm B (2010) Global phytoplankton decline over the past century. Nature 466 (7306):591-596. doi:10.1038/nature09268
Brewin RJW, Lavender SJ, Hardmanmountford NJ (2010) Mapping size-specific phytoplankton primary production on a global scale. Journal of Maps 2010:448-462. doi:10.4113/jom.2010.1122
Brimblecombe P, Hammer CU, Rodhe H, Ryaboshapko AG, Boutron CF (1989) Human influence on the sulphur cycle. In: Brimblecombe P, Lein AYU (eds) Evolution of the global biogeochemical sulphur cycle. Wiley, Chichester, pp 77–121
Brimblecombe P, Shooter D (1986) Photo-oxidation of dimethylsulphide in aqueous solution. Marine Chemistry 19 (4):343-353
Brock TD (1981) Calculating solar radiation for ecological studies. Ecological Modelling 14 (1-2):1-19
Brugger A, Slezak D, Obernosterer I, Herndl GJ (1998) Photolysis of dimethylsulfide in the northern Adriatic Sea: Dependence on substrate concentration, irradiance and DOC concentration. Marine Chemistry 59 (3-4):321-331. doi:10.1016/s0304-4203(97)00090-x
Bucciarelli E, Sunda WG (2003) Influence of CO2, nitrate, phosphate, and silicate limitation on intracellular dimethylsulfoniopropionate in batch cultures of the

coastal diatom Thalassiosira pseudonana. Limnology and Oceanography 48 (6):2256-2265
Buitenhuis E, Le Quéré C, Aumont O, Beaugrand G, Bunker A, Hirst A, Ikeda T, O'Brien T, Piontkovski S, Straile D (2006) Biogeochemical fluxes through mesozooplankton. Global Biogeochemical Cycles 20 (2). doi:10.1029/2005gb002511
Burkill PH, Archer SD, Robinson C, Nightingale PD, Groom SB, Tarran GA, Zubkov MV (2002) Dimethyl sulphide biogeochemistry within a coccolithophore bloom (DISCO): An overview. Deep-Sea Research Part II: Topical Studies in Oceanography 49 (15):2863-2885. doi:10.1016/s0967-0645(02)00061-9
Cainey JM, Harvey M (2002) Dimethylsulfide, a limited contributor to new particle formation in the clean marine boundary layer. Geophysical Research Letters 29 (7):32-31
Caldeira K, Wickett M (2005) Ocean model predictions of chemistry changes from carbon dioxide emissions to the atmosphere and ocean. Journal of Geophysical Research C: Oceans 110 (9):1-12. doi:10.1029/2004jc002671
Carr ME, Friedrichs MAM, Schmeltz M, Noguchi Aita M, Antoine D, Arrigo KR, Asanuma I, Aumont O, Barber R, Behrenfeld M, Bidigare R, Buitenhuis ET, Campbell J, Ciotti A, Dierssen H, Dowell M, Dunne J, Esaias W, Gentili B, Gregg W, Groom S, Hoepffner N, Ishizaka J, Kameda T, Le Quéré C, Lohrenz S, Marra J, Mélin F, Moore K, Morel A, Reddy TE, Ryan J, Scardi M, Smyth T, Turpie K, Tilstone G, Waters K, Yamanaka Y (2006) A comparison of global estimates of marine primary production from ocean color. Deep-Sea Research Part II: Topical Studies in Oceanography 53 (5-7):741-770. doi:10.1016/j.dsr2.2006.01.028
Carslaw KS, Boucher O, Spracklen DV, Mann GW, L. Rae JG, Woodward S, Kulmala M (2010) A review of natural aerosol interactions and feedbacks within the Earth system. Atmospheric Chemistry and Physics 10 (4):1701-1737
Charlson RJ, Lovelock JE, Andreae MO, Warren SG (1987) Oceanic phytoplankton, atmosperic sulphur, cloud albedo and climate. Nature 326 (6114):655-661
Chow WS, Melis A, Anderson JM (1990) Adjustments of photosystem stoichiometry in chloroplasts improve the quantum efficiency of photosynthesis. Proceedings of the National Academy of Sciences of the United States of America 87 (19):7507-7511
Ciotti AM, Bricaud A (2006) Retrievals of a size parameter for phytoplankton and spectral light absorption by colored detrital matter from water-leaving radiances at SeaWiFS channels in a continental shelf region off Brazil. Limnology and Oceanography: Methods 4 (JUL.):237-253
Corbett JJ, Fischbeck PS, Pandis SN (1999) Global nitrogen and sulfur inventories for oceangoing ships. Journal of Geophysical Research D: Atmospheres 104 (D3):3457-3470
Corbett JJ, Koehler HW (2003) Updated emissions from ocean shipping. Journal of Geophysical Research Atmospheres 108 (D20):4650–4666. doi:10.1029/2003JD003751
Crutzen PJ (1976) The possible importance of OCS for the sulfate layer of the stratosphere. Geophysical Research Letters 3:73–76

Curson ARJ, Todd JD, Sullivan MJ, Johnston AWB (2011) Catabolism of dimethylsulphoniopropionate: Microorganisms, enzymes and genes. Nature Reviews Microbiology 9 (12):849-859

Dacey JWH, Howse FA, Michaels AF, Wakeham SG (1998) Temporal variability of dimethylsulfide and dimethylsulfoniopropionate in the Sargasso Sea. Deep-Sea Research Part I: Oceanographic Research Papers 45 (12):2085-2104. doi:10.1016/s0967-0637(98)00048-x

Dacey JWH, Wakeham SG (1986) Oceanic dimethylsulfide: Production during zooplankton grazing on phytoplankton. Science 233 (4770):1314-1316

Dacey JWH, Wakeham SG, Howes BL (1984) HENRY'S LAW CONSTANTS FOR DIMETHYLSULFIDE IN FRESHWATER AND SEAWATER. Geophysical Research Letters 11 (10):991-994

de Boyer Montégut CD, Madec G, Fischer AS, Lazar A, Iudicone D (2004) Mixed layer depth over the global ocean: An examination of profile data and a profile-based climatology. Journal of Geophysical Research-Oceans 109 (C12). doi:C1200310.1029/2004jc002378

De Bruyn WJ (1995) Henry's law solubilities and Setchenow coefficients for biogenic reduced sulfur species obtained from gas-liquid uptake measurements. Journal of Geophysical Research 100 (D4):7245-7251

Dentener F, Drevet J, Lamarque JF, Bey I, Eickhout B, Fiore AM, Hauglustaine D, Horowitz LW, Krol M, Kulshrestha UC, Lawrence M, Galy-Lacaux C, Rast S, Shindell D, Stevenson D, Van Noije T, Atherton C, Bell N, Bergman D, Butler T, Cofala J, Collins B, Doherty R, Ellingsen K, Galloway J, Gauss M, Montanaro V, Müller JF, Pitari G, Rodriguez J, Sanderson M, Solmon F, Strahan S, Schultz M, Sudo K, Szopa S, Wild O (2006) Nitrogen and sulfur deposition on regional and global scales: A multimodel evaluation. Global Biogeochemical Cycles 20 (4). doi:10.1029/2005gb002672

Derevianko GJ, Deutsch C, Hall A (2009) On the relationship between ocean DMS and solar radiation. Geophysical Research Letters 36 (17). doi:10.1029/2009gl039412

Devred E, Sathyendranath S, Platt T (2007) Delineation of ecological provinces using ocean colour radiometry. Marine Ecology Progress Series 346:1-13. doi:10.3354/meps07149

Devred E, Sathyendranath S, Stuart V, Maass H, Ulloa O, Platt T (2006) A two-component model of phytoplankton absorption in the open ocean: Theory and applications. Journal of Geophysical Research C: Oceans 111 (3). doi:10.1029/2005jc002880

Dickson DMJ, Kirst GO (1986) The role of β-dimethylsulphoniopropionate, glycine betaine and homarine in the osmoacclimation of Platymonas subcordiformis. Planta 167 (4):536-543. doi:10.1007/bf00391230

Elliott S (2009) Dependence of DMS global sea-air flux distribution on transfer velocity and concentration field type. Journal of Geophysical Research G: Biogeosciences 114 (2). doi:10.1029/2008jg000710

Eppley RW (1972) Temperature and phytoplankton growth in the sea. Fishery Bulletin 70 (4):1063-1085

Evans C, Kadner SV, Darroch LJ, Wilson WH, Liss PS, Malin G (2007) The relative significance of viral lysis and microzooplankton grazing as pathways of dimethylsulfoniopropionate (DMSP) cleavage: An Emiliania huxleyi culture study. Limnology and Oceanography 52 (3):1036-1045

Fairall CW, Yang M, Bariteau L, Edson JB, Helmig D, McGillis W, Pezoa S, Hare JE, Huebert B, Blomquist B (2011) Implementation of the Coupled Ocean-Atmosphere Response Experiment flux algorithm with CO 2, dimethyl sulfide, and O 3. Journal of Geophysical Research C: Oceans 116 (10). doi:10.1029/2010jc006884

Faloona I (2009) Sulfur processing in the marine atmospheric boundary layer: A review and critical assessment of modeling uncertainties. Atmospheric Environment 43 (18):2841-2854

Fowler D, Smith R, Muller J, Cape JN, Sutton M, Erisman JW, Fagerli H (2007) Long term trends in sulphur and nitrogen deposition in Europe and the cause of non-linearities. Water, Air, and Soil Pollution: Focus 7 (1-3):41-47. doi:10.1007/s11267-006-9102-x

Gabric A, Murray N, Stone L, Kohl M (1993) Modelling the production of dimethylsulfide during a phytoplankton bloom. Journal of Geophysical Research 98 (C12):22,805-822,816

Galí M, Saló V, Almeda R, Calbet A, Simó R (2011) Stimulation of gross dimethylsulfide (DMS) production by solar radiation. Geophysical Research Letters 38 (15). doi:10.1029/2011gl048051

Garcia-Pichel F (1998) Solar ultraviolet and the evolutionary history of cyanobacteria. Origins of Life and Evolution of the Biosphere 28 (3):321-347

Geider RJ, Delucia EH, Falkowski PG, Finzi AC, Philip Grime J, Grace J, Kana TM, La Roche J, Long SP, Osborne BA, Platt T, Colin Prentice I, Raven JA, Schlesinger WH, Smetacek V, Stuart V, Sathyendranath S, Thomas RB, Vogelmann TC, Williams P, Ian Woodward F (2001) Primary productivity of planet earth: Biological determinants and physical constraints in terrestrial and aquatic habitats. Global Change Biology 7 (8):849-882. doi:10.1046/j.1365-2486.2001.00448.x

Gibson JAE, Garrick RC, Burton HR, McTaggart AR (1990) Dimethylsulfide and the alga Phaeocystis pouchetii in antarctic coastal waters. Marine Biology 104 (2):339-346

Goldblatt C, Lenton TM, Watson AJ (2006) Bistability of atmospheric oxygen and the Great Oxidation. Nature 443 (7112):683-686. doi:10.1038/nature05169

Graf HF, Feichter J, Langmann B (1997) Volcanic sulfur emissions: Estimates of source strength and its contribution to the global sulfate distribution. Journal of Geophysical Research D: Atmospheres 102 (9):10727-10738

Hader DP, Kumar HD, Smith RC, Worrest RC (2003) Aquatic ecosystems: effects of solar ultraviolet radiation and interactions with other climatic change factors. Photochemical & Photobiological Sciences 2 (1):39-50. doi:10.1039/b211160h

Halloran PR, Bell TG, Totterdell IJ (2010) Can we trust empirical marine DMS parameterisations within projections of future climate? Biogeosciences 7 (5):1645-1656. doi:10.5194/bg-7-1645-2010

Harvey M (2007) The iron CLAW. Environmental Chemistry 4 (6):396-399

Hatton AD (2002) Influence of photochemistry on the marine biogeochemical cycle of dimethylsulphide in the northern North Sea. Deep-Sea Research Part II: Topical Studies in Oceanography 49 (15):3039-3052. doi:10.1016/s0967-0645(02)00070-x

Herman JR, Celarier EA (1997) Earth surface reflectivity climatology at 340-380 nm from TOMS data. Journal of Geophysical Research-Atmospheres 102 (D23):28003-28011

Hill RW, White BA, Cottrell MT, Dacey JWH (1998) Virus-mediated total release of dimethylsulfoniopropionate from marine phytoplankton: A potential climate process. Aquatic Microbial Ecology 14 (1):1-6

Hind AJ, Rauschenberg CD, Johnson JE, Yang M, Matrai PA (2011) The use of algorithms to predict surface seawater dimethyl sulphide concentrations in the SE Pacific, a region of steep gradients in primary productivity, biomass and mixed layer depth. Biogeosciences 8 (1):1-16. doi:10.5194/bg-8-1-2011

Hirata T, Hardman-Mountford NJ, Brewin RJW, Aiken J, Barlow R, Suzuki K, Isada T, Howell E, Hashioka T, Noguchi-Aita M, Yamanaka Y (2011) Synoptic relationships between surface Chlorophyll-a and diagnostic pigments specific to phytoplankton functional types. Biogeosciences 8 (2):311-327. doi:10.5194/bg-8-311-2011

Ho DT, Bliven LF, Wanninkhof R, Schlosser P (1997) The effect of rain on air-water gas exchange. Tellus, Series B: Chemical and Physical Meteorology 49 (2):149-158

Ho DT, Law CS, Smith MJ, Schlosser P, Harvey M, Hill P (2006) Measurements of air-sea gas exchange at high wind speeds in the Southern Ocean: Implications for global parameterizations. Geophysical Research Letters 33 (16)

Hopkins FE, Turner SM, Nightingale PD, Steinke M, Bakker D, Lissa PS (2010) Ocean acidification and marine trace gas emissions. Proceedings of the National Academy of Sciences of the United States of America 107 (2):760-765. doi:10.1073/pnas.0907163107

Howard EC, Henriksen JR, Buchan A, Reisch CR, Bürgmann H, Welsh R, Ye W, González JM, Mace K, Joye SB, Kiene RP, Whitman WB, Moran MA (2006) Bacterial taxa that limit sulfur flux from the ocean. Science 314 (5799):649-652

Huebert BJ, Blomquist BW, Hare JE, Fairall CW, Johnson JE, Bates TS (2004) Measurement of the sea-air DMS flux and transfer velocity using eddy correlation. Geophysical Research Letters 31 (23):1-4

Huebert BJ, Blomquist BW, Yang MX, Archer SD, Nightingale PD, Yelland MJ, Stephens J, Pascal RW, Moat BI (2010) Linearity of DMS transfer coefficient with both friction velocity and wind speed in the moderate wind speed range. Geophysical Research Letters 37 (1). doi:10.1029/2009gl041203

Jerlov NG (1974) A simple method for measuring quanta irradiance in the ocean, Rep. 24. Inst. Fysik Oceanografi,Kobenhavens Universitet.

Jerlov NG (1977) Classification of sea water in terms of quanta irradiance. 37 (3):281–287

Jickells TD, An ZS, Andersen KK, Baker AR, Bergametti C, Brooks N, Cao JJ, Boyd PW, Duce RA, Hunter KA, Kawahata H, Kubilay N, LaRoche J, Liss PS, Mahowald N, Prospero JM, Ridgwell AJ, Tegen I, Torres R (2005) Global iron connections between desert dust, ocean biogeochemistry, and climate. Science 308 (5718):67-71. doi:10.1126/science.1105959

Jickells TD, Liss PS, Broadgate W, Turner S, Kettle AJ, Read J, Baker J, Cardenas LM, Carse F, Hamren-Larssen M, Spokes L, Steinke M, Thompson A, Watson A, Archer SD, Bellerby RGJ, Law CS, Nightingale PD, Liddicoat MI, Widdicombe CE, Bowie A, Gilpin LC, Moncoiffé G, Savidge G, Preston T, Hadziabdic P, Frost T, Upstill-Goddard R, Pedrós-Alió C, Simó R, Jackson A, Allen A, DeGrandpre MD (2008) A Lagrangian biogeochemical

study of an eddy in the Northeast Atlantic. Progress in Oceanography 76 (3):366-398. doi:10.1016/j.pocean.2008.01.006
Jitts HR, Morel A, Saijo Y (1976) The relation of oceanic primary production to available photosynthetic irradiance. Aust J Mar Freshw Res 27:441–454
Jodwalis CM, Benner RL, Eslinger DL (2000) Modeling of dimethyl sulfide ocean mixing, biological production, and sea-to-air flux for high latitudes. Journal of Geophysical Research D: Atmospheres 105 (D11):14387-14399
Johnson MT (2010) A numerical scheme to calculate temperature and salinity dependent air-water transfer velocities for any gas. Ocean Science 6 (4):913-932. doi:10.5194/os-6-913-2010
Joint I, Pomroy A (1993) Phytoplankton biomass and production in the southern North Sea. Marine Ecology Progress Series 99 (1-2):169-182
Joint I, Pomroy A, Savidge G, Boyd P (1993) Size-fractionated primary productivity in the northeast Atlantic in May-July 1989. Deep-Sea Research Part II 40 (1-2):423-440
Kahru M, Kudela R, Manzano-Sarabia M, Mitchell BG (2009) Trends in primary production in the California Current detected with satellite data. Journal of Geophysical Research C: Oceans 114 (2). doi:10.1029/2008jc004979
Karsten U, Kuck K, Vogt C, Kirst GO (1996) Dimethylsulfoniopropionate production in phototrophic organisms and its physiological function as a cryoprotectant. Biological and Environmental Chemistry of DMSP and Related Sulfonium Compounds:143-153
Keller MD, Bellows WK, Guillard RRL (1989) Dimethyl Sulfide Production in Marine Phytoplankton. In: Saltzman ES, Cooper WJ (eds) Biogenic Sulfur in the Environment. Am. Chem. Soc. , Washington D. C., pp 167-182
Kettle AJ, Andreae MO (2000) Flux of dimethylsulfide from the oceans: A comparison of updated data sets and flux models. Journal of Geophysical Research D: Atmospheres 105 (D22):26793-26808
Kettle AJ, Andreae MO, Amouroux D, Andreae TW, Bates TS, Berresheim H, Bingemer H, Boniforti R, Curran MAJ, DiTullio GR, Helas G, Jones GB, Keller MD, Kiene RP, Leck C, Levasseur M, Malin G, Maspero M, Matrai P, McTaggart AR, Mihalopoulos N, Nguyen BC, Novo A, Putaud JP, Rapsomanikis S, Roberts G, Schebeske G, Sharma S, Simó R, Staubes R, Turner S, Uher G (1999) A global database of sea surface dimethylsulfide (DMS) measurements and a procedure to predict sea surface DMS as a function of latitude, longitude, and month. Global Biogeochemical Cycles 13 (2):399-444
Kettle AJ, Kuhn U, Von Hobe M, Kesselmeier J, Andreae MO (2002) Global budget of atmospheric carbonyl sulfide: Temporal and spatial variations of the dominant sources and sinks. Journal of Geophysical Research D: Atmospheres 107 (22). doi:10.1029/2002jd002187
Kieber DJ, Jiao J, Kiene RP, Bates TS (1996) Impact of dimethylsulfide photochemistry on methyl sulfur cycling in the equatorial Pacific Ocean. Journal of Geophysical Research C: Oceans 101 (C2):3715-3722
Kiene RP, Linn LJ (2000) Distribution and turnover of dissolved DMSP and its relationship with bacterial production and dimethylsulfide in the Gulf of Mexico. Limnology and Oceanography 45 (4):849-861
Kiene RP, Linn LJ, Bruton JA (2000) New and important roles for DMSP in marine microbial communities. Journal of Sea Research 43 (3-4):209-224. doi:10.1016/s1385-1101(00)00023-x

Kiene RP, Slezak D (2006) Low dissolved DMSP concentrations in seawater revealed by small-volume gravity filtration and dialysis sampling. Limnology and Oceanography: Methods 4 (APR.):80-95

Kirschvink JL (1992) Late Proterozoic low-latitude global glaciation: The snowball Earth. In: Schopf J, Klein C (eds) The Proterozoic Biosphere: A Multidisciplinary Study. Cambridge University Press, Cambridge, pp 51–52

Kirschvink JL, Gaidos EJ, Bertani LE, Beukes NJ, Gutzmer J, Maepa LN, Steinberger RE (2000) Paleoproterozoic snowball Earth: Extreme climatic and geochemical global change and its biological consequences. Proceedings of the National Academy of Sciences of the United States of America 97 (4):1400-1405. doi:10.1073/pnas.97.4.1400

Kniveton DR, Todd MC, Sciare J, Mihalopoulos N (2003) Variability of atmospheric dimethylsulphide over the southern Indian Ocean due to changes in ultraviolet radiation. Global Biogeochemical Cycles 17 (4). doi:109610.1029/2003gb002033

Kopp RE, Kirschvink JL, Hilburn IA, Nash CZ (2005) The paleoproterozoic snowball Earth: A climate disaster triggered by the evolution of oxygenic photosynthesis. Proceedings of the National Academy of Sciences of the United States of America 102 (32):11131-11136. doi:10.1073/pnas.0504878102

Korhonen H, Carslaw KS, Spracklen DV, Mann GW, Woodhouse MT (2008) Influence of oceanic dimethyl sulfide emissions on cloud condensation nuclei concentrations and seasonality over the remote Southern Hemisphere oceans: A global model study. Journal of Geophysical Research D: Atmospheres 113 (15). doi:10.1029/2007jd009718

Kowalewsky S, Dambach M, Mauck B, Dehnhardt G (2006) High olfactory sensitivity for dimethyl sulphide in harbour seals. Biology Letters 2 (1):106-109

Kroeker KJ, Kordas RL, Crim RN, Singh GG (2010) Meta-analysis reveals negative yet variable effects of ocean acidification on marine organisms. Ecology Letters 13 (11):1419-1434. doi:10.1111/j.1461-0248.2010.01518.x

Lana A, Bell TG, Simó R, Vallina SM, Ballabrera-Poy J, Kettle AJ, Dachs J, Bopp L, Saltzman ES, Stefels J, Johnson JE, Liss PS (2011a) An updated climatology of surface dimethlysulfide concentrations and emission fluxes in the global ocean. Global Biogeochemical Cycles 25 (1). doi:10.1029/2010gb003850

Lana A, Simó R, Vallina SM, Dachs J (2011b) Re-examination of global emerging patterns of ocean DMS concentration. Biogeochemistry (this issue). doi:10.1007/s10533-011-9677-9

Laroche D, Vézina AF, Levasseur M, Gosselin M, Stefels J, Keller MD, Matrai PA, Kwint RLJ (1999) DMSP synthesis and exudation in phytoplankton: A modeling approach. Marine Ecology Progress Series 180:37-49

Le Clainche Y, Levasseur M, Vézina A, Dacey JWH, Saucier FJ (2004) Behaviour of the ocean DMS(P) pools in the Sargasso Sea viewed in a coupled physical-biogeochemical ocean model. Canadian Journal of Fisheries and Aquatic Sciences 61 (5):788-803

Le Clainche Y, Vezina A, Levasseur M, Cropp RA, Gunson JR, Vallina SM, Vogt M, Lancelot C, Allen JI, Archer SD, Bopp L, Deal C, Elliott S, Jin M, Malin G, Schoemann V, Simo R, Six KD, Stefels J (2010) A first appraisal of

prognostic ocean DMS models and prospects for their use in climate models. Global Biogeochemical Cycles 24 (3). doi:10.1029/2009gb003721
Leck C, Bigg EK (2005) Source and evolution of the marine aerosol - A new perspective. Geophysical Research Letters 32 (19):1-4
Leck C, Bigg EK (2007) A modified aerosol-cloud-climate feedback hypothesis. Environmental Chemistry 4 (6):400-403
Leck C, Larsson U, Baagander LE, Johansson S, Hajdu S (1990) Dimethylsulfide in the Baltic Sea: annual variability in relation to biological activity. Journal of Geophysical Research 95:3353-3363
Lee PA, De Mora SJ, Levasseur M (1999) A review of dimethylsulfoxide in aquatic environments. Atmosphere - Ocean 37 (4):439-456
Levine NM, Varaljay VA, Toole DA, Dacey JWH, Doney SC, Moran MA (2012) Environmental, biochemical and genetic drivers of DMSP degradation and DMS production in the Sargasso Sea. Environmental Microbiology 14 (5):1210-1223. doi:10.1111/j.1462-2920.2012.02700.x
Liss PS, Merlivat L (1986) Air– sea gas exchange rates: Introduction and synthesis. In: Buat-Me´nard P (ed) The Role of Air– Sea Exchange in Geochemical Cycling. Springer, New York, pp 113 – 127
Liss PS, Slater PG (1974) Flux of gases across the Air-Sea interface. Nature 247 (5438):181-184. doi:10.1038/247181a0
Longhurst A (1995) Seasonal cycles of pelagic production and consumption. Progress in Oceanography 36 (2):77-167. doi:10.1016/0079-6611(95)00015-1
Lovelock JE, Margulis L (1974a) Atmospheric homeostasis by and for biosphere - Gaia hypothesis. Tellus 26 (1-2):2–10
Lovelock JE, Margulis L (1974b) Homeostatic tendencies of the Earth's atmosphere. Origins of Life 5 (1-2):93-103. doi:10.1007/bf00927016
Macintyre HL, Kana TM, Geider RJ (2000) The effect of water motion on short-term rates of photosynthesis by marine phytoplankton. Trends in Plant Science 5 (1):12-17. doi:10.1016/s1360-1385(99)01504-6
Mahowald NM, Baker AR, Bergametti G, Brooks N, Duce RA, Jickells TD, Kubilay N, Prospero JM, Tegen I (2005) Atmospheric global dust cycle and iron inputs to the ocean. Global Biogeochemical Cycles 19 (4). doi:10.1029/2004gb002402
Malin G, Kirst GO (1997) Algal production of dimethyl sulfide and its atmospheric role. Journal of Phycology 33 (6):889-896. doi:10.1111/j.0022-3646.1997.00889.x
Malin G, Turner S, Liss P, Holligan P, Harbour D (1993) Dimethylsulphide and dimethylsulphoniopropionate in the Northeast atlantic during the summer coccolithophore bloom. Deep-Sea Research Part I 40 (7):1487-1508
Malin G, Wilson WH, Bratbak G, Liss PS, Mann NH (1998) Elevated production of dimethylsulfide resulting from viral infection of cultures of Phaeocystis pouchetii. Limnology and Oceanography 43 (6):1389-1393
Marañón E, Behrenfeld MJ, González N, Mouriño B, Zubkov MV (2003) High variability of primary production in oligotrophic waters of the Atlantic Ocean: Uncoupling from phytoplankton biomass and size structure. Marine Ecology Progress Series 257:1-11
Marra J (1997) Analysis of diel variability in chlorophyll fluorescence. Journal of Marine Research 55 (4):767-784

Marra J (2002) Approaches to the Measurement of Plankton Production. In: Williams PJ, Thomas DN, Reynolds CS (eds) Phytoplanton Productivity. 1 edn. Blackwell Science, pp 79-107
Masotti I, Belviso S, Alvain S, Johnson JE, Bates TS, Tortell PD, Kasamatsu N, Mongin M, Marandino CA, Saltzman ES, Moulin C (2010) Spatial and temporal variability of the dimethylsulfide to chlorophyll ratio in the surface ocean: An assessment based on phytoplankton group dominance determined from space. Biogeosciences 7 (10):3215-3237. doi:10.5194/bg-7-3215-2010
Matrai P, Vernet M, Wassmann P (2007) Relating temporal and spatial patterns of DMSP in the Barents Sea to phytoplankton biomass and productivity. Journal of Marine Systems 67 (1-2):83-101. doi:10.1016/j.jmarsys.2006.10.001
Matrai PA (1997) Dynamics of the vernal bloom in the marginal ice zone of the Barents Sea: Dimethyl sulfide and dimethylsulfoniopropionate budgets. Journal of Geophysical Research C: Oceans 102 (C10):22965-22979
Matrai PA, Keller MD (1993) Dimethylsulfide in a large-scale coccolithophore bloom in the Gulf of Maine. Continental Shelf Research 13 (8-9):831-843
Meskhidze N, Nenes A (2006) Phytoplankton and cloudiness in the southern ocean. Science 314 (5804):1419-1423
Miles CJ, Bell TG, Lenton TM (2009) Testing the relationship between the solar radiation dose and surface DMS concentrations using in situ data. Biogeosciences 6 (9):1927-1934. doi:10.1029/1999JC000111
Miles CJ, Bell TG, Suntharalingam P (2012) Investigating the inter-relationships between water attenuated irradiance, primary production and DMS(P). Biogeochemistry 110 (1-3):201-213. doi:10.1007/s10533-011-9697-5
Miller JN, Miller JC (2000) Statistics and Chemometrics for Analytical Chemistry. Prentice Hall, Harlow, UK
Mojzsis SJ, Arrhenius G, McKeegan KD, Harrison TM, Nutman AP, Friend CRL (1996) Evidence for life on Earth before 3,800 million years ago. Nature 384 (6604):55-59. doi:10.1038/384055a0
Monahan AH, Denman KL (2004) Impacts of atmospheric variability on a coupled upper-ocean/ecosystem model of the subarctic Northeast Pacific. Global Biogeochemical Cycles 18 (2):GB2010 2011-2016
Moran MA, Reisch CR, Kiene RP, Whitman WB (2012) Genomic insights into bacterial DMSP transformations. Annual Review of Marine Science 4:523-542. doi:10.1146/annurev-marine-120710-100827
Morel A (1988) Optical modeling of the upper ocean in relation to its biogeneous matter content (case I waters). Journal of Geophysical Research 93 (C9):10749-10768
Morel A, Berthon JF (1989) Surface pigments, algal biomass profiles, and potential production of the euphotic layer: relationships reinvestigated in view of remote-sensing applications. Limnology & Oceanography 34 (8):1545-1562
Morel A, Claustre H, Gentili B (2010) The most oligotrophic subtropical zones of the global ocean: Similarities and differences in terms of chlorophyll and yellow substance. Biogeosciences 7 (10):3139-3151. doi:10.5194/bg-7-3139-2010
Morel A, Gentili B, Claustre H, Babin M, Bricaud A, Ras J, Tièche F (2007) Optical properties of the "clearest" natural waters. Limnology and Oceanography 52 (1):217-229
Murphy DM, Anderson JR, Qulnn PK, McLnnes LM, Brechtel FJ, Kreidenwels SM, Middlebrook AM, Pósfai M, Thomson DS, Buseck PR (1998) Influence of

sea-salt on aerosol radiative properties in the Southern Ocean marine boundary layer. Nature 392 (6671):62-65. doi:10.1038/32138
Nelson D, Cox M (2000) Principles of Biochemistry. 3rd edn. Worth Publishing, New York
Nevitt GA, Haberman K (2003) Behavioral attraction of Leach's storm-petrels (Oceanodroma leucorhoa) to dimethyl sulfide. Journal of Experimental Biology 206 (9):1497-1501
Nevitt GA, Veit RR, Kareiva P (1995) Dimethyl sulphide as a foraging cue for Antarctic Procellariiform seabirds. Nature 376 (6542):680-682
Nguyen BC, Belviso S, Mihalopoulos N, Gostan J, Nival P (1988) Dimethyl sulfide production during natural phytoplanktonic blooms. Marine Chemistry 24 (2):133-141
Nightingale PD, Liss PS, Schlosser P (2000) Measurements of air-sea gas transfer during an open ocean algal bloom. Geophysical Research Letters 27 (14):2117-2120
O'Dowd CD, Lowe JA, Smith MH, Kaye AD (1999) The relative importance of non-sea-salt sulphate and sea-salt aerosol to the marine cloud condensation nuclei population: An improved multi-component aerosol-cloud droplet parametrization. Quarterly Journal of the Royal Meteorological Society 125 (556):1295-1313
O'Dowd CD, Smith MH (1993) Physicochemical properties of aerosols over the northeast Atlantic: evidence for wind-speed-related submicron sea-salt aerosol production. Journal of Geophysical Research 98 (D1):1137-1149
Pandis SN, Russell LM, Seinfeld JH (1994) The relationship between DMS flux and CCN concentration in remote marine regions. Journal of Geophysical Research 99 (D8):16,945-916,957
Paytan A, Mackey KRM, Chen Y, Lima ID, Doney SC, Mahowald N, Labiosa R, Post AF (2009) Toxicity of atmospheric aerosols on marine phytoplankton. Proceedings of the National Academy of Sciences of the United States of America 106 (12):4601-4605. doi:10.1073/pnas.0811486106
Pincus R, Baker MB (1994) Effect of precipitation on the albedo susceptibility of clouds in the marine boundary layer. Nature 372 (6503):250-252
Pirjola L, O'Dowd CD, Brooks IM, Kulmala M (2000) Can new particle formation occur in the clean marine boundary layer? Journal of Geophysical Research D: Atmospheres 105 (D21):26531-26546
Platt T, Sathyendranath S (1993) Estimators of primary production for interpretation of remotely sensed data on ocean color. Journal of Geophysical Research 98 (C8):14,561-514,576
Polimene L, Archer SD, Butenschön M, Allen JI (2012) A mechanistic explanation of the Sargasso Sea DMS "summer paradox". Biogeochemistry 110 (1-3):243-255
Polovina JJ, Howell EA, Abecassis M (2008) Ocean's least productive waters are expanding. Geophysical Research Letters 35 (3). doi:10.1029/2007gl031745
Poulton AJ, Holligan PM, Hickman A, Kim YN, Adey TR, Stinchcombe MC, Holeton C, Root S, Woodward EMS (2006) Phytoplankton carbon fixation, chlorophyll-biomass and diagnostic pigments in the Atlantic Ocean. Deep-Sea Research Part II: Topical Studies in Oceanography 53 (14-16):1593-1610. doi:10.1016/j.dsr2.2006.05.007
Putaud JP, Mihalopoulos N, Nguyen BC, Campin JM, Belviso S (1992) Seasonal variations of atmospheric sulfur dioxide and dimethylsulfide concentrations

at Amsterdam Island in the southern Indian Ocean. Journal of Atmospheric Chemistry 15 (2):117-131
Quinn PK, Bates TS (2011) The case against climate regulation via oceanic phytoplankton sulphur emissions. Nature 480 (7375):51-56. doi:10.1038/nature10580
Reisch CR, Moran MA, Whitman WB (2011a) Bacterial catabolism of dimethylsulfoniopropionate (DMSP). Frontiers in Microbiology 2 (AUG)
Reisch CR, Stoudemayer MJ, Varaljay VA, Amster IJ, Moran MA, Whitman WB (2011b) Novel pathway for assimilation of dimethylsulphoniopropionate widespread in marine bacteria. Nature 473 (7346):208-211
Sagan C, Mullen G (1972) Earth and Mars: Evolution of atmospheres and surface temperatures. Science 177 (4043):52-56
Sathyendranath S, Cota G, Stuart V, Maass H, Platt T (2001) Remote sensing of phytoplankton pigments: A comparison of empirical and theoretical approaches. International Journal of Remote Sensing 22 (2-3):249-273. doi:10.1080/014311601449925
Savidge G, Gilpin L (1999) Seasonal influences on size-fractionated chlorophyll a concentrations and primary production in the north-west Indian Ocean. Deep-Sea Research Part II: Topical Studies in Oceanography 46 (3-4):701-723. doi:10.1016/s0967-0645(98)00124-6
Sciare J, Baboukas E, Mihalopoulos N (2001) Short-term variability of atmospheric DMS and its oxidation products at Amsterdam Island during summer time. Journal of Atmospheric Chemistry 39 (3):281-302
Shaw GE (1983) Bio-controlled thermostasis involving the sulfur cycle. Climatic Change 5 (3):297-303
Siegel DA, Michaels AF (1996) Quantification of non-algal light attenuation in the Sargasso Sea: Implications for biogeochemistry and remote sensing. Deep-Sea Research Part II -Topical Studies in Oceanography 43 (2-3):321-345
Simó R (2001) Production of atmospheric sulfur by oceanic plankton: biogeochemical, ecological and evolutionary links. Trends in Ecology & Evolution 16 (6):287-294
Simó R (2004) From cells to globe: Approaching the dynamics of DMS(P) in the ocean at multiple scales. Canadian Journal of Fisheries and Aquatic Sciences 61 (5):673-684. doi:10.1139/f04-030
Simó R, Archer SD, Pedrós-Alió C, Gilpin L, Stelfox-Widdicombe CE (2002) Coupled dynamics of dimethylsulfoniopropionate and dimethylsulfide cycling and the microbial food web in surface waters of the North Atlantic. Limnology and Oceanography 47 (1):53-61
Simó R, Dachs J (2002) Global ocean emission of dimethylsulfide predicted from biogeophysical data. Global Biogeochemical Cycles 16 (4). doi:107810.1029/2001gb001829
Simo R, Grimalt JO, Pedros-Alio C, Albaiges J (1995) Occurrence and transformation of dissolved dimethyl sulfur species in stratified seawater (western Mediterranean Sea). Marine Ecology Progress Series 127 (1-3):291-299
Simó R, Pedrós-Alió C (1999a) Role of vertical mixing in controlling the oceanic production of dimethyl sulphide. Nature 402 (6760):396-399
Simó R, Pedrós-Alió C (1999b) Short-term variability in the open ocean cycle of dimethylsulfide. Global Biogeochemical Cycles 13 (4):1173-1181. doi:10.1029/1999gb900081

Simó R, Pedrós-Alió C, Malin G, Grimalt JO (2000) Biological turnover of DMS, DMSP and DMSO in contrasting open-sea waters. Marine Ecology Progress Series 203:1-11
Six KD, Maier-Reimer E (2006) What controls the oceanic dimethylsulfide (DMS) cycle? A modeling approach. Global Biogeochemical Cycles 20 (4)
Slezak D, Brugger A, Herndl GJ (2001) Impact of solar radiation on the biological removal of dimethylsulfoniopropionate and dimethylsulfide in marine surface waters. Aquatic Microbial Ecology 25 (1):87-97
Smith GC, Clark T, Knutsen L, Barrett E (1999) Methodology for analyzing dimethyl sulfide and dimethyl sulfoniopropionate in seawater using deuterated internal standards. Analytical Chemistry 71 (24):5563-5568. doi:10.1021/ac990211q
Smith MH (2007) Sea-salt particles and the CLAW hypothesis. Environmental Chemistry 4 (6):391-395
Smith RC, Baker KS (1981) Optical properties of the clearest natural waters (200-800 nm). Applied Optics 20 (2):177-184
Smyth TJ (2011) Penetration of UV irradiance into the global ocean. Journal of Geophysical Research: Oceans 116 (C11):C11020. doi:10.1029/2011jc007183
Stefels J (2000) Physiological aspects of the production and conversion of DMSP in marine algae and higher plants. Journal of Sea Research 43 (3-4):183-197. doi:10.1016/s1385-1101(00)00030-7
Stefels J, Steinke M, Turner S, Malin G, Belviso S (2007) Environmental constraints on the production and removal of the climatically active gas dimethylsulphide (DMS) and implications for ecosystem modelling. Biogeochemistry 83 (1-3):245-275. doi:10.1007/s10533-007-9091-5
Stefels J, Van Leeuwe MA (1998) Effects of iron and light stress on the biochemical composition of antarctic Phaeocystis sp. (Prymnesiophyceae). I. Intracellular DMSP concentrations. Journal of Phycology 34 (3):486-495
Steiger JH (1980) Tests for comparing elements of a correlation matrix. Psychological Bulletin 87 (2):245-251. doi:10.1037/0033-2909.87.2.245
Steinke M, Malin G, Gibb SW, Burkill PH (2002) Vertical and temporal variability of DMSP lyase activity in a coccolithophorid bloom in the northern North Sea. Deep-Sea Research Part Ii-Topical Studies in Oceanography 49 (15):3001-3016
Steinke M, Stefels J, Stamhuis E (2006) Dimethyl sulfide triggers search behavior in copepods. Limnology and Oceanography 51 (4):1925-1930
Steinke M, Wolfe GV, Kirst GO (1998) Partial characterisation of dimethylsulfoniopropionate (DMSP) lyase isozymes in 6 strains of Emiliania huxleyi. Marine Ecology-Progress Series 175:215-225
Stern DI (2006) Reversal of the trend in global anthropogenic sulfur emissions. Global Environmental Change 16 (2):207-220. doi:10.1016/j.gloenvcha.2006.01.001
Strom S (2002) Novel interactions between phytoplankton and microzooplankton: Their influence on the coupling between growth and grazing rates in the sea. Hydrobiologia 480:41-54. doi:10.1023/a:1021224832646
Strom S, Wolfe G, Slajer A, Lambert S, Clough J (2003) Chemical defense in the microplankton II: Inhibition of protist feeding by β-dimethylsulfoniopropionate (DMSP). Limnology and Oceanography 48 (1 I):230-237

Sunda W, Kieber DJ, Kiene RP, Huntsman S (2002) An antioxidant function for DMSP and DMS in marine algae. Nature 418 (6895):317-320. doi:10.1038/nature00851

Suntharalingam P, Kettle AJ, Montzka SM, Jacob DJ (2008) Global 3-D model analysis of the seasonal cycle of atmospheric carbonyl sulfide: Implications for terrestrial vegetation uptake. Geophysical Research Letters 35 (19). doi:10.1029/2008gl034332

Tedetti M, Sempere R (2006) Penetration of ultraviolet radiation in the marine environment. A review. Photochemistry and Photobiology 82 (2):389-397. doi:10.1562/2005-11-09-ir-733

Todd JD, Curson ARJ, Dupont CL, Nicholson P, Johnston AWB (2009) The dddP gene, encoding a novel enzyme that converts dimethylsulfoniopropionate into dimethyl sulfide, is widespread in ocean metagenomes and marine bacteria and also occurs in some Ascomycete fungi. Environmental Microbiology 11 (6):1376-1385

Todd JD, Curson ARJ, Kirkwood M, Sullivan MJ, Green RT, Johnston AWB (2011) DddQ, a novel, cupin-containing, dimethylsulfoniopropionate lyase in marine roseobacters and in uncultured marine bacteria. Environmental Microbiology 13 (2):427-438

Todd JD, Curson ARJ, Nikolaidou-Katsaraidou N, Brearley CA, Watmough NJ, Chan Y, Page PCB, Sun L, Johnston AWB (2010) Molecular dissection of bacterial acrylate catabolism - unexpected links with dimethylsulfoniopropionate catabolism and dimethyl sulfide production. Environmental Microbiology 12 (2):327-343

Todd JD, Kirkwood M, Newton-Payne S, Johnston AWB (2012) DddW, a third DMSP lyase in a model Roseobacter marine bacterium, Ruegeria pomeroyi DSS-3. ISME Journal 6 (1):223-226

Todd JD, Rogers R, You GL, Wexler M, Bond PL, Sun L, Curson ARJ, Malin G, Steinke M, Johnston AWB (2007) Structural and regulatory genes required to make the gas dimethyl sulfide in bacteria. Science 315 (5812):666-669

Toole DA, Kieber DJ, Kiene RP, Siegel DA, Nelson NB (2003) Photolysis and the dimethylsulfide (DMS) summer paradox in the Sargasso Sea. Limnology and Oceanography 48 (3):1088-1100

Toole DA, Kieber DJ, Kiene RP, White EM, Bisgrove J, del Valle DA, Slezak D (2004) High dimethylsulfide photolysis rates in nitrate-rich Antarctic waters. Geophysical Research Letters 31 (11):L11307 11301-11304. doi:10.1029/2004gl019863

Toole DA, Siegel DA (2004) Light-driven cycling of dimethylsulfide (DMS) in the Sargasso Sea: Closing the loop. Geophysical Research Letters 31 (9). doi:L0930810.1029/2004gl019581

Toole DA, Slezak D, Kiene RP, Kieber DJ, Siegel DA (2006) Effects of solar radiation on dimethylsulfide cycling in the western Atlantic Ocean. Deep-Sea Research Part I: Oceanographic Research Papers 53 (1):136-153. doi:10.1016/j.dsr.2005.09.003

Turner SM, Harvey MJ, Law CS, Nightingale PD, Liss PS (2004) Iron-induced changes in oceanic sulfur biogeochemistry. Geophysical Research Letters 31 (14):L14307 14301-14304. doi:10.1029/2004gl020296

Turner SM, Malin G, Bågander LE, Leck C (1990) Interlaboratory calibration and sample analysis of dimethyl sulphide in water. Marine Chemistry 29 (C):47-62

Turner SM, Malin G, Liss PS, Harbour DS, Holligan PM (1988) The seasonal variation of dimethyl sulfide and dimethylsulfoniopropionate concentrations in nearshore waters. Limnology & Oceanography 33 (3):364-375
Turpin DH (1991) Effects of inorganic N availability on algal photosynthesis and carbon
metabolism. Journal of Phycology 27 (1):14-20. doi:10.1111/j.0022-3646.1991.00014.x
Twohy CH, Anderson JR (2008) Droplet nuclei in non-precipitating clouds: Composition and size matter. Environmental Research Letters 3 (4). doi:10.1088/1748-9326/3/4/045002
Twomey S (1991) Aerosols, clouds and radiation. Atmospheric Environment - Part A General Topics 25 A (11):2435-2442
Twomey S, Inst.Atmos.Phys (1977) Atmospheric aerosols.
Uitz J, Huot Y, Bruyant F, Babin M, Claustre H (2008) Relating phytoplankton photophysiological properties to community structure on large scales. Limnology and Oceanography 53 (2):614-630
Vairavamurthy A, Andreae MO, Inverson RL (1985) Biosynthesis of dimethylsulfide and dimethylpropiothetin by *Hymenomonas carterae* in relation to sulfur source and salinity variations. Limnology and Oceanography 30:59–70
Vallina SM, Simó R (2007) Strong relationship between DMS and the solar radiation dose over the global surface ocean. Science 315 (5811):506-508. doi:10.1126/science.1133680
Vallina SM, Simó R, Anderson TR, Gabric A, Cropp R, Pacheco JM (2008) A dynamic model of oceanic sulfur (DMOS) applied to the Sargasso Sea: Simulating the dimethylsulfide (DMS) summer paradox. Journal of Geophysical Research G: Biogeosciences 113 (1). doi:10.1029/2007jg000415
Vallina SM, Simó R, Gassó S (2006) What controls CCN seasonality in the Southern Ocean? A statistical analysis based on satellite-derived chlorophyll and CCN and model-estimated OH radical and rainfall. Global Biogeochemical Cycles 20 (1). doi:10.1029/2005gb002597
Vallina SM, Simó R, Gasso S, De Boyer-Montegut C, del Rio E, Jurado E, Dachs J (2007) Analysis of a potential "solar radiation dose-dimethylsulfide-cloud condensation nuclei" link from globally mapped seasonal correlations. Global Biogeochemical Cycles 21 (2):16. doi:Gb200410.1029/2006gb002787
Van Der Giezen M, Lenton TM (2012) The rise of oxygen and complex life. Journal of Eukaryotic Microbiology 59 (2):111-113. doi:10.1111/j.1550-7408.2011.00605.x
Van Rijssel M, Gieskes WWC (2002) Temperature, light, and the dimethylsulfoniopropionate (DMSP) content of Emiliania huxleyi (Prymnesiophyceae). Journal of Sea Research 48 (1):17-27. doi:10.1016/s1385-1101(02)00134-x
Vernet M, Matrai PA, Andreassen I (1998) Synthesis of particulate and extracellular carbon by phytoplankton at the marginal ice zone in the Barents Sea. Journal of Geophysical Research C: Oceans 103 (C1):1023-1037
Vichi M, Allen JI, Masina S, Hardman-Mountford NJ (2011) The emergence of ocean biogeochemical provinces: A quantitative assessment and a diagnostic for model evaluation. Global Biogeochemical Cycles 25 (2). doi:10.1029/2010gb003867

Vogt M, Vallina SM, Buitenhuis ET, Bopp L, Le Quéré C (2010) Simulating dimethylsulphide seasonality with the Dynamic Green Ocean Model PlankTOM5. Journal of Geophysical Research C: Oceans 115 (6). doi:10.1029/2009jc005529
Von Glasow R (2007) A look at the CLAW hypothesis from an atmospheric chemistry point of view. Environmental Chemistry 4 (6):379-381
von Glasow R, Crutzen PJ (2004) Model study of multiphase DMS oxidation with a focus on halogens. Atmospheric Chemistry and Physics 4 (3):589-608
Wallcraft AJ, Kara AB, Barron CN, Metzger EJ, Pauley RL, Bourassa MA (2009) Comparisons of monthly mean 10 m wind speeds from satellites and NWP products over the global ocean. Journal of Geophysical Research D: Atmospheres 114 (16)
Wanninkhof R (1992) Relationship between wind speed and gas exchange over the ocean. Journal of Geophysical Research 97 (C5):7373-7382
Wanninkhof R, McGillis WR (1999) A cubic relationship between air-sea CO2 exchange and wind speed. Geophysical Research Letters 26 (13):1889-1892
Watts SF (2000) The mass budgets of carbonyl sulfide, dimethyl sulfide, carbon disulfide and hydrogen sulfide. Atmospheric Environment 34 (5):761-779
Weisberg S (2005) Applied Linear Regression. Wiley Series on Probability and Statistics, 3 edn. John Wiley & Sons, Inc, New Jersey
Welschmeyer NA (1994) Fluorometric analysis of chlorophyll a in the presence of chlorophyll b and pheopigments. Limnology and Oceanography 39 (8):1985-1992
Wilcox R (2010) Fundamentals of Modern Statistical Methods: Substantially Improving Power and Accuracy. 2 edn. Springer, New York
Wolfe GV, Steinke M (1996) Grazing-activated production of dimethyl sulfide (DMS) by two clones of Emiliania huxleyi. Limnology and Oceanography 41 (6):1151-1160
Wolfe GV, Steinke M, Kirst GO (1997) Grazing-activated chemical defence in a unicellular marine alga. Nature 387 (6636):894-897. doi:10.1038/43168
Wolfe GV, Strom SL, Holmes JL, Radzio T, BradyOlson M (2002) Dimethylsulfoniopropionate cleavage by marine phytoplankton in response to mechanical, chemical, or dark stress. Journal of Phycology 38 (5):948-960. doi:10.1046/j.1529-8817.2002.t01-1-01100.x
Woodhouse MT, Carslaw KS, Mann GW, Vallina SM, Vogt M, Halloran PR, Boucher O (2010) Low sensitivity of cloud condensation nuclei to changes in the sea-air flux of dimethyl-sulphide. Atmospheric Chemistry and Physics 10 (16):7545-7559. doi:10.5194/acp-10-7545-2010
Yoch DC (2002) Dimethylsulfoniopropionate: Its sources, role in the marine food web, and biological degradation to dimethylsulfide. Applied and Environmental Microbiology 68 (12):5804-5815
Yost DM, Mitchelmore CL (2009) Dimethylsulfoniopropionate (DMSP) lyase activity in different strains of the symbiotic alga symbiodinium microadriaticum. Marine Ecology Progress Series 386:61-70
Zappa CJ, Asher WE, Jessup AT (2001) Microscale wave breaking and air-water gas transfer. Journal of Geophysical Research C: Oceans 106 (C5):9385-9391
Zemmelink HJ, Gieskes WWC, Klaassen W, Beukema WJ, De Groot HW, De Baar HJW, Hintsa EJ, McGillis WD, Dacey JWH (2004) Relaxed-eddy accumulation measurements of the sea-to-air transfer of dimethylsulfide over

the northeastern Pacific. Journal of Geophysical Research C: Oceans 109 (1):C01025 01021-01010
Zepp RG, Schlotzhauer PF, Sink RM (1985) Photosensitized transformations involving electronic energy transfer in natural waters: Role of humic substances. Environmental Science and Technology 19 (1):74-81